Insulin-Like Growth Factor Binding Protein-6: Posttranslational modifications and sorting in polarized MDCK cells

Dissertation

zur Erlangung des Doktorgrades
der Mathematisch-Naturwissenschaftlichen Fakultäten
der Georg-August-Universität zu Göttingen

vorgelegt von

Liliana Dimitrova Shalamanova-Malinowski
(geb. Shalamanova)

aus Sofia / Bulgarien

Göttingen 2001

D 7

Referent: **Prof. Dr. K. von Figura**

Koreferent: **Prof. Dr. G. Gottschalk**

Tag der mündlichen Prüfung: **30.10.2001**

PUBLICATIONS AND PRESENTATIONS ARISING FROM THIS THESIS

Publications

Shalamanova L., Kubler B., Scharf J. G., Braulke T., (2000): Ligand blotting: iodinated vs biotinylated IGF. *Growth Horm IGF Res* 10: 294

Shalamanova L., Kübler B., Scharf J. G., Braulke T.: MDCK cells secrete neutral proteases cleaving insulin-like growth factor-binding protein-2 to –6. *Am J Endocrinol Metab*. In press

Presentations

Shalamanova L., Kubler B., Scharf J. G., Braulke T., (2000): Madin-Darby canine kidney cells secrete two distinct insulin-like growth factor binding protein –6 degrading proteases. *Biol Chem* 381: S 142

Shalamanova L., Kübler B., Braulke T., (1999): Prteolysis of IGF-binding protein-6 in media from kidney cells. *Growth Horm IGF Res* 9: 377

CONTENTS

ABBREVIATIONS

Units

bp, kb	Base pair, kilobase
Da, kDa	Dalton, kilodalton
g, mg, µg, ng	Gram, milligram, microgram, nanogram
l, ml, µl	Liter, milliliter, microliter
M, mM, µM, nM	Molar, millimolar, micromolar, nanomolar
nm	Nanometer
OD, A	Optical density, absorbance
rpm	Rotations per minute
v/v	Volume for volume
w/v	Weight for volume

Cell lines

BHK	Baby Hamster Kidney
CHO	Chinese Hamster Ovary
MDBK	Madin-Darby Bovine Kidney
MDCK	Madin-Darby Canine Kidney

Genes and Proteins

ASA	Arylsulfatase A
cDNA	complementary DNA
DNA, RNA	2-deoxy D-ribonucleic acid, ribonucleic acid
IGF	Insulin-like Growth Factor
IGFBP	IGF-Binding Protein
IgG	Immunoglobulin G
HRP	Horseradish peroxidase
VEGF	Vascular Endothelial Growth Factor
WT	Wild type

Methods and Chemicals

BSA	Bovine Serum Albumin
CHAPS	3-([3-Cholamidopropyl]dimethylammonio)-1-propanesulfonate
ddH_2O	double distilled water
DEAE	2-diethylamino-ethyl
DMEM	Dulbecco's Modified Essential Medium
DMSO	Dimethyl sulfoxyde
dNTP	Deoxyribonucleoside triphosphate
DTT	1,4-Dithio-DL-threitol
ECL	Enhanced chemiluminescence
EDTA	Ethylenediamine tetraacetic acid
FCS	Fetal Calf Serum
HCl	Hydrochloric acid, hydrochloride
HEPES	4-(2-hydroxyethyl)-1-piperazine ethanesulphonic acid
HBS	HEPES Buffered Saline

LB	Luria Bertani medium
MOPS	3-(N-Morpholino)propanesulfonic acid
NaCl	Sodium chloride
NC	Nitrocellulose membrane
PBS	Phosphate Buffered Saline
PBST	PBS-Tween 20
PCR	Polymerase Chain Reaction
SDS	Sodium dodecyl sulphate
SDS-PAGE	SDS-polyacrylamide gel electrophoresis
TEMED	N,N,N',N'-Tetramethylethylenediamine
TFMS	Trifluoromethanesulfonic acid

ABSTRACT

The insulin-like growth factors (IGFs) promote proliferation and differentiation of a variety of cell types. The IGF availability and interactions with specific cell surface IGF-receptors are modulated by six structurally related IGF-binding proteins (IGFBPs). Among the IGFBPs, IGFBP-6 has the highest binding affinity for IGF II. Limited proteolysis of IGFBPs by specific proteases decreases the affinity of IGFBPs for IGFs, thus maintaining higher levels of free IGFs.

This study represents the first report on the secretion and sorting of IGFBPs and IGFBP-proteases in polarized epithelial Madin-Darby canine kidney (MDCK) cell line. It was found that MDCK cells secrete a variety of neutral proteases cleaving IGFBP-2 to –5 into fragments of defined sizes. IGFBP-6, the main sequestrating binding protein of IGF II, was completely degraded with transient fragment formation. The IGFBP-6 fragments, even after a minor proteolytic cleavage, displayed no affinity for IGF II, demonstrating the importance of the proteolysis of IGFBP-6 for maintainance of free-IGF II levels. Protease inhibitor profile and partial purification of IGFBP-6 proteases from media of MDCK cells showed that IGFBP-6 is degraded by two different proteases – a serine and a disintegrin metalloprotease (ADAM). Polypeptides in partially purified metalloprotease-containing fractions cross-reacted with antibodies against conserved domains of ADAM 12 S in Western blots. These data suggest that the IGFBP-6 metalloprotease may belong to the ADAM/ADAMTS family.

MDCK cells secreted IGFBP-4 and –6 proteases preferentially from the basolateral side, whereas the IGFBPs were secreted mainly from the apical side as a result of specific intracellular sorting processes. MDCK cells stably transfected with mouse IGFBP-6 cDNA, demonstrated a preferential apical secretion of mIGFBP-6. Structural characterization of mIGFBP-6 overexpressed in MDCK cells revealed the presence of a variety of posttranslational modifications (O-glycosylation, phosphorylation and sulfation), which physiological functions are unclear. Substitution of a putative O-glycosylation site of mIGFBP-6 with an alanine residue resulted in a faster electrophoretic mobility and in marginal changes of the polarized secretion of the protein. Overexpression of mIGFBP-6 inhibited the proliferation of MDCK cells presumably by sequestration of the endogenous IGF II, and suppressed the migration of MDCK cells.

The present study indicates that the complex regulation of IGF actions in MDCK cells involves IGFBPs and IGFBP-proteases. The results suggest that mIGFBP-6 is capable of modulating important biological processes such as proliferation and migration. Posttranslational modifications of mIGFBP-6 including O-glycosylation, sulfation, and

phosphorylation, lead to a high molecular heterogeneity of the protein, and may be important for the maintainance of its physiological functions, polarized sorting, proteolytic stability, and affinity to IGF II. The data provide evidence that in addition to the presence of IGF receptors in the basolateral membrane of MDCK cells, sorting of at least IGFBPs and IGFBP proteases to distinct sides contributes to the complexity and the fine regulation of the epithelial cell functions.

1 INTRODUCTION

1.1 The insulin-like growth factor (IGF) system

The insulin-like growth factor (IGF) system plays an important role in the regulation of proliferation and differentiation of normal and malignant cells. The established components of the IGF system include the families of IGFs, IGF receptors, IGF-binding proteins (IGFBPs), and IGFBP proteases (Figure 1).

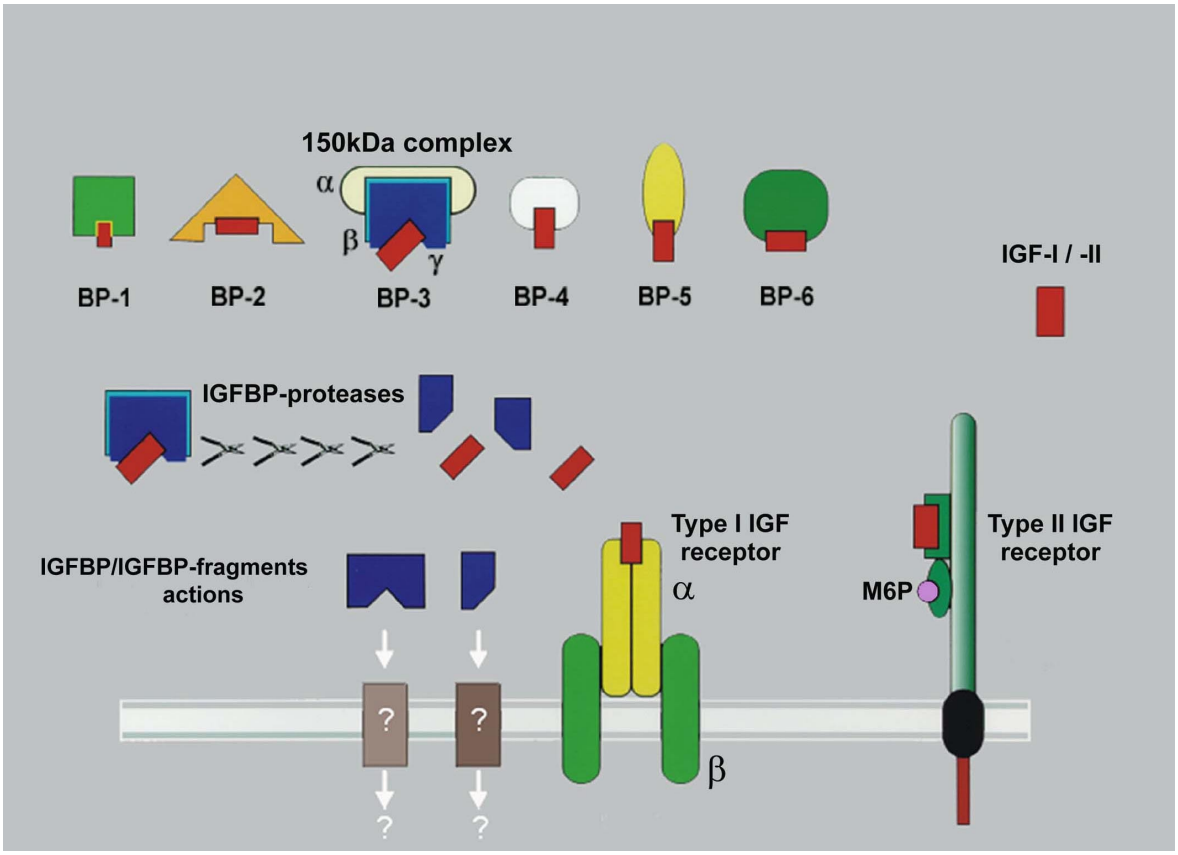

Figure 1: The insulin-like growth factor system

1.1.1 Insulin-like growth factors

IGF I and II are highly homologous 7 kDa single-chain polypeptides, sharing structural homology to proinsulin. IGFs are widely expressed and regulate proliferation, survival and differentiation of normal and malignant cells (Kurihara et al., 2000; Granerus at al., 2001) in endocrine, paracrine, as well as autocrine manner (Jones et al., 1995).

1.1.2 IGF receptors

IGFs exert their effects by binding to specific cell surface receptors designated type 1 and type 2 IGF receptors, as well as by interacting with the insulin receptor. The mitogenic effects of IGFs are mediated mainly through interactions with the type 1 IGF receptor (IGF 1R) (Le Roith, 2000). The type 2 IGF receptor (IGF 2R) is structurally distinct, binds primarily IGF II (K_D range 0.017-0.07 nM), but also serves as a receptor for mannose 6-phosphate-containing ligands (Braulke, 1999 a).

Type 1 IGF receptor

IGF 1R is a member of the transmembrane tyrosine kinase receptor family that includes also the insulin receptor (IR). IGF 1R is a heterotetramer, which consists of two α subunits of 130-135 kDa and two β chains of 90-95 kDa (Figure 1) with several α-α and α-β disulfide bridges (Ullrich et al. 1986). The ligand-binding domain of IGF 1 receptor is located on the extracellular α subunit. It binds preferentially IGF I with $K_D \leq 1$ nM and has a several-fold lower affinity for insulin and IGF II (Feld and Hirschberg, 1996). The intracellular region of the β-subunit contains a cytoplasmic tyrosine kinase domain that phosphorylates upon ligand binding tyrosine residues in the respective contralateral β-subunit within the same receptor (Brodt et al., 2000). This autophosphorylation reaction leads to phosphorylation of insulin receptor substrates (IRS), and Shc. Subsequent to tyrosine phosphorylation, these proteins bind various Src homology (SH) 2 domain-containing proteins such as Grb-2, Crk, and Nck, which mediate various biological processes like mitogenesis and inhibition of apoptosis via the Ras/Raf/MAP kinase pathway, and phosphatidyl inositol-3 (PI-3) kinase pathway (Liu et al., 2001).

Type 2 IGF receptor

The IGF 2 receptor is identical with the monomeric 300 kDa mannose-6-phosphate (M6P) receptor. Distinct regions in its extracytoplasmic domain interact with two classes of ligands – IGF II and proteins that bear mannose 6-phosphate (M6P) residues (Kornfeld, 1990). The binding of IGF II to IGF 2R at the cell surface results in internalization and degradation of the ligand, thereby down-regulating the extracellular IGF II level of this mitogenic factor (Oka and Czech, 1986). The role of IGF 2R in signal transduction is discussed controversely (Nishimoto, 1993; Körner et al., 1995; Ludwig et al., 1996). In

addition, the IGF 2R binds M6P-containing proteins, mainly soluble lysosomal hydrolases, in the Golgi or at the plasma membrane, and mediates their targeting to the lysosomes.
The IGF 2R appears also to be involved in the activation of the growth inhibitor transforming growth factor-β (TGF-β1). The M6P containing precursor of TGF-β1 is part of the latent extracellular TGF-β1 complexes (Dennis and Rifkin, 1991; Munger et al., 1997). After activation, TGF-β1 exerts effects on cellular proliferation by interacting with its own serine/threonine kinase receptors, usually resulting in growth inhibition (Alevizopoulos and Mermod, 1997). The physiological significance of two other types of IGF 2R ligands described recently, retinoic acid and the urokinase-type plasminogen activator receptor (Kang et al., 1999; Nykjaer et al., 1998) is still unclear.

1.1.3 Insulin-like growth factor-binding protein (IGFBP) family

Circulating and tissue IGFs are largely bound to a family of six structurally related IGF binding proteins (IGFBP-1 to –6). IGFs bind to IGFBPs with higher affinities (K_D ~10^{-10} M) than to IGF 1R (K_D ~10^{-8}-10^{-9} M). Therefore, IGFBPs act not only as carriers of IGFs, prolonging their half-life in the circulation, but also function as modulators of IGF availability and activity (Hwa et al., 1999). In addition, it has been described that some of the IGFBPs mediate important IGF-independent effects such as IGFBP-3, which promotes growth-inhibition in breast cancer cells (Oh, 1998) or induces apoptosis in lung cells (Besnard et al., 2001). Whether the cross-linked products of IGFBP-3 with proteins from the cell surface of Hs578T human breast cancer cells (Oh et al., 1993; Yamanaka et al., 1999) or the type V TGF-β receptor (Leal et al., 1997) represent IGFBP-3 receptors is unclear. Additionally, it has been reported that the apoptotic effect of IGFBP-3 is mediated by direct binding of IGFBP-3 to the nuclear retinoid X receptor-α (Liu et al., 2000).
The IGFBPs are cysteine rich proteins (16-20 cysteines residues) with high homology in their primary amino acid sequences. Structurally, the cysteine residues are clustered at the conserved N-terminal and in the C-terminal part of the proteins. The N- and C-terminal domains are separated by a central region of low similarity among the IGFBPs. It has been reported that the N-terminal domain of IGFBP-5 (Zeslawski et al., 2001), the C-terminal domain of IGFBP-2 (Forbes et al., 1998), or both domains of IGFBP-3 and –4 (Hwa et al., 1999; Ständker et al., 2000) bind the IGFs, however, with greatly reduced affinity compared to those of the intact IGFBP molecules.

N-terminal domain

The N-terminal part of the six mature IGFBPs comprises 80-93 amino acid residues and shares approximately 58% similarity among the IGFBPs. Ten to 12 of the 16-20 cysteine residues found in the IGFBPs are located in this domain. In IGFBP-1 to –5, the 12 cysteines are fully conserved, whereas in IGFBP-6 10 of the 12 cysteine residues are invariant. The N-terminus is highly structured with a maximum of 6 disulfide bonds formed (5 in the case of IGFBP-6). Recent studies have demonstrated that the cysteines in the N-terminal part of IGFBP-4 and –6 form interdomain disulfide bonds and are not linked to C-terminal cysteine residues (Neumann et al., 1998; Ständker et al., 2000).

Central region

The central region of the IGFBPs comprises 55 to 95 amino acid residues, sharing less than 15% similarity among the IGFBPs. Posttranslational modifications of the IGFBPs (glycosylation, phosphorylation, and proteolytic cleavage) are restricted to this domain.

C-terminal domain

The C-terminal part of IGFBPs, like the N-terminal domain, is highly conserved and shares a similarity of approximately 34% among the human IGFBPs. The disulfide linkages involve all six cysteine residues with a proposed disulfide bond pattern 1-2, 3-4, and 5-6 (Forbes et al., 1998; Ständker et al., 2000). Interestingly, heparin binding motifs (XBBBXXBX, where B is a basic residue, Arg, Lys, or His, and X stands for any residue) are found within the C-terminal domains of IGFBP-3, -5, and –6. For IGFBP-3 and –5 it is demonstrated that the heparin binding domain is involved in binding of IGFBPs to the cell surface and/or the extracellular matrix (Booth et al., 1996; Fowlkes et al., 1997).

1.1.3.1 Posttranslational modifications of human IGFBP-1 to –6

Human IGFBPs differ not only in the size of the mature proteins and the number of conserved cysteines (Table 1), but also in the posttranslational modifications (N- and O-glycosylation or phosphorylation) of their central region.

	Mw (kDa)	Amino acids	No. of cysteines	Glycosylation (N- or O-)	Phosphorylation
IGFBP-1	25.3	234	18		P
IGFBP-2	31.4	289	18		
IGFBP-3	28.7	264	18	N	P
IGFBP-4	26.0	237	20	N	
IGFBP-5	28.6	252	18	O	P
IGFBP-6	22.8	216	16	O	

Table 1: Characteristics of the human IGFBP family (Hwa et al., 1999)

Glycosylation of IGFBPs

N-Glycosylation occurs only on an asparagine residue that is part of the consensus sequence Asn-X-Ser/Thr, where X is any amino acid other than proline. In contrast, there is no consensus amino acid sequence that determines whether an individual serine or threonine residue will be O-glycosylated. As shown in Table 1, IGFBP-3 and –4 are N-glycosylated, and IGFBP-5 and –6 are O-glycosylated (Hwa et al., 1999). It has been reported that glycosylation protects IGFBPs from proteolysis (Neumann et al., 1998). Because proteolysis of IGFBPs appears to be a major mechanism to release IGFs from IGF/IGFBP complexes, glycosylation may affect the bioavailability of IGFs.

Phosphorylation of IGFBPs

Three of the six IGFBPs, IGFBP-1, -3, and –5, are phosphorylated predominantly at serine residues in the central region (Coverley and Baxter, 1997). The involved kinases, however, are unknown. Whereas the importance of phosphorylation of IGFBPs is unclear, there is evidence that in human IGFBP-1 phosphorylation enhances the affinity to IGFs 5-fold (Westwood et al., 1997). Thus, phosphorylated IGFBP-1 inhibits the IGF I-stimulated amino acid uptake in trophoblast cells, whereas nonphosphorylated IGFBP-1 has the opposite effect (Yu et al., 1998). In contrast, the phosphorylation of IGFBP-3 does not affect its binding to IGFs (Hoeck and Mukku, 1994).

1.1.3.2 IGFBP-6 – a unique member of the IGFBP family

The main feature that makes IGFBP-6 unique among the other IGFBPs is its high binding affinity for IGF II (K_D 1~4 x 10^{-11} M (Roghani et al., 1991)), whereas it binds to IGF I with a 20-100-fold lower affinity (Forbes et al., 1990). Thus, the inhibitory effects of IGFBP-6

on IGF II-induced proliferation and differentiation of cells are most likely due to sequestration of IGF II, preventing its interaction with IGF-receptors (Bach et al., 1995; Srinivasan et al., 1996). However, there are data suggesting that IGFBP-6 initiates IGF-independent effects (Babajko et al., 1997), as described for IGFBP-3 (Besnard et al., 2001). Thus, recent studies have demonstrated that IGFBP-6 activates the process of apoptosis in non-small cell lung cancer cells (NSCLC). Additionally, IGFBP-6 is able to reduce the size of NSCLC xenografts in nu/nu mice (Sueoka et al., 2000), which makes it a potential target in cancer therapeutics.

Human, rat and mouse IGFBP-6 are O-glycosylated in different stochiometry (Bach, 1999). In human IGFBP-6 the residues Thr126, Ser144, Thr145, Thr146, and Ser152 have been identified to be glycosylated (Neumann et al., 1998). It is proposed that O-glycosylation prevents the binding of IGFBP-6 to glycosaminoglycans resulting in a 10-fold higher affinity for IGF II (Marinaro et al., 2000 b).

1.1.4 IGFBP proteases

Proteolysis of IGFBPs is the main mechanism to release IGFs from IGF/IGFBP complexes and to increase their availability for binding to the IGF receptors. Three known groups of IGFBP proteases, kallikrein-like serine proteases, cathepsins, and metalloproteases, are known so far.

Kallikrein-like serine proteases, like the prostate-specific antigen (PSA, hK3) or the nerve growth factor-γ, have been demonstrated to cleave IGFBP-3 *in vitro* (Rajah et al., 1996). Furthermore, hK3 has been described to degrade IGFBP-4 but not IGFBP-2 and -5, whereas hK2 degrades all of the IGFBPs (Rehault et al., 2001). Recently, the serine protease complement component C1s was identified as a specific IGFBP-5 protease (Busby et al., 2000).

The cathepsin family comprises a broad variety of acidic lysosomal cysteine and aspartic proteases like cathepsin L, B, and D, respectively, as well as non-lysosomal proteases with neutral pH optimum like cathepsin C and G. Cathepsins have been described to degrade a variety of IGFBPs: cathepsin G cleaves IGFBP-1 to –6 (Gibson and Cohen, 1999); cathepsin D degrades IGFBP-1 to –5 but fails to cleave IGFBP-6 (Conover and De Leon, 1994; Claussen et al., 1997). Several acid-activated proteases have been described to be involved in the proteolysis of IGFBP-6 in media from NIH-3T3 cells or human keratinocytes (Claussen et al., 1995; Marinaro et al., 1999 a).

The metalloproteases form the most diverse group of peptidases, including more than 30 families (Creemers et al., 2001). Members of metzincin superfamily of metalloproteases, including the reprolysin and the matrix metalloprotease (MMP) families, have been described to degrade IGFBPs (Conover, 2000). It has been demonstrated that recombinant human MMP-3 cleaves human IGFBP-3 and endogenous rat IGFBP-3 in non-pregnancy serum (Wu et al., 1999) whereas MMP-1 uses IGFBP-2 and IGFBP-3 as proteolytic substrates in asthmatic airway tissue extracts (Rajah et al., 1999).

ADAMs (a disintegrin and metalloproteases) belong to the reprolysin family of zinc metalloproteases and are composed by a pro-, a metalloprotease, a disintegrin, and a cysteine-rich domains. Additionally, membrane-ancored ADAMs contain a transmembrane and cytoplasmic domains (Loechel et al., 1998). ADAMs are involved in the proteolysis of IGFBP-3, -4, and –5 during pregnancy (Kübler et al., 1998). Recently, ADAM 12 S has been shown to be the responsible protease in pregnancy serum cleaving IGFBP-3 (Shi et al., 2000). Additionally, it has been demonstrated that this enzyme degrades also IGFBP-5 (Loechel et al., 2000). Furthermore, the metalloprotease pregnancy associated plasma protein A (PAPP-A) is identical with the IGF II-stimulated IGFBP-4 protease in media of human ovarian granulosa cells (Conover et al., 2001) and in pregnancy serum (Byun et al., 2001).

1.2 Polarized sorting of proteins

Epithelial cell types, like kidney tubular or intestinal cells, that form permeability barriers between two compartments in the body, have a unique structural and functional cell organization. The plasma membrane of these cells is divided by tight junctions into two distinct domains, termed apical and basolateral, which face the lumen of the organ and underlying cells and connective tissue, respectively. Each domain is comprised of specific subsets of proteins and lipids. The differences in the protein distribution are maintained by a complex machinery which utilizes distinct signals for apical and basolateral sorting (Mostov et al., 2000). These signals are best investigated for integral membrane proteins.

1.2.1 Pathways of polarized protein traffic

In the exocytic pathway, newly synthesized proteins are transported to the Golgi complex, where they undergo a variety of posttranslational modifications. In the trans-Golgi network (TGN), proteins and lipids are packed into vesicles and are further transported to the

plasma membrane by three different pathways. In the direct pathway, TGN derived vesicles are targeted directly to the correct, i.e., apical or basolateral domain. In the indirect pathway, membrane proteins are first delivered to the basolateral domain. From there, apical proteins are endocytosed and transported to the apical domain by transcytosis. Third, proteins can be sorted randomly to both membrane surfaces. (Zegers and Hoekstra, 1998).

1.2.2 Apical sorting of membrane proteins

Multiple signals seem to play a role in the apical targeting of membrane proteins. One mechanism for apical sorting is based on the association of proteins with glycosphingolipid and cholesterol enriched microdomains (rafts) in the Golgi. Many glycosyl-phosphatidylinositol (GPI)-anchored proteins are directly sorted to the apical membrane after raft-association (Hannan and Edidin, 1996; Schmidt et al., 2001). However, some GPI-ancored proteins are directed to the basolateral domain of epithelial cells (McGwire et al., 1999; Lipardi et al., 2000).

N-linked carbohydrate chains have also been reported to serve as apical determinants (Gut et al., 1998). It is thought that the N-glycans interact with TGN lectin sorters, which mediate incorporation of the transported proteins into apical carrier vesicles. Two lectin-like proteins localized in TGN and post-Golgi compartments, VIP-36, and the thyroglobulin receptor, have been proposed to be involved in apical sorting (Fiedler and Simons, 1995; Miquelis et al., 1993). Recent studies, however, have shown that VIP-36 does not exit the Golgi and cycles in the early secretory pathway (Fullekrug et al., 1999).

O-linked carbohydrate chains have been shown to be required for the correct apical targeting of the membrane proteins dipeptidyl peptidase IV and pro-sucrase isomaltase (Naim et al., 1999; Alfalah et al., 1999). Monlauzeur et al. (1998) have demonstrated that the apical localization of the human neurotrophin receptor p75 (p75(NTR)) is neither affected by truncation of the cytoplasmic domain nor by the replacement of the transmembrane domain by a GPI-anchor, whereas the substitution of potential O-glycosylation sites leads to intracellular cleavage and secretion of the ectodomain into the basolateral medium.

Finally, a number of different determinants located in the transmembrane or cytoplasmic domains have been described to function in membrane proteins as apical sorting signals (Lin et al., 1998; Sun et al., 1998).

1.2.3 Basolateral sorting of membrane proteins

The importance of the cytoplasmic domain as a basolateral-sorting determinant for integral membrane proteins is demonstrated for a variety of proteins (Martens et al., 2000; Kroepfl and Gardinier, 2001; Nadler et al., 2001). Thereby, single tyrosine residues as a part of the coated pit localisation signals play the major role as basolateral targeting signals (Caplan, 1997; Moll et al., 2001). These motifs appear to interact with the epithelial-specific subunit of the AP-1 clathrin adaptor complex, μIb (Folsch et al., 1999). Another type of signals, unrelated to the endocytic signal motifs, comprises short sequences at the extreme carboxyl terminus of many membrane proteins, which have been found to bind proteins containing PDZ (PSD-95/discs-large/ZO-1) domains (Fanning and Anderson, 1999; Mostov et al., 2000; Peifer and Tepass, 2000; Le Maout et al., 2001). PDZ-containing proteins are found to be involved in localization, clustering, or linking of receptors to different signaling pathways (Kim, 1997).

1.2.4 Sorting of soluble proteins

In comparison with the targeting determinants of membrane proteins, the sorting signals for soluble proteins are far less studied. Carbohydrate modifications are considered to play an important role in apical sorting of secretory proteins. Scheiffele et al. (1995) have demonstrated that the rat growth hormone (rGH), a protein secreted randomly in MDCK cells, is directed to the apical domain after introduction of one or two N-glycosylation sites. In addition N-glycans have also been shown to be important for the apical targeting of erythropoetin or rGH in MDCK cells (Kitagawa et al., 1994; Benting et al., 1999). However, analyses of secretory proteins with mutated N-glycosylation sites expressed in MDCK cells, have provided evidence against the executive role of N-glycosylation in the apical sorting (Larsen et al., 1999; Yeaman et al., 1997; Marmorstein et al., 2000). The role of O-glycosylation as a putative signal for targeting of secretory proteins is not well defined. O-gycans appear to present apical determinants for some soluble proteins such as the secreted soluble form of p75NTR or IGFBP-6 (Yeaman et al., 1997; Pommier et al., 1995; Remacle-Bonnet et al., 1995).

2 MATERIAL AND METHODS

2.1 General

2.1.1 Chemicals and Reagents

Except where stated, all media, enzymes and supplements for cell culture were purchased from Life Technologies, Inc.. Chemicals and enzymes were bought from Fluka (Switzerland), Merck, Amersham Pharmacia Biotech (Freiburg), Roth (Karlsruhe), Sigma, Serva (Heidelberg), Roche (Mannheim) or New England Biolabs, unless indicated otherwise. X-Omat AR films (Kodak, Rochester, NY) were used for autoradiography or chemical luminescence.

2.1.2 Buffers and Solutions

PBS	10 mM sodium phosphate, 150 mM NaCl, pH 7.4
TBS	20 mM Tris/HCl, 10 mM NaCl, pH 7.4

2.2 Cell Biological Methods

2.2.1 Cell culture

All cell lines were grown in DMEM supplemented with 4.5 g/l glucose, 25 mM HEPES, 2 mM glutamine, 10% FCS, 100 U/ml penicillin, and 100 µg/ml streptomycin, and cultured at 37°C in 5% CO_2. Depending on the purpose, cells were grown on plastic dishes with different sizes (Greiner, Germany), or on 24 mm Transwell (Costar, Cambridge, MA) polycarbonate filters (0.4 µm pore size) when experiments with polarized cells were performed.

For conditioning of cells, serum-free medium (DMEM, 0.1-0.005% (w/v) BSA, antibiotics) was used. Cells were washed two times with PBS and starved in serum-free medium for 2 h at 37°C. After removal of the media, conditioning was carried out with fresh medium for 24-72 h at 37°C.

2.2.1.1 Cell lines

Baby hamster kidney 21 (BHK 21), Madin-Darby canine kidney (MDCK), and Madin-Darby bovine kidney (MDBK) cell lines were kindly provided by Dr. K. von Figura (University of Göttingen, Germany).

2.2.1.2 Trypsinization

Cells were washed twice with sterile PBS and incubated in minimal amount trypsin-EDTA (0.5 g/l trypsin, 0.2 g/l EDTA) at 37°C until they had detached from the dish. The process was controlled under an inverted microscope. Trypsin was inhibited by addition of growth medium in which the cells were subsequently resuspended. Cell counting was performed, when necessary, using an improved Neubauer chamber, and the cells were plated out or harvested for cryoconservation.

2.2.1.3 Cryoconservation and thawing

Resuspended cells were spun down (1000 g for 5 minutes at 4°C) in 4 ml growth medium. The supernatant was aspirated and the cells resuspended (1-5 x 10^7 cells/ml) in ice-cold freezing medium (DMEM, 20% FCS, 10% DMSO). Cells were kept for 16 h at –80°C and then stored in liquid nitrogen.

For revitalization, frozen cells were quickly thawed, gently transferred to disposable Falcon tubes containing 4 ml cold growth medium and spun down as described above. Supernatant was discarded by aspiration, and cells were plated out after being resuspended in a suitable amount of growth medium.

2.2.1.4 Stable transfection of mammalian cells

The protocol for stable transfection of mammalian cells by calcium-phosphate was adapted from Chen and Okayama (1987). MDCK cells (2 x 10^5) were plated out in growth medium on 60 mm petri dishes. After 16 hours the medium was changed and 3 hours later a DNA precipitation reaction was set up. Ten micrograms plasmid DNA were added to 31.3 µl 2 M $CaCl_2$ and filled up to 250 µl with sterile H_2O. The solution was dropwise pipetted into a second vial containing 250 µl 2x HBS (50 mM HEPES, 1.5 mM Na_2HPO_4, 280 mM NaCl, pH 7.1) under a weak air-bubbling produced by a pasteur pipette. The mixture was

incubated for 1 h at room temperature and then dropwise added into the petri dishes. After 16 h, an antibiotic selection with hygromycine or neomycine was started at initial concentration of 0.1 mg/ml. The amount of antibiotic was increased daily by 0.1 mg/ml to a final concentration of 0.8 mg/ml at which the cell selection was carried out up to the moment when single cell colonies were formed.

2.2.2 Metabolic labeling

For metabolic labeling studies subconfluent cells grown on 60 mm plastic dishes or confluent cells grown on 24 mm Transwell polycarbonate filters were used. The cells were preincubated at 37°C for 2 h in a respective MEM containing 0.005% BSA before being labeled for 20 h at 37°C. The labeling media were centrifuged down (1000 rpm for 10 min) to remove cell debris, and were further subjected to immunoprecipitation or two-dimensional gel electrophoresis.

2.2.2.1 Metabolic labeling with [^{35}S]-methionine

For labeling of newly synthesized proteins, cells were labeled in methionine-free medium (1642454, ICN Biomedicals, Inc.) containing 100 μCi of [^{35}S]-methionine (Amersham Pharmacia Biotech).

2.2.2.2 Metabolic labeling with [^{35}S]-sulfur

Cells were labeled with 150 μCi [^{35}S]-sulfur (ICN Biomedicals, Inc.) in sulfate-free medium (51200, Life Technologies, Inc.) supplemented with 5,958 mg/l HEPES, 300 mg/l glutamine and 75 mg/l $MgCl_2$.

2.2.2.3 Metabolic labeling with [^{33}P]-orthophosphate

Cells were labeled in phosphate-free medium (M-3786, Sigma) in the presence of 100 μCi [^{33}P]-orthophosphate (Amersham Pharmacia Biotech).

2.2.2.4 Metabolic Labeling with [^{3}H]-galactose

Glycosylated proteins were labeled with 100 µCi [^{3}H]-galactose (Amersham Pharmacia Biotech) in conditioning medium with reduced glucose concentration (450 mg/l) (11966, Life Technologies, Inc.).

2.2.3 Cell Migration Assay

The migration assays were performed according to Schmidt et al. (1999) using modified 96-well Boyden chambers (Neuroprobe Inc., Cabin John, MD). VEGF, IGF I, IGF II and mouse IGFBP-6 were diluted in serum-free medium containing 0.1% (w/v) BSA and loaded into the lower wells of the Boyden chamber in triplicate. The wells were covered with a filter of 8 µm pore size (Nucleopore Corp., Pleasanton, CA) coated overnight with Vitrogen 100 (Collagen Corp., Palo Alto, CA). The cells were trypsinized and resuspended in serum-free basal medium containing 0.1% (w/v) BSA. Cell suspension (50 µl) was loaded onto the upper wells of the Boyden chamber and the chambers were incubated for 6 h at 37°C. Nonmigrated cells were scraped off the filter. The number of cells that had migrated to the lower chamber was counted under the microscope (Leica, Bensheim, Germany) after staining with Diff Quick (Dade Behring, Dudingen, Switzerland). For each factor or combination of factors, three fields of three different filters were evaluated.

2.2.4 Proliferation Assay

5-Bromo-2´-deoxy-uridine (BrdU) labeling and detection kit III (Roche, Mannheim) was used for determination of cellular proliferation. Briefly, 5,000 cells/well were seeded and allowed to attach for 24 h at 37°C in a 96-well microtiter ELISA plate. The cells were preincubated for 2 h at 37°C in conditioning medium supplemented with 0.005% BSA. After an incubation for 14 h in the presence or absence of VEGF, IGFBP-6, IGF I, or IGF II in conditioning medium, BrdU reagent which labels the newly synthesized DNA was added for 7.5 h. Cell proliferation rate was estimated with ELISA reader (Tecan Mini, Tecan Group Ltd) by measuring absorbance at 405 nm.

2.3 Molecular Biological Methods

2.3.1 Bacterial work

2.3.1.1 Strain genotypes

DH5α F´/*end*A1, *hsd*R17(r_K^-,mK^+), *sup*E44, *thi*-1, *rec*A1, *gyr*A($Na1^r$), *rel*A1, D(*lac*ZYA-*arg*F)$_{U169}$, (j80*lac*ZDM15)

2.3.1.2 Media and solutions

LB medium	10 g/l Bacto-tryptone, 5 g/l bacto-yeast extract, 5 g/l NaCl, pH 7.0
LB agar	18 g/l bacto-agar into LB medium
TFB 1	30 mM potassium acetate, 50 mM $MnCl_2$, 100 mM RbCl, 10 mM $CaCl_2$, 15% (w/v) glycerol, pH 5.8, adjusted with 0.2 M acetic acid
TFB 2	10 mM Na-MOPS, 75 mM $CaCl_2$, 10 mM RbCl, 15% (w/v) glycerol, pH 7.0, adjusted with NaOH

2.3.1.3 Preparation of competent cells

The protocol used for transforming bacteria was adapted from Hanahan (1985).
TFB 1 and TFB 2 were freshly prepared, sterile filtered and kept on ice. A single colony of strain *E. coli* DH5α was grown overnight in 3 ml LB medium without antibiotics. One milliter of cell suspension was inoculated into 100 ml LB medium, and the flask was shaken at 37°C for 2-2.5 h until OD_{600} of 0.4-0.5 was reached. After 10 min incubation on ice the cells were spun down (4,000 g at 4°C). The pellet was resuspended in 30 ml TFB 1, placed on ice for 10 min and spun down again. The bacteria were resuspended in 4 ml TFB 2, incubated on ice for 10 min, and stored in aliquots of 100 µl at –80°C.

2.3.1.4 Transformation of competent cells

Frozen competent cells were thawed out on ice and mixed with a small volume (≥10 µl) of plasmid DNA (1-100 ng). Incubation on ice for 20 min was followed by a heat shock for 2 min at 42°C. Cells were placed back on ice for 2 min and 400 µl antibiotic-free LB medium were added. After incubation for 1 h at 37°C, 25 µl and 75 µl cell suspension were

plated out on agar plates supplemented with 200 µg/ml ampicillin. The plates were then incubated overnight at 37°C, single colonies were picked and inoculated into 5 ml LB medium supplemented with 100 µg/ml ampicillin. The cell suspension was further used for plasmid preparations or preparation of glycerol stock cultures.

2.3.1.5 Preparation of glycerol stock cultures

To 1 ml bacteria in LB medium, 250 µl 80% (v/v) sterile glycerol was added. The suspension was mixed well and stored at –80°C.

2.3.2 DNA Plasmid Preparation

Mini- and midi-preparation kits were used for isolation of plasmid DNA, following the protocols of the manufacturer (Qiagen, Hilden, Germany).
Plasmid concentrations were determined by spectrophotometry at 260 nm (BioPhotometer, Eppendorf, Germany), with a conversion of 50 µg/ml per OD unit. OD_{260}/OD_{280} ratios were used to evaluate protein contamination.

2.3.3 Separation of DNA on agarose gels

50x TAE	242 g Tris base, 57.1 ml glacial acetic acid, 37.2 g Na_2EDTA x $2H_2O$, H_2O to 1 liter
1x TAE	40 mM Tris-acetate, 2 mM Na_2EDTA
5x Loading buffer	50% glycerol in 2x TAE buffer, traces of bromphenol blue

Depending on the size of the DNA fragments, agarose gels with different matrix concentration (0.8 – 2%) were cast. Agarose was melted in 1x TAE buffer. The solution was cooled down to 55°C, and ethidium bromide was added to a final concentration of 0.5 µg/ml. Mixed with a respective amount of 5x loading buffer DNA samples were separated in the agarose gel under tension of 3–4 V/cm. The DNA fragments were visualized under UV light by means of a CCD camera (Diana II, Raytest, Germany).

2.3.4 Cloning and site directed mutagenesis

2.3.4.1 Vectors and cDNA

pcDNA 3.1. (+)	Invitrogen, Leek, The Netherlands
pGK Hygro	Mortensen et al., 1991
pBEH	Artelt et al., 1988

Mouse IGFBP-6 WT cDNA containing 43 bp of the 5´untranslated region and 229 bp of the 3´untranslated region with 20 bp of polyA was kindly provided by Dr. A. Schuller (Department of Neuroscience and Cell Biology, University of Medicine and Dentistry New Jersey, USA) (Schuller et al., 1994). In order to study the role of O-glycosylation for the sorting of mIGFBP-6 in epithelial cells, two potential O-glycosylation sites, S126 and S143, were mutated to alanine residues. mIGFBP-6 WT cDNA subcloned into two different vectors, pBEH and pcDNA 3.1. (+), was used as a template for obtaining the following mutants S126A, S143A and S126A/S143A mIGFBP-6 by means of PCR-based site directed mutagenesis.

2.3.4.2 PCR-based site directed mutagenesis

For substitution of S126 and S143 against alanine residues in mIGFBP-6 WT, mismatch primer sets (Table 2) were used to construct the following point mutations:

	Primer sequence
S126A F	5´-caa gga ggt gcc g*cc cgc tct cgt gac-3´
S126A R	5´-gtc acg aga gcg ggc* ggc acc tcc ttg-3´
S143A F	5´-aat cca cgg acc g*ct gct gcc cct ata-3´
S143A R	5´-tat agg ggc agc agc* ggt ccg tgg att-3´

Table 2: Sequences of mismatch primers for substitution of S126 with A126, and S143 with A143 in mIGFBP-6

In order to minimize the number of undesirable mutations occurring during the PCR reaction, *Pfu-Turbo*™-DNA-Polymerase (Stratagene, La Jolla, USA) with 3′→5′ exonuclease proofreading activity that enables the polymerase to correct nucleotide-misincorporation errors was used. The PCR reactions were carried out using the following reagents:

Stock solutions

dNTP mix (Life Technologies, Inc.)	25 mM each nucleotide
10x *Pfu-Turbo*-reaction buffer (Stratagene, La Jolla, USA)	

PCR reaction mix

Primer 1	200 ng
Primer 2	200 ng
dNTP	0.2 mM
1x *Pfu-Turbo*-reaction buffer	
Pfu-Turbo Polymerase	2.5 U
DMSO	2% (v/v)
DNA plasmid template	50 ng
ddH_2O	up to 50 µl

The PCR-based site directed mutagenesis was carried out for 18 cycles in Mastercycler gradient (Eppendorf, Hamburg, Germany) as follows:

Denaturation (1^{st} cycle only)	98°C	10 sec
Denaturation	98°C	2 sec
Annealing	45°C	1 min
Extension	68°C	14 min

For digestion of methylated bacterial DNA template 10 U *DpnI* (New England Biolabs) were added to the PCR product and the mixture was incubated for 2 h at 37°C. DH5α competent cells were transformed with 25 µl *DpnI* digested PCR product.

2.3.5 Sequencing

For sequencing of double stranded DNA, ABI PRISM® BigDye™ Terminators v3.0 Cycle Sequencing Kit (Applied Biosystems, Langen, Germany) was used. The kit components were mixed with 250-500 ng DNA template and 10 pmol primer. Twenty-five amplification cycles were run on a Mastercycler gradient under the following conditions:

Denaturation	96°C	10 sec
Annealing	50°C	5 sec
Extension	60°C	4 min

The PCR product was added to 2 µl 3 M sodium acetate (pH 5.2) and 50 µl 96% ethanol. The mixture was incubated for 10 min on ice and centrifuged (10 min at 14,000 rpm). The resulting DNA pellet was washed two times with 70% ethanol, air-dried and subjected to sequencing. Sequencing was performed by means of ABI PRISM® 377 DNA Sequencer (Applied Biosystems, Langen, Germany) at the Central Service Laboratory, Institute for Cell Biology and Clinical Neurobiology, UKE.

2.4 Biochemical Methods

2.4.1 SDS-Polyacrylamide Gel Electrophoresis (SDS-PAGE)

The SDS-PAGE is based on the ability of SDS, an anionic detergent, to denaturate and charge uniformly negatively protein molecules. Thus, the proteins undergoing an electrophoresis are separated only according to their molecular weight. For better sample resolution, a discontinuous SDS-PAGE was performed according to Laemmli (1970).
SDS-PAGE was performed using SE 600 vertical slab gel unit, 1.5 mm combs and spacers, 180x140 mm glass plates, and EPS 1001 power supply (AmershamPharmaciaBiotech).

Acrylamide solution	30% (w/v) acrylamide, 0.8% bisacrylamide
4x Running gel buffer	1.5 M Tris/HCl (pH 6.8), 0.4% (w/v) SDS
4x Stacking gel buffer	0.5 M Tris/HCl (pH 8.8), 0.4% (w/v) SDS
Ammonium persulfate	10% (w/v) APS
TEMED	
2x Sample buffer	250 mM Tris/HCl (pH 6.8), 2% (w/v) SDS, 20% (w/v) glycerol, 20 mM DTT (only for reducing conditions)
Anode buffer	192 mM glycine, 50 mM Tris/HCl (pH 8.6)
Cathode buffer	192 mM glycine, 50 mM Tris/HCl (pH 8.6), 0.1% (w/v) SDS, 0.001% (w/v) bromphenol blue

Discontinuous electrophoresis consisted of a separating gel (5-15% acrylamide, 0.375 M Tris/HCl pH 8.8, 0.1% SDS, 0.8% APS, 0.08% TEMED) and stacking gel (4% acrylamide, 0.125 M Tris/HCl pH 6.8, 0.1% SDS, 0.33% APS, 0.1% TEMED). The separating gel solution was carefully pipetted down between the glass plates, overlayed with ddH_2O and allowed to polymerize at room temperature for 30 min. After pouring off the overlaying ddH_2O, the stacking gel solution was pipetted down and a comb was inserted. The gel was allowed to polymerize for 60 min. The comb was removed and wells were rinsed with ddH_2O, which was discarded by aspiration. Probes solubilized in a sample buffer, and boiled at 95°C for 5 min, were loaded on the gel and overlaid with cathode buffer. Prestained molecular weight markers (RPN 756, low range 14,300-220,000, Amersham Pharmacia Biotech) were used as standards. Electrophoresis was run at 50 mA/gel in a chamber filled with anode buffer, typically for 2-3 h.

2.4.2 Detection of proteins in SDS-polyacrylamide gels

2.4.2.1 Coomassie Staining

After SDS-PAGE, the gel was simultaneously fixed and stained in 50% methanol, 10% acetic acid and Coomassie blue R250 at room temperature for 30 min. The gel was destained in 50% methanol, 10% acetic acid, washed with ddH_2O, and dried between celophane sheets with an air gel dryer (BioRad, Munich, Germany).

2.4.2.2 Silver staining

(according to Blum et al., 1987)

Gel was fixed in 40% (v/v) ethanol and 10% (v/v) acetic acid for 60 min. Washing with 30% (v/v) ethanol (3x20 min) was followed by an incubation in 0.02% (w/v) sodium thiosulfate for exactly 1 min. The gel was washed in ddH_2O (3x 20 sec) and stained in 0.2% (w/v) silver nitrate, and formaldehyde (250 µl 35% formaldehyde per 1 l) for 20 min. Protein bands were developed in 3% (w/v) Na_2CO_3 and formaldehyde (500 µl 35% formaldehyde per 1 l) for 2-5 min. The reaction was terminated in 1% (w/v) glycine for 10 min, the gel was washed in ddH_2O, and subsequently air-dried.

2.4.3 Protein transfer from SDS-PAGE gels to membranes

Protein electrotransfer from SDS-gels to nitrocellulose membranes was carried out according to Towbin et al. (1979).

Transfer buffer 25 mM Tris/HCl, 192 mM Glycine, 20% Methanol (v/v)

Separating gel, nitrocellulose membrane (0.2 µm pore size, Sartorius, Germany), 2 sponges and 4 sheets of 3MM Whatman paper were equilibrated in transfer buffer for 5 min. A transfer sandwich (sponge, 2 sheets of paper, nitrocellulose membrane, running gel, 2 sheets of paper, sponge) kept together by a plastic cassette, was assembled under transfer buffer to minimize trapping of air bubbles. The cassette was inserted in the buffer tank and the transfer was run at 900 mA for 90 min in TE 62X and 400 mA for 1 h in TE 22 unit

(Tank Transphor TE 62X or TE 22 Mighty Small Transphor, Hoefer Scientific Instruments, San Francisco, USA).

2.4.4 Detection of proteins on nitrocellulose membranes

2.4.4.1 Western immunoblot

PBST 0.1% (w/v) Tween 20 in PBS
Blotto 5% (w/v) fat-free milk powder in PBST

Membranes were blocked for 1 h at room temperature in Blotto. The blots were incubated with rocking for 2 h at room temperature with the primary antibodies (Table 3) diluted in Blotto. The membranes were rinsed five times with PBST and the respective secondary antibody (Table 4) was added. After incubation for 1 h at room temperature, the blots were rinsed as before and the antibody binding was visualised with ECL kit (SuperSignal, Pierce, Rockford, IL) by means of X-Omat AR films.

Primary Antibody	Host	Dilution	Producer
Anti-human IGFPB-1	rabbit	1:1000	UBI, Lake Placid, NY
Anti-bovine IGFBP-2	rabbit	1:1000	UBI, Lake Placid, NY
Anti-human IGFBP-4	rabbit	1:1000	UBI, Lake Placid, NY
Anti-human IGFBP-5	rabbit	1:1000	UBI, Lake Placid, NY
Anti-human IGFBP-6	rabbit	1:600	van Doorn et al., 1999
Anti-mouse IGFBP-6	goat	1:450	Santa Cruz Biotechnology, Inc.
Anti-human ADAM-12 disintegrin domain (rb 119)	rabbit	1:500	Dr. U. Wewer[1]
Anti-human ADAM-12 cysteine-rich domain (rb 122)	rabbit	1:500	Dr. U. Wewer[2]
Anti-human ADAM-12 prodomain (rb 132)	rabbit	1:500	Dr. U. Wewer[2]

Table 3: Primary antibodies used in Western immunoblotting

[1] The antibody was kindly provided by Dr. U. Wewer, University of Copenhagen, Denmark.

Secondary Antibody	Dilution	Producer
Peroxidase-conjugated rabbit anti goat IgG	1:7000	Jackson Immuno Researach Lab., Inc.
Peroxidase-conjugated goat anti rabbit IgG	1:7000	Jackson Immuno Researach Lab., Inc.

Table 4: Secondary antibodies used in Western immunoblotting

2.4.4.2 Western ligand blot (WLB)

For detection of target protein(s) in Western ligand blotting, a labeled ligand is used instead of a primary antibody. For a successful protein-ligand binding, preservation of the secondary protein structure is necessary, which requires exclusion of reducing agents from the SDS-PAGE.
For detection of IGFBPs, biotin- or [^{125}I]-labeled IGF I or II were used.

2.4.4.2.1 Biotinylated IGF I and IGF II (bIGF) WLB

bIGF I and bIGF II, and streptavidin-HRP were purchased from GroPep, Adelaide, Australia and Jackson Immuno Research Laboratories, Inc., respectively.

PBT	8 mM Na_2HPO_4, 2 mM NaH_2PO_4, 10 mM NaCl, pH 7.5, 0.1% Tween 20
BSA-PBT	1% (w/v) BSA in PBT

Membranes were blocked in BSA-PBT for 1 h at room temperature and incubated with bIGF II (20 ng/ml in BSA-PBT) for 16 h at 4°C. The blots were rinsed five times with PBT and incubated with streptavidin-HRP/BSA-PBT (1:7,000) for 45 min at room temperature. The membranes were washed as mentioned before, and the proteins detected by ECL, as described earlier (2.4.4.2).

2.4.4.2.2 [^{125}I]-IGF II WLB

Recombinant human IGF II (GroPep, Adelaide, Australia) was iodinated by the chloramine T-procedure (Zapf et al., 1981) to a specific activity of 80 µCi/µg of protein.

Blocking buffer	50 mM Tris/HCl pH 7.4, 150 mM NaCl,
	0.5% (w/v) fish gelatin (G7765, Sigma)
Washing buffer	50 mM Tris/HCl pH 7.4, 150 mM NaCl,
	0.5% (w/v) fish gelatin, 0.2% (w/v) NP-40

After electrotransfer of proteins, the nonspecific binding sites of the nitrocellulose membranes were blocked in blocking buffer at 4°C overnight. The blots were incubated with [^{125}I]-IGF II (600,000-800,000 cpm/ml) in blocking buffer for 2 to 16 h, then washed 3x 20 min with washing buffer, and were air-dried. The membranes were sealed in a plastic bags and exposed to Kodak X omat AR films at –80°C for 2-4 days.

2.4.5 Nonreducing Two-Dimensional (2D) Electrophoresis

The method uses two protein properties (native net charge and mass) in two discrete steps to achieve better separation of target protein(s). During the so called „first dimension“ or „isoelectric focusing“ (IEF), the proteins migrate in an electric field through ampholyte containing gel strips with defined pH gradient, driven by their positive or negative net charge towards the cathode or anode, respectively. The protein migration stops when the isoelectric point (pI) is reached. After IEF, the strips are subjected to discontinuous SDS-PAGE (second dimension), where the isoelectrically focused proteins are resolved according to their molecular weight.

Materials and equipment for the first dimension

Multiphor II Electrophoresis unit with Immobiline DryStrip Kit, Ready-made Immobilized pH Gradient (IPG) strips (11 cm, with 3-10 (linear) and 6-11 (linear) pH gradient), IPG buffer with pH range identical to that of the IPG strip, were purchased from Amersham PharmaciaBiotech.

Rehydration buffer	8 M urea, 2% (w/v) Chaps, 0.5% (v/v) IPG buffer, trace of bromphenol blue
SDS equilibration buffer	50 mM Tris/HCl pH 8.8, 6 M urea, 30% (v/v) glycerol, 2% (w/v) SDS, trace of bromphenol blue

Depending on the aim, broad (pH 3-10) or narrow (pH 6-11) range IPG strips were used. The strips were rehydrated in 200 µl of rehydration buffer at room temperature for 16 h. Samples were dissolved in 100 µl rehydration buffer as well, and applied on the IPG gel. The isoelectric focusing was run at 20° C with 18 100 Volt-hours (200 V x 30 min, 3000 V x 6 h), followed by equilibration (room temperature, 30 min) of the IPG strips in equilibration buffer. The strips were then subjected to SDS-PAGE.

2.4.6 Iodination of IGFBPs

IGFBPs were labeled with [^{125}I] according to the method of Parker et al. (1983) which is based on oxydation of the hydroxy group in tyrosine residues by [^{125}I]-NaI substituting the hydrogene atom against [^{125}I], in the presence of the catalyser 1,3,4,6-tetrachloro-3α,6α-diphenylglycouril (Iodo-Gen, Pierce, Rockford, IL).

Borate buffer	20 mM H_3BO_3, pH 8.0
Elution buffer	10 mM PBS, 0.1% KI (w/v), 0.05% (w/v) BSA
Iodo-Gen solution	1 mM Iodo-Gen in dichloromethane

Eighty microliters of Iodo-Gen solution was pipetted into a conical glass tube, and the solvent dichloromethane was evaporated under a stream of N_2. The coated tubes can be stored at -20°C for 2 months. One hundred and fifty µCi [^{125}I]-NaI were added to 0.25-1 µg protein dissolved in borate buffer. After incubation on ice for 2 min the mixture was transferred to the Iodo-Gen-covered glass tube under constant rotation in an ice/water bath for 8 min. The reaction was stopped by transfer of the reaction mixture to a new glass tube. The Iodo-Gen glass tube was rinsed with 140 µl borate buffer. The buffer was applied together with the reaction mixture onto a preequilibrated PD-10 Sephadex G-25 column (Amersham Pharmacia Biotech). Four milliliters elution buffer were added and fractions of 500 µl were collected. The iodinated proteins were typically eluted in fraction 5-8.

2.4.7 IGFBP protease assay

[^{125}I]-labeled IGFBPs were used as substrates for determining the IGFBP-proteolytic activity in different samples (conditioned media or purified IGFBP-protease containing fractions).

Fifty microliters of conditioned media or 5-40 µl of column fractions dialyzed against 20 mM Tris/HCl, pH 7.4, containing 10 mM NaCl were incubated with [^{125}I]-IGFBPs (5,000–10,000 cpm) at 37°C for 6-18 hours. When indicated, protein inhibitors were included. After solubilization, the samples were subjected to SDS-PAGE (12.5% acrylamide) and visualized by autoradiography as described (2.4.8.1) or by phosphorimaging (2.4.8.2). To examine the IGFBP-6 proteolysis in the presence of cells, MDCK cells grown on 24 well tissue plates were preincubated in a serum-free medium containing 0.05% BSA for 2 h at 37°C. Thereafter the medium was replaced by serum-free medium containing [^{125}I]-IGFBP-6 (65,000 cpm/ml) for 24 h at 37°C. At the end of the incubation 0.09 ml aliquots of the medium were analyzed by SDS-PAGE and autoradiography or by trichloroacetic acid precipitation (2.4.13).

2.4.8 Visualization of radioactively labeled proteins after SDS-PAGE

2.4.8.1 Autoradiography

After SDS-PAGE of [^{125}I]-labeled proteins, the gel was shortly washed in ddH_2O and dried as described earlier. Two Kodak X-Omat AR films were exposed on the gel between Cornex intesifying screens (Cornex Lightning Plus, Dupont) in a film cassette at –70°C.

2.4.8.2 Phosphoimaging

Dried gels were exposed to phosphoimaging screens (Cyclone Storage Phosphor Screens, Packard, Meriden, CT) at room temperature and images were developed by means of Cyclone™ Storage Phosphor System (Packard, Meriden, CT).

2.4.8.3 Fluorography of [^{3}H]-, [^{33}P]-, and [^{35}S]- labeled proteins

In order to enhance the β-radioactive signal emitted by [^{3}H]-, [^{33}P]-, and [^{35}S]-isotops, the SDS-gels were dehydrated in DMSO (3x 20 min) and incubated in 20% (w/v) PPO (2,5-

diphenyloxazole, Roth, Germany) in DMSO for 3-16 h at room temperature (Laskey and Mills, 1975). After rehydration the gels were dried and the labeled protein bands were visualized as described above (2.4.8.1).

2.4.9 Immunoprecipitation

For immunoprecipitation of mIGFBP-6, conditioned medium from MDCK cells overexpressing mIGFBP-6 was collected and centrifuged (1000 rpm for 10 min at 4°C) to remove cell debris. Six milligrams of Protein-A immobilized on agarose (Sigma) were preswelled and extensively washed with PBS. In order to decrease unspecific binding, 10 µg rabbit IgG were mixed with Protein-A, 1 ml conditioned medium, 0.5% (v/v) Triton X-100, and protease-inhibitor cocktail (Sigma). The mixture was incubated on a rotating wheel for 1 h. After centrifugation the supernatant was transferred into a vial containing 10 µg goat anti-mouse IGFBP-6 antibody (Santa Cruz Biotechnology, Inc.) bound to Protein-A agarose. The formation of immunocomplexes occurred for 4 h at 4°C. After centrifugation the resulting pellet was extensively washed with PBS / 0.1% Triton X-100, boiled for 5 min at 95°C in sample buffer, centrifuged, and the supernatant was subjected to SDS-PAGE.

2.4.10 Deglycosylation

Overexpressing mIGFBP-6 subconfluent MDCK cells grown on 35 mm petri dishes were metabolically labeled for 20 h with [^{35}S]-methionine as described previously (2.2.2.1) and immunoprecipitation of mIGFBP-6 was carried out (2.4.9). The resulting pellets were subjected to chemical or enzymatic deglycosylation.

2.4.10.1 Chemical deglycosylation of O-linked oligosaccharides

(according to Edge et al., 1981)

The immunoprecipitated mIGFBP-6 was eluted by boiling for 5 min at 95°C in 200 µl 4-fold concentrated solubilizer without reducing agents. The proteins in the supernatant were precipitated by the addition of 600 µl ice-cold acetone for 6 h at –20°C. After

centrifugation for 15 min at 14,000 rpm the resulting pellet was air-dried and dissolved in 30 µl precooled mixture of TFMS (Sigma) and anisole (Fluka) (2:1, v/v). The vial was capped after bubbling N_2 through the solution and left for 2.5 h at 0°C. The reaction was terminated by addition of 125 µl of pyridine/water (4:1, v/v) in 10 µl portions. During this treatment the vial was immersed in a slurry of acetone/dry ice. The solution was precipitated with 3 volumes of ice-cold acetone and washed twice with acetone. The resulting pellet was boiled for 5 min at 95°C in solubilizer and subjected to SDS-PAGE under nonreducing conditions.

2.4.10.2 Enzymatic deglycosylation of O-linked oligosaccharides

mIGFBP-6 was eluted from the Protein-A complexes pellet by boiling for 5 min at 95°C in 220 µl 4-fold concentrated solubilizer without reducing agents. The supernatant was split into two equal parts, and to each 100 mU neuraminidase (Sigma) were added. After incubation for 1.5 h at 37°C the samples were boiled again for 1 min at 100°C and chilled on ice. To one of the test vials 16 mU O-glycanase (Oxford Glycosystems Inc., UK) were added, followed by incubation for 3 h at 37°C. The enzyme was inactivated by boiling for 5 min at 95°C and the samples were analyzed by SDS-PAGE and fluorography (2.4.8.3).

2.4.11 Purification of IGFBP-6 protease

IGFBP-6 protease was partially purified from 300 ml of 48 h conditioned medium from MDCK cells grown in 250 ml tissue culture flasks (Greiner, Germany).

2.4.11.1 Ammonium sulfate protein precipitation

Proteins in the MDCK conditioned medium were subsequently precipitated by 30 and 45% ammonium sulfate. The respective amount of ammonium sulfate was slowly added to the medium under stirring and the mixture was further stirred for 16 h at 4°C. After centrifugation for 30 min at 10,000 rpm (JA-10 rotor), the precipitates were dissolved in 3 ml TBS.

2.4.11.2 Gel chromatography

The solved ammonium sulfate precipitates were desalted by means of Sephadex G25 column (Amersham Pharmacia Biotech, 1.0 x 35 cm) preequilibrated in TBS. Proteins were eluted with TBS at a constant flow rate of 0.8 ml/min, and collected in 2 ml fractions. Protein concentration was measured at λ=280 nm and 50 µl aliquots were tested for IGFBP-6 protease activity.

2.4.11.3 DEAE anion-exchange chromatography

IGFBP-6 protease containing fractions were pooled and loaded onto a 2 ml DEAE-Sephadex column equilibrated with TBS. The column was washed with the same buffer (1 ml/min) until absorbance (280 nm) had return to the base line. Bound proteins were eluted by a stepwise gradient of 0.1, 0.25, 0.5, 0.75 and 1.0 M NaCl in 20 mM Tris buffer pH 7.5. One-milliliter fractions were collected, dialyzed against TBS and tested for IGFBP-6 protease activity. Protease-containing fractions were pooled (fraction 7 and 8 to pool I and fractions 13-15 to pool III), as well as the inactive fractions (fraction 9-12 to pool II). The pools were dialyzed against 50 mM Tris buffer, pH 7.4.

2.4.11.4 Hydroxyapatite ion-exchange cromatography

Pool fractions I, II, and III of the DEAE-eluates were applied to a hydroxyapatite column (Amersham Pharmacia Biotech; 1.0 x 1.0 cm), washed with 50 mM Tris buffer, pH 7.4 and bound proteins were eluted with a two-step gradient of 3 ml of 150 and 300 mM KP_i in 50 mM Tris buffer pH 7.4. Fractions of 1 ml were collected, dialyzed against TBS and tested for IGFBP-6 protease activity.

2.4.12 Acetone precipitation

Proteins were precipitated in ice-cold acetone (1:3 v/v) for 16 h at –20°C, centrifuged for 10 min at 14,000 rpm, and the pellet was air-dried.

2.4.13 Trichloroacetic acid (TCA) precipitation

TCA precipitation was used to estimate the amount of radioactivity incorporated into proteins. Five or 10 µl of labeled conditioned medium were incubated in 0.5 ml 10% (w/v) TCA on ice for at least 1 h. After centrifugation for 10 min at 14,000 rpm, the supernatant was aspirated and the pellet was subsequently washed with 0.5 ml of 5% (w/v) TCA, ddH_2O, and 96% ethanol. After drying the [^{3}H]-, [^{33}P]-, or [^{35}S]- containing protein pellets were solubilized in 50 µl 1 N NaOH at 95°C for 5 min. The solution was cooled down on ice and neutralized with 50 µl of 1 M HCl. After transfer into scintillation vials and addition of 5 ml scintillation solution (Roth), the samples were measured in a β-counter (LS 1800, Beckman Coulter, Inc.).

To determine the degradation rate of [^{125}I]-labeled proteins, aliquots of media were mixed with TCA (final concentration 10%), incubated for at least 1 h on ice, and after centrifugation and washing the pellets with 5% TCA, the radioactivity in the pellets was counted directly in a γ-counter (1470 Wizard, Wallac, Finnland).

2.4.14 Protein measurement

(according to Lowry et al., 1951)

The method is based on formation of a cupper-protein complex that is subsequently oxydized by Folin reagent.

Solution A	100:1:1 of 3% (w/v) Na_2CO_3 in 0.1 N NaOH,
	4% (w/v) K-Na-tartrat x 4 H_2O, 2% (w/v) $CuSO_4$ x 5 H_20
Solution B	1:2 of 33% (v/v) Folin reagent (Merck), ddH_2O

Both solutions were freshly prepared. As a protein standard, 2-20 µl of 1 mg/ml BSA solution (Pierce, Rockford, Illinois) was used. The samples were filled up to 100 µl with ddH_2O, followed by addition of 1 ml solution A. After an incubation of 10 min at room temperature, 100 µl of solution B was added, vortexed, and left at room temperature for 10 min. The absorbance of the samples was measured at λ=600 nm.

3 AIMS OF THE PRESENT STUDY

IGFs, IGFBPs, and IGF receptors have been reported to contribute to processes of cell proliferation and differentiation of epithelial cells. Prerequisite for the constitution of an epithelial permeability barrier are highly polarized cells characterized by morphologically, functionally and biochemically distinct apical and basolateral plasma membranes. Because little is known about the role of the different members of the IGF-system for the maintainance of epithelial cell properties, first aim of the present work was to examine and characterize secreted IGFBPs and IGFBP-proteases using as a model Madin-Darby canine kidney (MDCK) cell line.

The second goal of the work was to investigate the sorting mechanism of IGFBPs in polarized cells. Because it is proposed that O-linked carbohydrate chains function as signal structures for apical sorting, IGFBP-6 mutants were generated, lacking putative O-glycosylation sites, followed by stable expression and analysis of their polarized distribution in MDCK cells.

Finally, the complex 2D-gel electrophoretic pattern of IGFBP-6 served as a basis to find and characterize additional posttranslational modifications, which might contribute to specific biological functions of IGFBP-6.

4 RESULTS

4.1 Sorting and proteolysis of IGFBPs in polarized MDCK cells

4.1.1 Sorting of IGFBPs

To examine whether IGFBPs are secreted in a polarized manner from MDCK cells, conditioned media from cells grown on permeable polycarbonate filters were collected after 24 and 48 h. [^{125}I]-IGF II ligand blotting revealed the presence of three 35, 28, and 25 kDa IGFBP bands in apical (lane 1 and 3) and basolateral (lane 2 and 4) media (Figure 2). Densitometric evaluation showed that the total amount of IGFBPs secreted to the apical side is 4.2-fold higher than that to the basolateral side.

In order to determine the identity of the IGFBPs secreted by MDCK cells, Western immunoblotting and Northern blotting were carried out. Because no anti-canine IGFBP antibodies are available, immunoblotting was performed with primary antibodies directed against human IGFBP-1, -4, -5, and –6, bovine IGFBP-2, and mouse IGFBP-6. IGFBP-3 was excluded due to its molecular mass of 43/45 kDa. For Northern blotting, specific cDNA probes for human IGFBP-1 to –6 were used for hybridization. Neither any of the antibodies tested nor the used cDNA probes cross-reacted or hybridized, respectively, with MDCK-material (not shown).

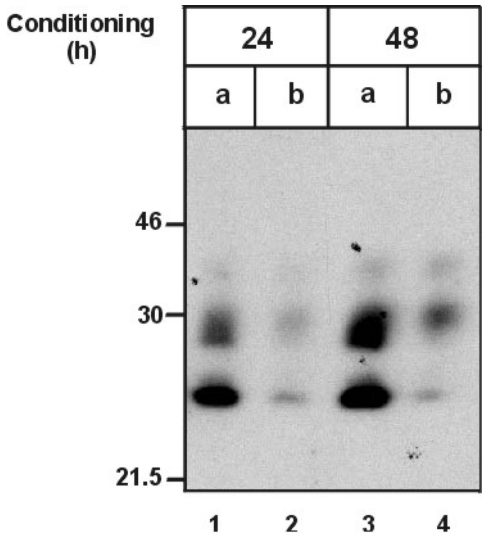

Figure 2: Polarized secretion of endogenous IGFBPs in MDCK cells

Conditioned media from filter-grown MDCK cells were collected after 24 and 48 h from the apical (lane 1 and 3) or basolateral side (lane 2 and 4) and analyzed by SDS-PAGE (12.5% acrylamide), [^{125}I]-IGF II ligand blot and autoradiography. The positions of molecular mass marker proteins (in kDa) are indicated on left.

4.1.2 Proteolysis of IGFBPs by conditioned media from MDCK cells

In order to determine if the apical abundance of IGFBPs is a result of preferential apical targeting of the IGFBPs or is due to degradation of IGFBPs in the basolateral side, conditioned medium from MDCK cells grown on plastic dishes was tested for proteolytic activity against [^{125}I]-labeled recombinant human IGFBP-1 to –6 at neutral pH (Figure 3). The results show no fragmentation of IGFBP-1 within a 6 h incubation, whereas after 12 h [^{125}I]-IGFBP-2 was cleaved into two fragments of 24 and 13.5 kDa; the 30 kDa non-glycosylated [^{125}I]-IGFBP-3 was cleaved into four fragments of 25, 21, 15 and approximately 8.5 kDa; [^{125}I]-IGFBP-4 was fragmented to 17 and 10 kDa products, and [^{125}I]-IGFBP-6 was almost completely hydrolyzed depending on the incubation time with a transient appearance of 24, 17, 10 and 6 kDa IGFBP-6 fragments. [^{125}I]-IGFBP-5 was cleaved to a 22 kDa doublet, 16, and 8 kDa peptide fragments after a 6 h incubation. When the unrelated 62 kDa [^{125}I]-ASA was incubated with conditioned MDCK medium for 14 h at 37°C under identical conditions as for [^{125}I]-IGFBP-3, no ASA proteolysis products were detected (not shown), indicating the specificity of the IGFBP protease(s) secreted by MDCK cells .

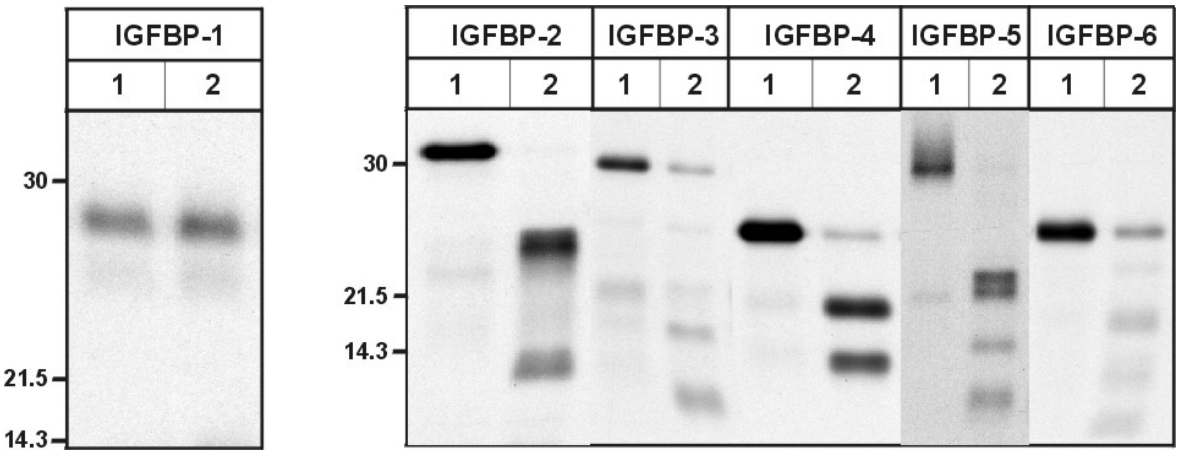

Figure 3: Proteolysis of IGFBPs by conditioned media from MDCK cells

[^{125}I] labeled IGFBP-1 to –6 were incubated with 50 µl nonconditioned (1) or conditioned (72 h) media from MDCK cells (2) at 37°C and pH 7.4 for 6 h (IGFBP-1 and -5) or 12 h (IGFBP-2, -3, -4, and –6). Samples were analyzed by SDS-PAGE and autoradiography.

As mentioned earlier (1.1.4), proteolysis of IGFBP-6 has only been demonstrated for acid-activated proteases. Because this is a first description of IGFBP-6 proteolysis at neutral pH in media from cultured cells, further studies were carried out to identify and characterize the unique neutral IGFBP-6 protease.

4.1.3 Polarized secretion of IGFBP proteases

Apical and basolateral conditioned media from MDCK cells grown on polycarbonate filters were tested for the presence of proteolytic activity against [^{125}I]-IGFBP-4 and –6 at neutral pH. Figure 4 shows that after an 8 h incubation at 37°C, the degradation of both [^{125}I]-IGFBP-4 and –6 was approximately four-fold higher in the basolateral than in the apical media, as estimated by densitometry of the formed fragments. In contrast, when β-hexosaminidase activity was determined as a control, a 2.6-fold (range 2.3 to 3.1, n=6) higher activity was measured in the apical than in the basolateral medium. The results indicate preferential basolateral sorting of the IGFBP-4 and IGFBP–6 proteases in MDCK cells.

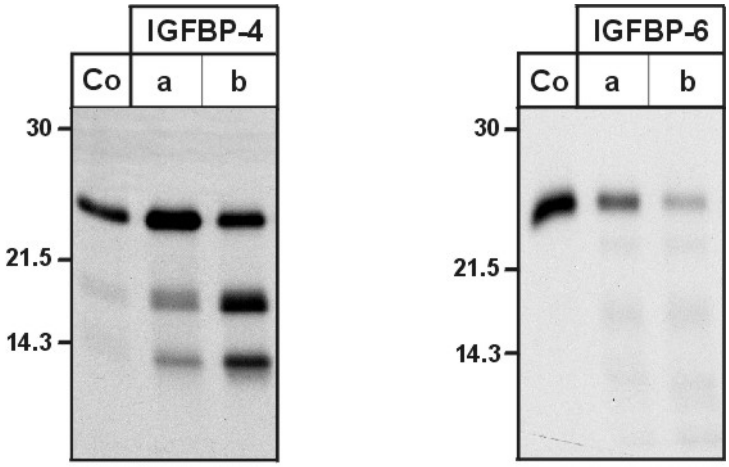

Figure 4: Polarized secretion of IGFBP proteases

Media were collected from the apical (a) or basolateral (b) side of filter grown MDCK cells conditioned for 24 h. Aliquots of the media (50 µl) were tested for protease activity against [^{125}I]–IGFBP-4, and [^{125}I]–IGFBP-6 for 8 h at neutral pH, followed by SDS-PAGE and autoradiography. As a control (Co), [^{125}I]–IGFBP-4 or -6 were incubated in nonconditioned medium under identical conditions. The autoradiograms of one representative experiment out of three are shown. The aliquots contain 12.2 (a) and 4.9 mU/ml (b) β hexosaminidase activity secreted within 24 h.

4.1.4 Proteolysis of IGFBP-6 in conditioned media from kidney cell lines

Different kidney cell lines, MDCK (dog kidney distal tubule/collecting duct cells), MDBK (bovine kidney distal tubule cells), and BHK (Baby hamster kidney fibroblasts) were compared for their ability to cleave IGFBP-6. For this purpose, 48 h conditioned media from cells grown on plastic dishes were incubated for 12 h with [^{125}I]-IGFBP-6 at neutral pH (Figure 5). As the results show, [^{125}I]-IGFBP-6 was cleaved in media from MDCK and MDBK cells into three transient fragments of approximately 24, 17, and 10 kDa. In contrast, the medium from BHK fibroblasts showed only a weak proteolytic activity, resulting in the formation of a 17 kDa IGFBP-6 fragment.

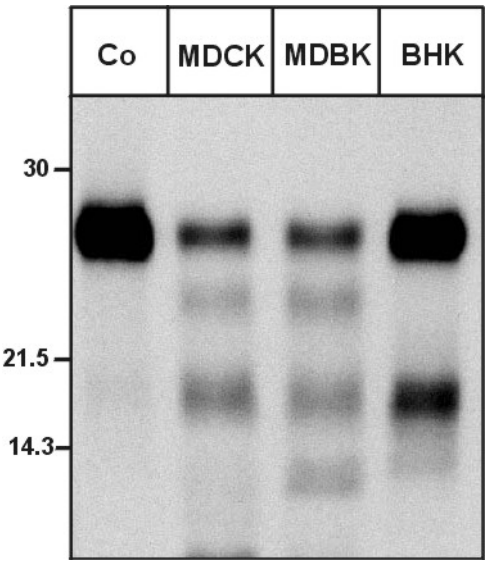

Figure 5: Proteolysis of [^{125}I]-IGFBP-6 in conditioned media from kidney cell lines

Conditioned media from MDCK, MDBK, and BHK cells grown on plastic dishes were collected after 48 h. Nonconditioned (Co) or conditioned media (50 µl) were incubated for 12 h at 37°C and pH 7.4 with 10,000 cpm [^{125}I]-IGFBP-6. Proteolytic fragments were detected by 12.5 % SDS-PAGE and autoradiography.

4.1.5 Effect of IGF II on proteolysis of IGFBPs

Claussen et al. (1995) have described inhibition of acid-activated proteolysis of IGFBP-6 by IGF II. The effect of 50 nM IGF II on the neutral proteolysis of IGFBP-6 in the presence of MDCK cells was examined (Figure 6). For comparison, the effects of IGF II on the proteolysis of IGFBP-4 were investigated. For this purpose, MDCK cells grown on 35 mm dishes were conditioned for 24 h with or without 50 nM IGF II. [^{125}I]-IGFBP-6 or [^{125}I]-IGFBP-4 were added to the cell media and incubated for 24 h at 37°C. The results show that IGF II did not affect the cleavage of [^{125}I]-IGFBP-4 into two fragments of 17 and 10 kDa. [^{125}I]-IGFBP-6 was completely degraded in the absence of IGF II. In the presence of MDCK cells, however, IGF II inhibited the proteolysis of [^{125}I]-IGFBP-6 by 49% as determined by the densitometric evaluation of the remaining intact IGFBP-6.

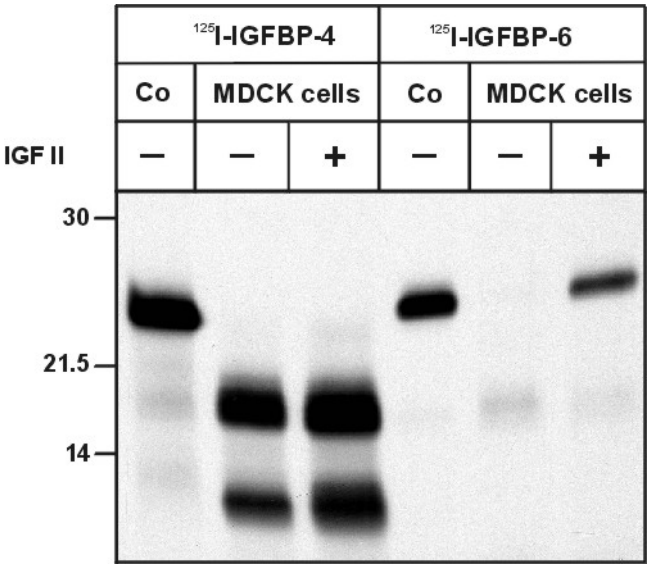

Figure 6: Effect of IGF II on proteolysis of [^{125}I]-IGFBP-4 and –6 by MDCK cells

MDCK cells grown on 35 mm plastic dishes were conditioned for 24 h at 37°C in the presence or absence of 50 nM IGF II. [^{125}I]-IGFBP-4 or –6 (100,000 cpm) was added to the media and incubated for 24 h at 37°C. Control (Co) represented 12,000 cpm of the respective [^{125}I]-IGFBP incubated on ice for 24 h in cell-free medium. Proteolytic fragments were resolved on a 12.5 % SDS-PAGE and visualized by autoradiography.

The inhibitory effect of IGF II on IGFBP-6 proteolysis by MDCK cells demonstrated in Figure 6 could be explained either by i) IGF II stimulated release of an unknown inhibitor, ii) IGF-induced reduction in IGFBP-6 protease secretion, iii) protection and stabilization of IGFBP-6 via binding to IGF II, or iv) direct inhibition of the IGFBP-6 protease by IGF II.

To determine whether the effect of IGF II on IGFBP-6 proteolysis is cell-mediated, [^{125}I]-IGFBP-6 and 50 nM IGF II were coincubated in 50 µl conditioned medium for 8 h at 37°C and neutral pH. For comparison, the effect of IGF II on [^{125}I]-IGFBP-4, and [^{125}I]-IGFBP-5 proteolysis was tested under identical conditions. Figure 7 shows that [^{125}I]-IGFBP-4 was cleaved into two fragments of 10 and 17 kDa. [^{125}I]-IGFBP-5 was hydrolyzed into a 22 kDa doublet, and two fragments of 16 and 8 kDa. [^{125}I]-IGFBP-6 was degraded into four fragments of 24, 17, 10, and 6 kDa. IGF II had no effect on the proteolysis of [^{125}I]-IGFBP-4, and –5, whereas it inhibited the degradation of [^{125}I]-IGFBP-6. The results suggest that IGF II protects IGFBP-6 fragmentation directly and not by regulation of secretion of inhibitors or proteases.

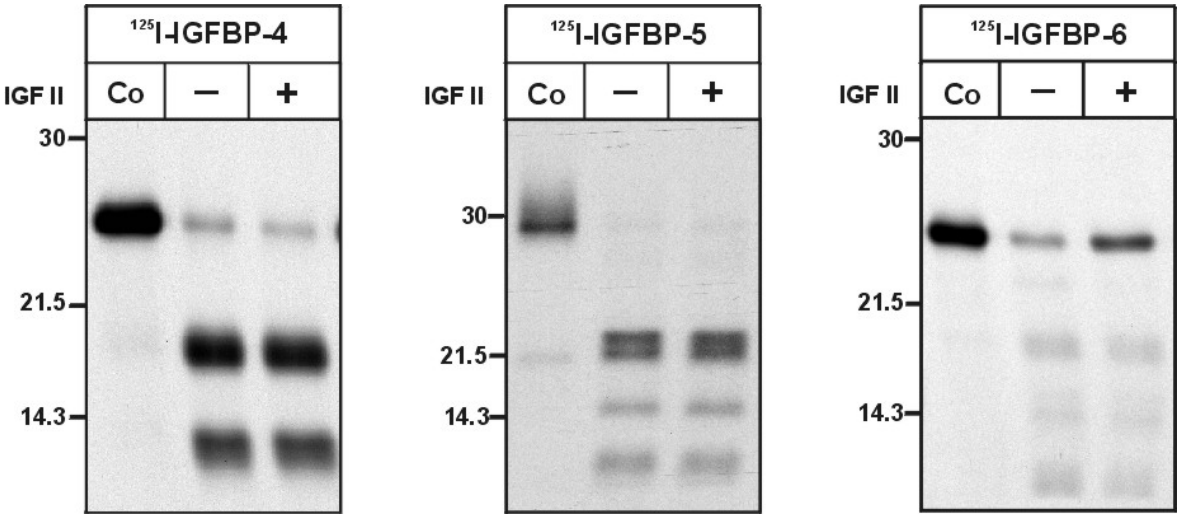

Figure 7: Effect of IGF II on the proteolysis of IGFBP-4, -5, and -6 in conditioned media from MDCK cells

[^{125}I] labeled IGFBP-4, -5 and -6 were incubated with 50 µl nonconditioned (Co) or conditioned media (48 h) for 8 h at 37°C at neutral pH. The aliquots of conditioned media were incubated with [^{125}I]–IGFBPs in the presence (+) or absence (-) of 50 nM IGF II followed by 12.5% SDS-PAGE and autoradiography.

4.1.6 Affinity of IGFBP-6 fragments for IGF II

Depending on time, IGFBP-6 was degraded in conditioned medium by MDCK cells completely with formation of transient fragments (Figure 7). To examine the ability of these fragments to bind IGF II, rhIGFBP-6 (0.2 µg) produced in mammalian cells (not specified by the company producer Gropep, Australia) was incubated in conditioned medium from MDCK cells for 0, 5, 10, and 25 h at 37°C and neutral pH. Each sample was divided into two parts which were subsequently analyzed by immunoblotting using anti-human IGFBP-6 antibody or [^{125}I]-IGFII ligand blotting (Figure 8). In SDS-PAGE the rhIGFBP-6 produced in mammalian cells showed an electrophoretic mobility of approximately 29 kDa, whereas the rhIGFBP-6 produced in yeast and used for the [^{125}I]-protease assays migrated at 26 kDa. The results shown in Figure 8 demonstrate almost a complete degradation of the intact IGFBP-6 after 25 h. The anti-human IGFBP-6 antibody detected one major and three minor IGFBP-6 fragments of approximately 28, 24, 22, and 21.5 kDa. [^{125}I]-IGFII, however, bound only to the intact IGFBP-6.

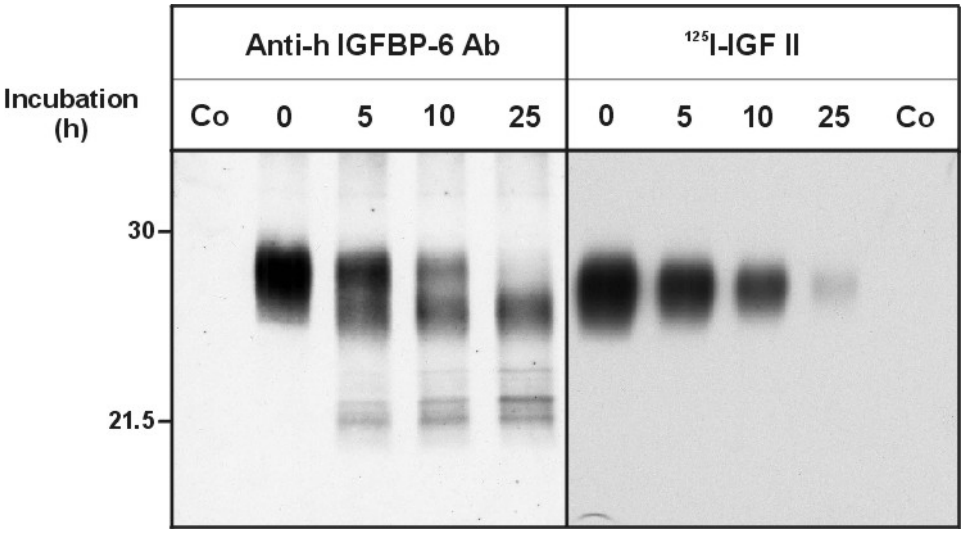

Figure 8: Affinity of IGFBP-6 fragments for IGF II

Glycosylated rhIGFBP-6 (0.2 µg) was incubated in 80 µl conditioned medium (48 h) from MDCK at 37°C and neutral pH for 0, 5, 10 or 25 h. Control (Co) indicates conditioned medium without addition of IGFBP-6. The samples were analyzed by 12.5% SDS-PAGE and immunoblot with anti-human IGFBP-6 antibody or [^{125}I]-IGF II ligand blotting.

4.1.7 Inhibitors of IGFBP –6 proteolysis

To characterize in more detail the neutral IGFBP-6 protease secreted by MDCK cells, cell-free conditioned media were supplememted with [^{125}I]-IGFBP-6 (200,000-360,000 cpm/ml), and aliquots of 25 µl were incubated in the presence or absence of protease inhibitors. For comparison, the effect of the inhibitors on [^{125}I]-IGFBP-5 proteolysis was tested under identical conditions (Figure 9). The proteolysis of [^{125}I]-IGFBP-6 was almost completely inhibited by the metalloprotease inhibitors 1,10 phenanthroline (10 mM) and TAPI (TNF-α protease inhibitor; a specific disintegrin metalloprotease inhibitor, 0.1 mM), whereas the serine protease inhibitor DCI (3,4-dichloroisocoumarin, 0.2 mM) affected weakly the proteolytic activity. In contrast, TAPI and aprotinin (serine protease inhibitor, 0.3 µM) completely inhibited the formation of the 8 kDa IGFBP-5 fragment resulting in accumulation of the 16 kDa fragment. The proteolysis of the intact IGFBP-5 and of the 23 kDa IGFBP-5 fragment was not affected by the inhibitors at the concentrations used. These results indicate that i) in conditioned media from MDCK cells at least two different proteases, a metalloprotease, and a serine protease, are involved in the degradation of IGFBP-6, and ii) distinct proteases are involved in the proteolysis of IGFBP-5 and -6.

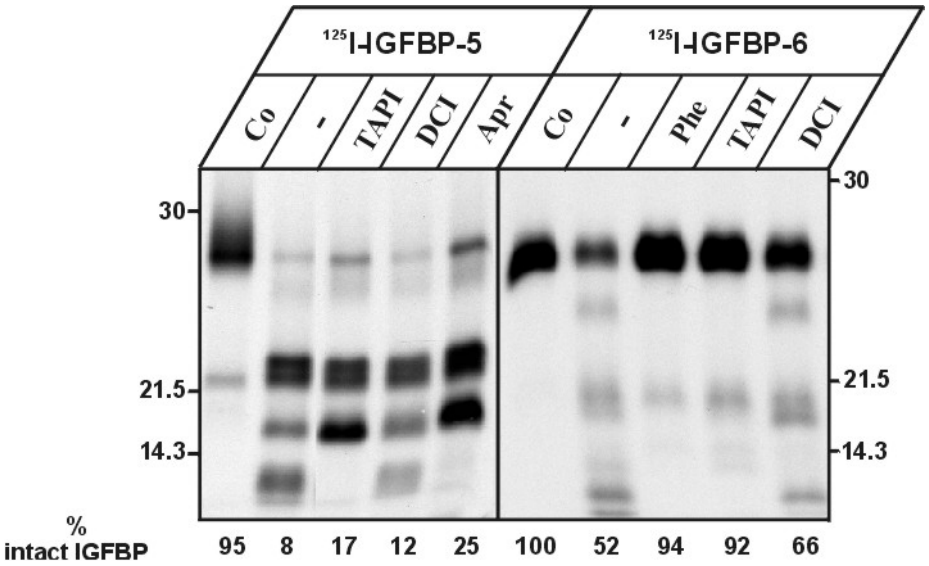

Figure 9: Effects of protease inhibitors on IGFBP-5, and -6 protease activity in MDCK medium

Aliquots of 48 h conditioned MDCK cell medium (25 µl) were incubated with [^{125}I]–IGFBP-5 or -6 (5,000 – 9,000 cpm) in the absence of inhibitors (-) for 10 h at 37°C. Equal amounts of radioactivity in each aliquot were confirmed by γ-counting. 1,10 Phenanthroline (Phe 10 mM), TAPI (0.1 mM), 3,4 dichloroisocoumarin (DCI; 0.2 mM) or aprotinin (Apr; 0.3 µM) were added as indicated. The reaction products were separated by SDS-PAGE and visualized by autoradiography. As controls (Co), [^{125}I]-IGFBP-5 or -6 were incubated in nonconditioned medium under identical conditions. The percentage of intact IGFBP-5 or –6 after the incubation determined by densitometry is listed below each lane.

4.1.8 Partial purification of IGFBP-6 proteases

In order to identify the IGFBP-6 proteases secreted by MDCK cells, 300 ml MDCK conditioned medium were subjected to a two-step (30 and 45%) ammonium sulfate precipitation. The resulting protein pellets were resolved and subjected to gel filtration. The collected fractions were tested for the presence of IGFBP-6 proteolytic activity. Degradation of [^{125}I]-IGFBP-6 was observed only in fractions 4 to 7 of the 45% ammonium sulfate precipitate. The active fractions were pooled and applied onto DEAE-Sephadex column. IGFBP-6 protease activity was detected in fractions eluted with 0.5 M NaCl (fraction 7 and 8) and with 1 M NaCl (fraction 13-15) (Figure 10 A). The active fractions were pooled (pool I and III, respectively) as well as the inactive fractions 9-12 (pool II) and each pool was applied separately to a hydroxyapatite column. The eluted fractions were dialyzed against TBS in a semi-permeable membranes with 6 kDa cut-off, and were tested for presence of [^{125}I]-IGFBP-6 proteolytic activity (Figure 10 B). No proteolytic activity was found in the flow through and in fractions of pool I. Strong IGFBP-6 proteolytic activity was found in fractions of pool III eluted at 150 mM KP_i (III-1) but not at 300 mM KP_i (III-2). When the IGFBP-6 proteolytic activity of fraction III-1 was estimated in the presence or absence of protease inhibitors, it was neither inhibited by phenanthroline nor by TAPI, but almost completely abolished by the serine protease inhibitors DCI and aprotinin (Figure 10 C).

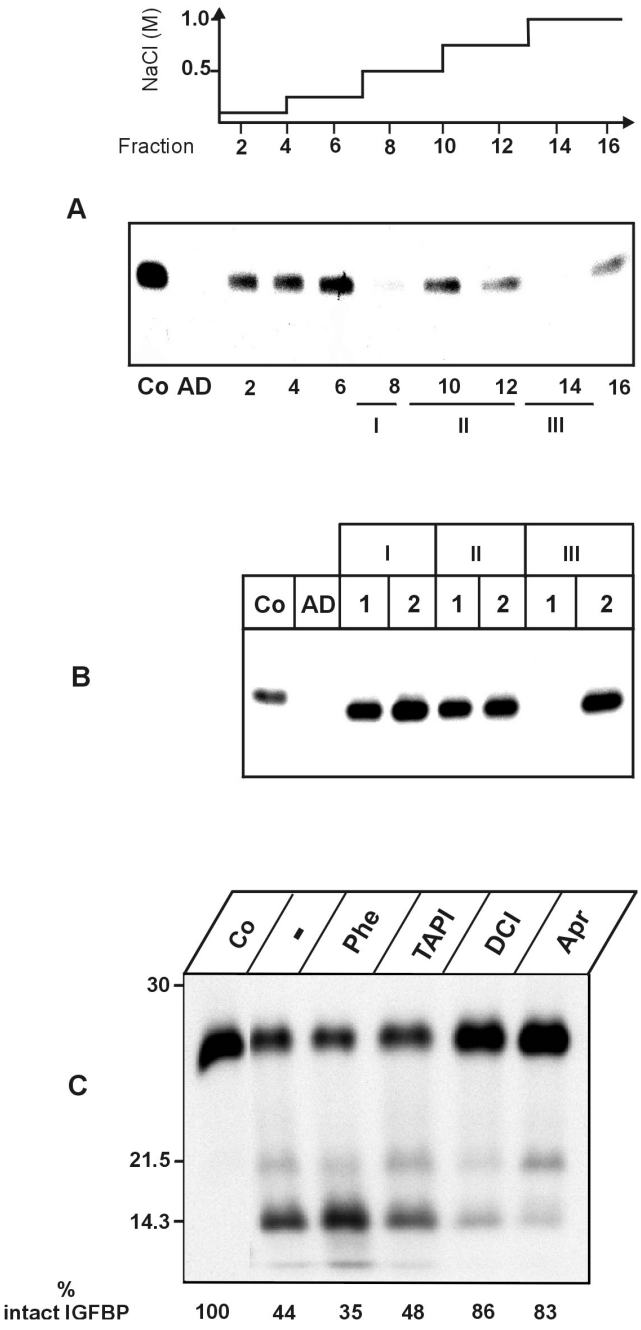

Figure 10: Partial purification of IGFBP-6 protease

A: Ammonium sulfate precipitates of conditioned medium from MDCK cells were dissolved and desalted on a gel chromatography column. Fractions (4-7 from 45% ammonium sulfate precipitate) containing IGFBP-6 proteolytic activity were pooled and applied on a DEAE-Sephadex column. Bound proteins were eluted by a stepwise NaCl-gradient (upper part). Dialyzed aliquots of every second fraction were tested for IGFBP-6 proteolytic activity followed by SDS-PAGE and autoradiography (lower part). Equal amounts of radioactivity in each aliquot were confirmed by γ-counting. Co: control incubation of [^{125}I]–IGFBP-6 with buffer in the presence of 0.1% BSA. AD: aliquots of applied sample on DEAE-Sephacel. The underlined fractions were pooled separately (pools I, II, and III).

B: After dialysis pool I, II, and III were applied separately to a hydroxyapatite column. Bound proteins were eluted at 150 mM (1) or 300 mM (2) KP_i. Dialyzed aliquots of these fractions were incubated with [^{125}I]–IGFBP-6 for 6 h at 37°C and analyzed by SDS-PAGE and autoradiography. Equal amounts of radioactivity in each aliquot were confirmed by γ-counting. Co: control incubation of [^{125}I]–IGFBP-6 with buffer without the presence of BSA. AD: aliquots of applied sample on DEAE-Sephadex.

C: Aliquots of the partially purified fraction III-1 eluted from hydroxyapatite column were incubated with [^{125}I]-IGFBP-6 for 8 h at 37 C in the presence or absence (-) of 1,10 phenanthroline (Phe; 10 mM), TAPI (0.1 mM), 3,4 dichloroisocoumarin (DCI; 0.2 mM), or aprotinin (Apr; 0.3 μM). The reaction products were separated by SDS-PAGE and visualized by phosphorimaging. Densitometric evaluation revealed the percentage of remaining intact IGFBP-6 given below each lane.

4.1.9 Characterization of IGFBP-6 disintegrin metalloprotease

The discrepancy between [^{125}I]-IGFBP-6 proteolytic activity in media from MDCK cells inhibited by serine and metalloprotease inhibitors (Figure 9), and the recovery of an IGFBP-6 protease in fraction III-1 inhibited only by serine protease inhibitors (Figure 10 C), suggests that pool I contains the IGFBP-6 metalloprotease activity. After chromatographic separation of pool I on a hydroxyapatite column, however, no IGFBP-6 protease activity was detected in the eluted fractions I-1 and I-2 (Figure 10 B). To determine whether the loss of proteolytic activity was due to the loss of required divalent cations, aliquots of fraction I-1 were supplemented with different concentrations of divalent cations, and their ability to degrade [^{125}I]-IGFBP-6 was tested. Figure 11 shows that 50 µM manganese (Mn^{2+}) and 1 mM calcium (Ca^{2+}) were able to recover the IGFBP-6 proteolytic activity of fraction I-1. These data indicate that the fraction I-1 contains a cation-dependent IGFBP-6 protease activity, which was deactivated by hydroxyapatite chromatography and/or the subsequent dialysis.

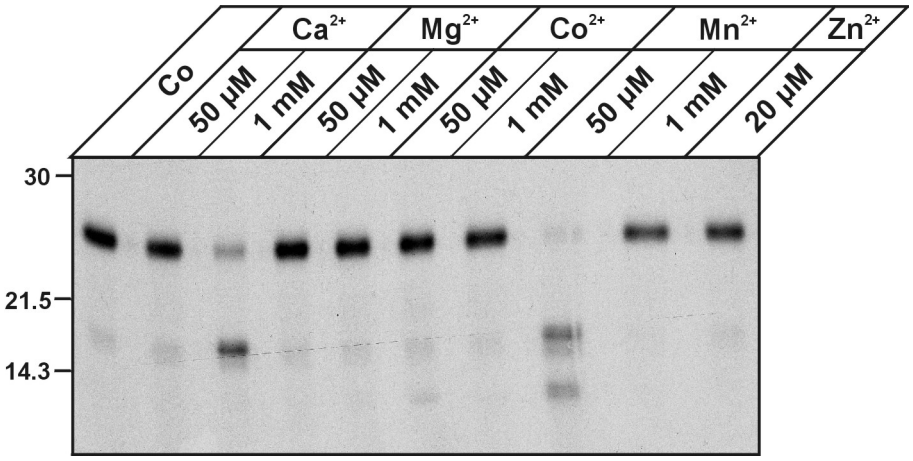

Figure 11: Retrieving of IGFBP-6 proteolytic activity of fraction I-1 by divalent cations

To 125 µl of fraction I-1, 50,000 cpm [^{125}I]-IGFBP-6 were added. Aliquots of 12.5 µl were incubated in the presence or absence (Co) of 50 µM or 1 mM $CaCl_2$, $MgCl_2$, $CoCl_2$, $MnCl_2$, or 20 µM $ZnCl_2$ for 6 h at 37°C. Equal amounts of radioactivity in each aliquot were confirmed by γ-counting. The samples were analyzed by SDS-PAGE and autoradiography.

Because the IGFBP-6 protease activity in conditioned media was inhibited by the disintegrin metalloprotease-specific inhibitor TAPI, the fractions eluted from the hydroxyapatite column were tested by immunoblotting with rb 119 antibody directed against the disintegrin domain of the secreted soluble form of human ADAM 12 (ADAM 12 S), a disintegrin and metalloprotease. A single immunoreactive band at 30 kDa was found exclusively in I-1 and I-2 but not in the pool III-eluted fractions (Figure 12). When the 5-fold concentrated I-1 and –2 fractions were analyzed by SDS-PAGE and silver staining, in addition to the major BSA band (deriving from the conditioned medium) several weak bands of 105, 88, 40, and 34 kDa were detected but no polypeptide of 30 kDa (not shown). In the initial fraction used for purification, a second disintegrin immunoreactive band at 35 kDa was detected.

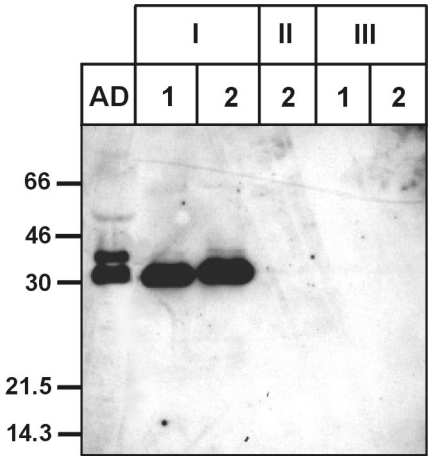

Figure 12: Anti-ADAM 12 S disintegrin immunoblotting of partially purified fractions from media of MDCK cells

Aliquots of the same fractions shown in Figure 10 B, eluted from hydroxyapatite column were solubilized under non-reducing conditions and analyzed by SDS-PAGE and anti-disintegrin immunoblotting using the rb 119 antibody. AD, aliquot of the sample applied on DEAE-Sephacel. Elution of proteins from the DEAE- or hydroxyapatite column in a second purification protocol with linear NaCl or KP_i gradients respectively, did not result in better separation of IGFBP-6 protease activities.

To examine whether the 30 kDa disintegrin immunoreactive band is a fragment of ADAM 12 S, aliquots of the fraction applied on the DEAE-column (AD) and of the pool I (Figure 10 A) were immunoblotted with antibodies against the prodomain (rb 132), the disintegrin domain (rb 119), and the cysteine-rich domain (rb 122) of human ADAM 12 S. The staining pattern of the two fractions with the three antibodies shown in Figure 13 is

partially consistent with the expected sizes of full-length ADAM-12 S (about 92 kDa) or the mature protease (about 65 kDa). All polypeptide bands of smaller molecular mass indicate the presence of truncated fragments.

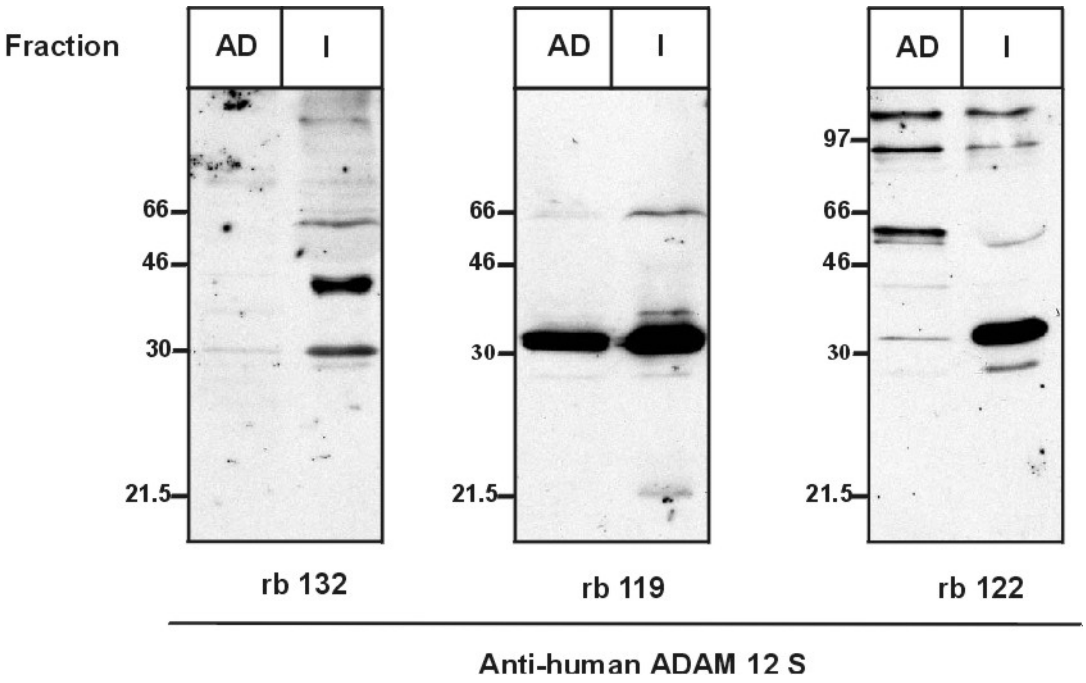

Figure 13: Immunoblot analysis of MDCK medium fractions with antibodies against different ADAM 12 S domains

Aliquots of MDCK medium applied on the DEAE-ion exchange column (AD) and of the pool I (I) were separated by SDS-PAGE under non-reducing conditions, transferred to nitrocellulose, and analyzed with antibodies against the prodomain (rb 132), the disintegrin domain (rb 119), and the cysteine-rich domain (rb 122) of ADAM 12 S. The immunoreactive polypeptides were visualized by peroxidase-conjugated secondary antibodies and ECL.

4.2 Overexpression of mouse IGFBP-6 in MDCK cells

It has been reported that IGFBP-6 is secreted from the apical side of HT29-D4 cells whereas IGFBP-2 and IGFBP-4 are directed to the basolateral side (Pommier et al., 1995). To get insight in the mechanism of preferential apical sorting of IGFBPs, MDCK cells were transfected with a mouse IGFBP-6 wild type (WT) cDNA.

After stable transfection of MDCK cells with mIGFBP-6 WT cDNA cloned into the mammalian expression vector pcDNA 3.1 + and followed by neomycin selection, none of the selected neomycin-resistant clones secreted mIGFBP-6, as proved by western or ligand blotting (not shown). Cotransfection of mIGFBP-6 cDNA, subcloned in the pBEH mammalian expression vector and pGK hygromycin resistance plasmid, and subsequent hygromycin selection yielded several cell clones which secreted similar amounts of mIGFBP-6. One of them, MDCK B1, was used in the further studies. For a control, an MDCK cell clone transfected with pGK vector alone was selected (pGK). Because no differences in the composition of IGFBPs in conditioned media from MDCK and pGK were observed (not shown), in all studies, unless indicated, nontransfected MDCK cells were used as a control. When different charges of conditioned media from MDCK B1 and pGK cells were tested for their ability to cleave [^{125}I]-IGFBP-6, surprisingly no proteolytic activity was observed (not shown).

4.2.1 [^{125}I]-IGF II vs. bIGF II Western ligand blotting

In the course of substituting [^{125}I]-IGF II by biotinylated IGF II for ligand blotting, the results revealed that bIGF II does not recognize any of the IGFBPs detected by [^{125}I]-IGF II in media from MDCK cells. Therefore, media of different cell lines expressing variable IGFBP-forms were tested in ligand blotting using [^{125}I]-IGF II or bIGF II (Figure 14). With the exception of a few IGFBPs (e.g. the 24 kDa IGFBP-4 in media from MCF7 (human breast tumor), or the 28 kDa IGFBP in media from Fao (rat hepatoma) cells) bIGF II bound to the IGFBPs in a comparable manner. However, the inability of bIGF II to bind to the canine IGFBPs proved to be an advantage for detection of heterologous IGFBPs overexpressed in MDCK cells.

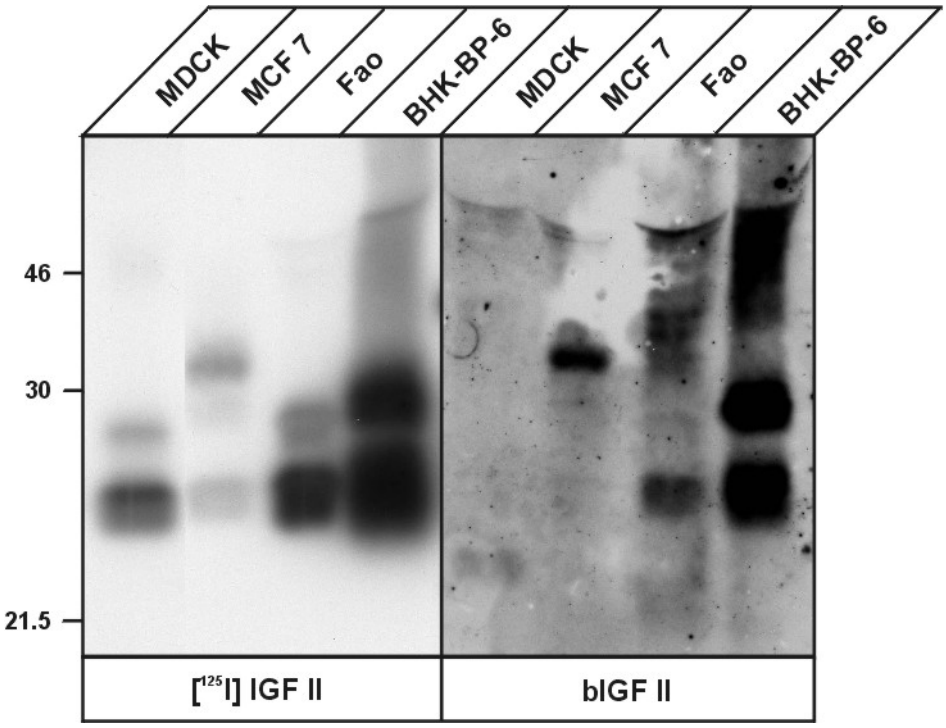

Figure 14: [^{125}I]-IGF II vs. bIGF II Western ligand blotting

Equal amounts of conditioned media (48 h) from MDCK, MCF7, Fao, and BHK-BP-6 (BHK overexpressing IGFBP-6) cell lines were separated on a 12.5% SDS-PAGE and subjected to ligand blotting using either [^{125}I]-IGF II (left panel) or bIGF II (right panel). The IGFBPs were visualized by autoradiography or ECL, respectively.

4.2.2 Polarized sorting of mIGFBP-6 in MDCK cells

In order to examine the sorting of mIGFBP-6 in MDCK cells, MDCK B1 and nontransfected MDCK cells were conditioned on polycarbonate filters. Apical (a) and basolateral (b) media were collected after 24, 48, or 72 h, and bIGF II ligand blotting was performed (Figure 15). Conditioned for 48 h medium from MDCK B1 grown on plastic dishes was used as an mIGFBP-6 control (Co). The results showed that no endogenous canine IGFBPs could be detected by bIGF II in MDCK and MDCK B1 media. In control medium mIGFBP-6 appeared as a broad band with an estimated molecular mass between 27.5 and 26 kDa. Additionally, mIGFBP-6 was secreted predominantly in the apical side from MDCK B1, with a basolateral time-dependent accumulation. As described previously (4.2), MDCK B1 cells lost their IGFBP-6 proteolytic activity after transfection, therefore the apical accumulation of mIGFBP-6 in MDCK B1 was not due to the presence of IGFBP-6 protease in the basolateral compartment. In order to test whether MDCK cells are able to transcytose IGFBP-6, and to maintain in this way its polar distribution, [^{125}I]-IGFBP-6 was added for 20 h to the apical or basolateral media of MDCK cells grown on

polycarbonate filters. As analyzed by γ-counting and SDS-PAGE followed by autoradiography, [^{125}I]-IGFBP-6 transcytosis was neither observed to the apical nor to the basolateral side (not shown).

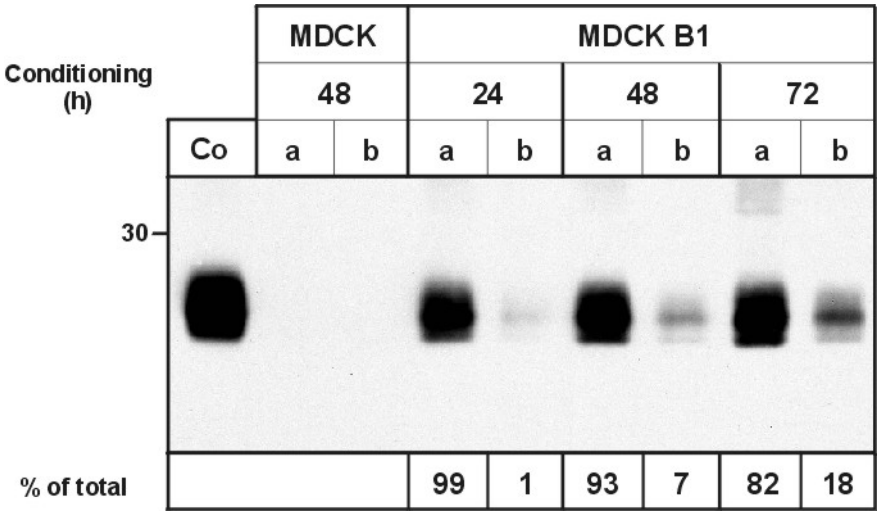

Figure 15: Polarized sorting of mIGFBP-6 in MDCK cells

Conditioned media (0.7 ml apical and 1 ml basolateral) were collected from MDCK (48 h) and MDCK B1 (24, 48, and 72 h) grown on polycarbonate filters. Proteins in 200 µl of 48 h conditioned medium from MDCK B1 grown on plastic dishes (Co), 200 µl from the apical (a), and 285 µl from the basolateral media (b) were precipitated by acetone. Samples were resolved in a 12.5% SDS-PAGE and bIGF II Western ligand blotting was used for detection of mIGFBP-6. The ability of bIGF II to recognize in ligand blotting specifically mIGFBP-6 in media from MDCK B1 cells was confirmed by immunoblotting with anti-mouse IGFBP-6 antibody.

4.2.3 Structural characterization of mIGFBP-6 expressed in MDCK cells

According to the SWISS-PROT database (accession number P47880), the molecular mass of the unprocessed mIGFBP-6 precursor is 25.4 kDa whereas the molecular mass of mIGFBP-6, expressed in MDCK cells was estimated to be between 27.5 and 26 kDa (Figure 15). The difference in the molecular mass and the fact that mIGFBP-6 overexpressed in MDCK cells runs as a broad band in SDS-PAGE suggests the presence of posttranslational modifications.

4.2.3.1 Isoforms of mIGFBP-6

Conditioned media from MDCK and MDCK B1 cells grown on plastic dishes were subjected to nonreducing 2D-electrophoresis and IGFBPs were subsequently detected by

bIGF II ligand blotting. Approximately ten major mIGFBP-6 spots were detected in medium by MDCK B1 (Figure 16 A). The mIGFBP-6 isoforms could be aligned to three groups according to their apparent molecular mass: spots 1, 2, 4, 5, and 7 of 27.5 kDa, spots 6, 8, 9, and 10 of 26.5 kDa, and spot 3 of 26 kDa, and to three groups according to their pI: pI 5.5-7 (spots 1 and 2), pI 7.5-8 (spots 3, 4, 5, and 6), and pI 9-9.7 (spots 7, 8, 9, and 10). None of these IGFBP spots were detected in media from nontransfected MDCK cells (Figure 16 B).

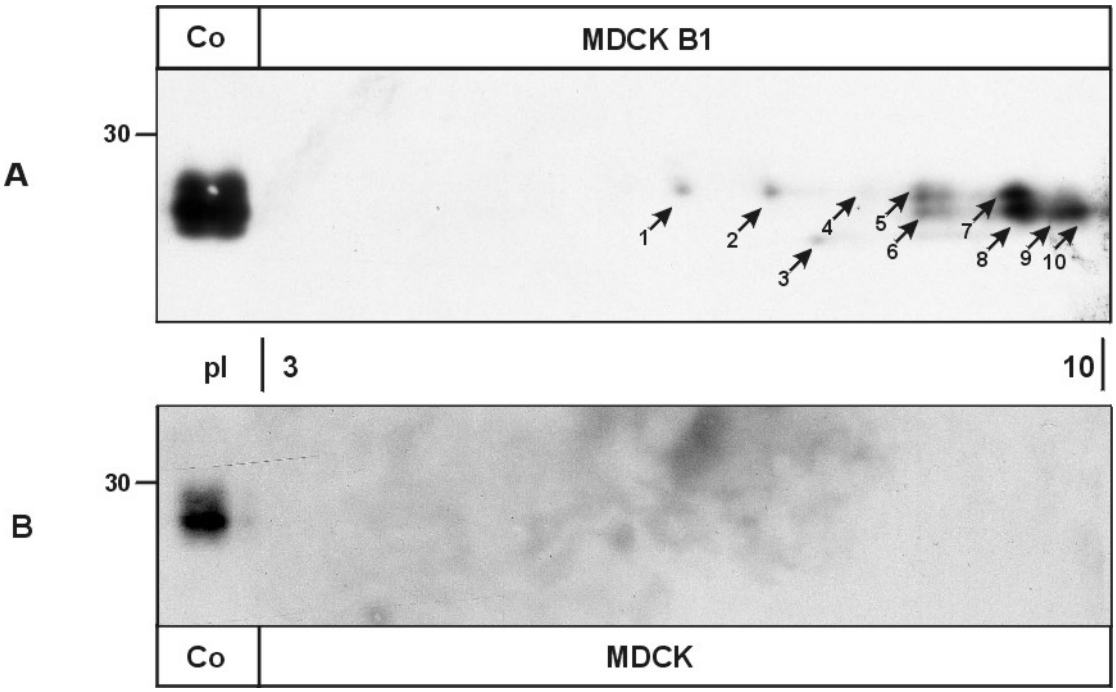

Figure 16: bIGF II ligand blot of nonreducing 2D-electrophoresis of MDCK B1 conditioned medium
MDCK and MDCK B1 cells were conditioned on plastic dishes for 48 h. Proteins in 300 µl medium were precipitated in acetone and subjected to nonreducing 2D-electrophoresis. Fifty microliters MDCK B1 conditioned medium (Co) were lyophilized, resolved in sample buffer and applied on the second dimension (12.5% SDS-PAGE). bIGF II ligand blotting was carried out for detection of IGFBPs.

4.2.3.2 Posttranslational modifications of mIGFBP-6

It has been reported that human and mouse IGFBP-6 have five, and one or two O-glycosylation sites, respectively (Neumann et al., 1998, Claussen et al., 1995). In order to examine whether other posttranslational modifications contribute to the diversity of mIGFBP-6 isoforms, MDCK B1 cells were metabolically labeled with [^{35}S]-methionine,

[^{3}H]-galactose, [^{33}P]-orthophosphate, or [^{35}S]-sulfate, for 20 h followed by immunoprecipitation of mIGFBP-6 from the media. When the cells were labeled with [^{35}S]-methionine, two major and one minor band with apparent molecular masses of 27, 26.5, and 26 kDa were precipitated (Figure 17 A). Labeling with [^{3}H]-galactose and [^{33}P]-orthophosphate revealed the presence of two mIGFBP-6 bands of 27 and 26.5 kDa. When the cells were labeled in the presence of [^{35}S]-sulfate very weakly labeled polypeptides were observed. The specificity of the anti-mouse IGFBP-6 antibody is shown in Figure 17 B. Immunoprecipitation of mIGFBP-6 from [^{35}S]-methionine labeled MDCK and MDCK B1 media showed the presence of three polypeptydes of 27.5, 26.5 and 26 kDa from mIGFBP-6 overexpressed cells but not from nontransfected MDCK cells. An unknown 97 kDa protein was immunoprecipitated from both media. The identity of the 64 and 39 kDa polypeptydes precipitated mainly from media of MDCK B1 cells, as well as of the 45 kDa polypeptide precipitated only from media of MDCK cells is unknown.

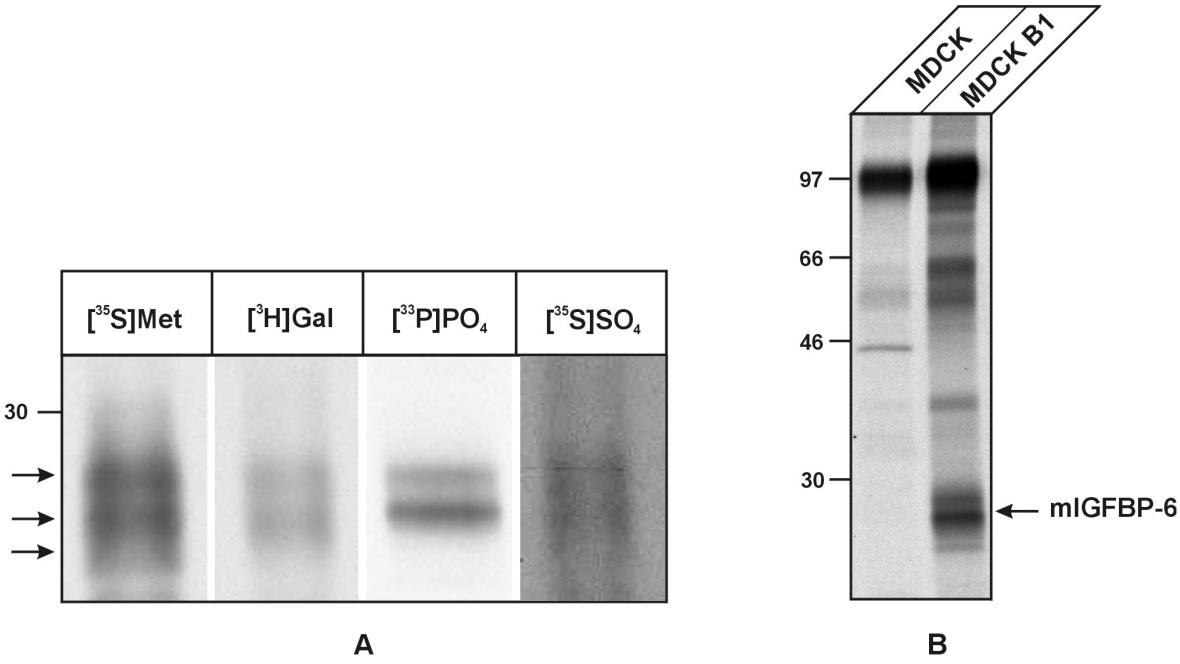

Figure 17: Posttranslational modifications of mIGFBP-6 expressed in MDCK cells

A: MDCK B1 cells grown on 60 mm plastic dishes were metabolically labeled for 20 h with [^{35}S]-methionine, [^{3}H]-galactose, [^{33}P]-orthophosphate, and [^{35}S]-sulfate. After immunoprecipitation with an antibody against mIGFBP-6, the complexes were separated by a 12.5% SDS-PAGE. The protein bands were visualized by fluorography after exposure for 10 days ([^{35}S]-methionine), 45 days ([^{3}H]-galactose), 20 days ([^{33}P]-orthophosphate), and 45 days ([^{35}S]-sulfate), respectively. Arrows indicate mIGFBP-6 polypeptides.
B: MDCK and MDCK B1 cells were labeled with [^{35}S]-methionine for 20 h. Immunoprecipitation with an antibody against mIGFBP-6 was followed by SDS-PAGE and fluorography. Arrow indicates the position of mIGFBP-6.

4.2.3.3 Deglycosylation of O-linked carbohydrates in mIGFBP-6

To verify whether the [^{3}H]-galactose incorporation in mIGFBP-6 reflects the presence of O-linked oligosaccharides, two approaches (enzymatic and chemical) to deglycosylate specifically O-glycosylated proteins were used. MDCK B1 grown on plastic dishes were metabolically labeled with [^{35}S]-methionine for 20 h followed by immunoprecipitation of the mIGFBP-6 from the medium. One third of the immunoprecipitate treated only with neuraminidase as a control (Co) revealed two bands with an apparent molecular mass of 27.5 (band 1) and 26.5 kDa (band 2) (Figure 18). The second sample was treated with neuraminidase and O-glycanase (enzymatic deglycosylation) which resulted in a shift of the molecular mass of band 1 from 27.5 to about 26.8 kDa (band 3). The same effect was observed in the third sample subjected to chemical removal of O-glycosydes (2.4.10.1). In addition, the 97 kDa protein (band 4) coprecipitated unspecifically from the medium appeared to be O-glycosylated too, because a shift after enzymatic and chemical deglycosylation to 88 kDa was observed (band 5). The data indicate that mIGFBP-6 expressed in MDCK cells is O-glycosylated and the oligosaccharides contribute with about 1 kDa or less to the molecular mass of the protein.

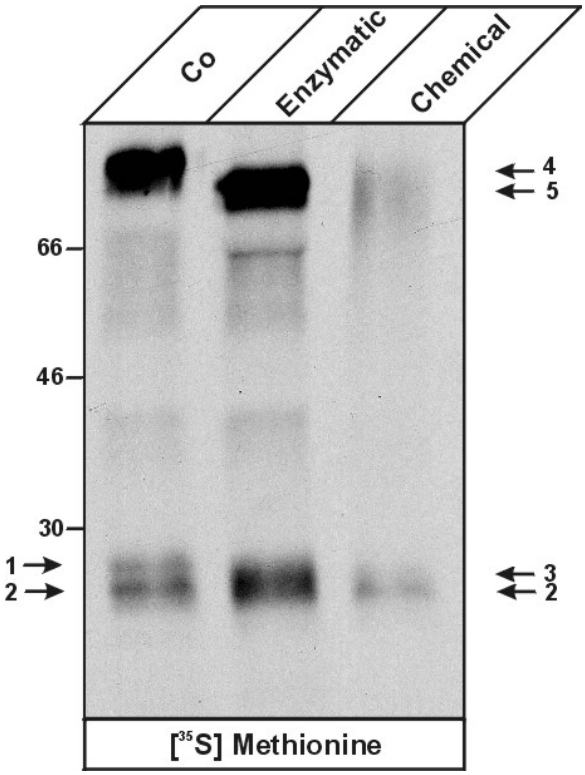

Figure 18: Deglycosylation of O-linked carbohydrates in mIGFBP-6

MDCK B1 cells grown on plastic dishes were metabolically labeled for 20 h with [^{35}S]-methionine. From the immunoprecipitated mIGFBP-6 each one third was either treated with neuraminidase alone (Co), with neuraminidase and O-glycanase (enzymatic deglycosylation) or TFMS and anisole (chemical deglycosylation). Proteins were resolved in a 12.5% SDS-PAGE and visualized by fluorography. With arrows are indicated: bands 1, 2 and 3 – forms of mIGFBP-6 with estimated molecular mass of 27.5, and 26.8 kDa respectively; bands 4, and 5 – an unknown protein of apparent molecular mass 97 and 88 kDa before and after deglycosylation, respectively.

4.2.3.4 Phosphorylation of mIGFBP-6

In order to identify which of the mIGFBP-6 isoforms are modified by phosphorylation, MDCK B1 and MDCK cells grown on plastic dishes were metabolically labeled with [^{33}P]-orthophosphate for 20 h. Under the conditions used for resolving samples in the absence of reducing agents for the isoelectric focusing (IEF, first dimension), the [^{33}P]-orthophosphate-mIGFBP-6 immunoprecipitates could not be recovered in the SDS-PAGE (second dimension). Therefore, proteins from 300 µl medium were precipitated by acetone at –20°C and subjected to 2D-electrophoresis and fluorography (Figure 19 B, C). For comparison, conditioned medium from non-labeled MDCK B1 cells was subjected to 2D-electrophoresis as well, and total mIGFBP-6 isoforms were detected by bIGF II ligand blotting (Figure 19 A). Metabolic labeling of MDCK B1 and MDCK cells with [^{33}P]-orthophosphate revealed that spots 1, 2, 8, and 10 are phosphorylated in medium from MDCK B1 cells (Figure 19 B), whereas none of these spots could be detected in medium from MDCK cells (Figure 19 C). The results show that MDCK B1 secrete four mIGFBP-6 phosphorylated isoforms with apparent molecular masses of 27.5 kDa (spot 1, and 2) and 26.5 kDa (spot 8, and 10). In Figure 19 B and C, spots of phosphorylated mIGFBP-6-unrelated proteins with molecular masses above 30 kDa are designated from **a** to **g.**

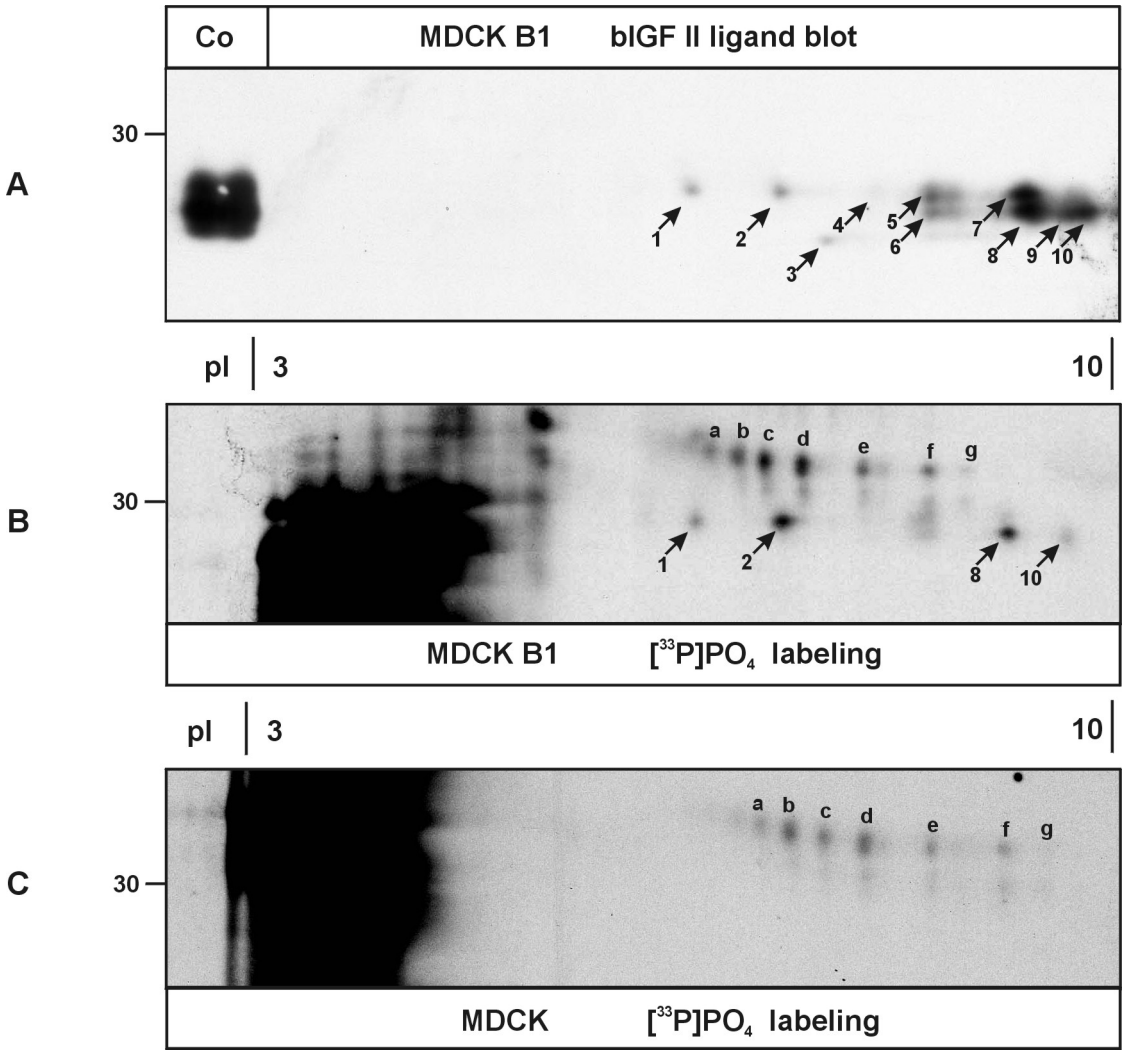

Figure 19: Phosphorylated mIGFBP-6 isoforms

A: Medium (300 µl) by MDCK B1 cells conditioned for 48 h medium was precipitated in acetone and subjected to 2D-electrophoresis with broad range (pI 3-10) strips. Isoforms of mIGFBP-6 were detected by bIGF II ligand blotting.

B, C: MDCK B1 or MDCK, respectively, grown on plastic dishes were metabolically labeled with [^{33}P]-orthophosphate for 20 h. Proteins in 300 µl medium were precipitated in acetone, subjected to 2 D-electrophoresis and detected by fluorography. Phosphorylated mIGFBP-6-unrelated proteins are designated from **a** to **g.**

4.2.3.5 Sulfation of mIGFBP-6 in MDCK cells

When media from MDCK and MDCK B1 cells labeled with [^{35}S]-sulfate were analyzed by 2D-electrophoresis, three spots were detected (Figure 20 B) corresponding to spots 5, 8, and 10 detected by bIGF II ligand blotting in conditioned medium from non-labeled MDCK B1 (Figure 20 A). These three spots were not detected in medium by MDCK cells labeled with [^{35}S]-sulfate (Figure 20 C). In Figure 20 B and C, spots of sulfated mIGFBP-6 unrelated proteins with molecular masses above 30 kDa are designated from **h** to **q**.

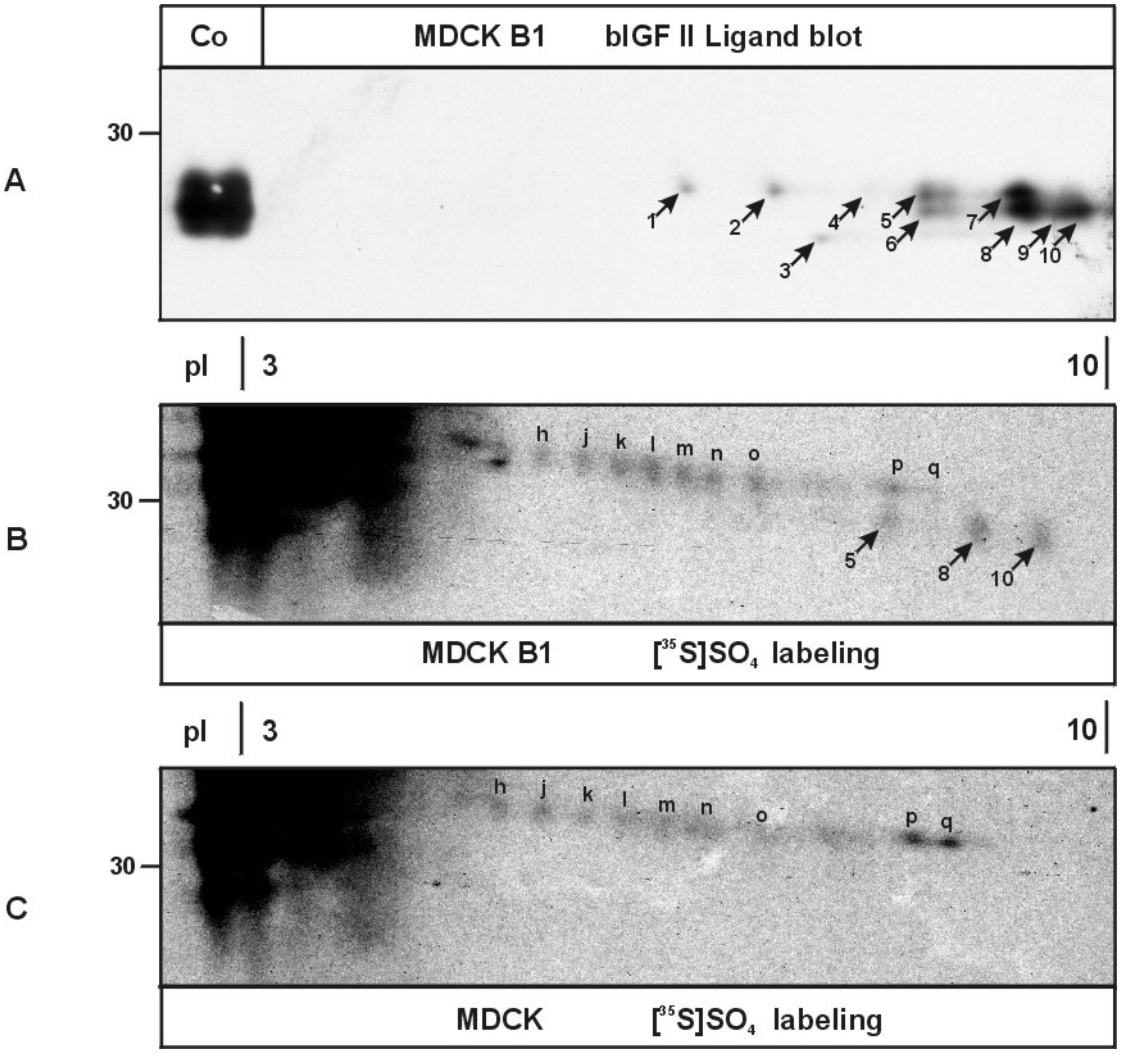

Figure 20: Sulfation of mIGFBP-6 in MDCK cells

A: Proteins in 300 µl medium by MDCK B1 cells conditioned for 48 h were precipitated in acetone and subjected to 2D-electrophoresis and mIGFBP-6 isoforms were detected by bIGF II ligand blotting

B, C: MDCK B1 and MDCK cells respectively, were metabolically labeled with [^{35}S]-sulfate. Proteins in 300 µl medium were precipitated in acetone and subjected to 2D-electrophoresis. Proteins labeled with [^{35}S]-sulfate were detected by fluorography. Spots of sulfated mIGFBP-6 unrelated proteins are designated from **h** to **q**.

4.2.4 Secretion of mIGFBP-6 isoforms from polarized MDCK cells

MDCK B1 cells secrete 82-99% of mIGFBP-6 preferentially towards the apical compartment (Figure 15). In order to determine whether MDCK cells maintain polarity of specific mIGFBP-6 isoforms, 48 h conditioned media from the apical and basolateral side of MDCK B1 cells grown on filters were subjected to 2D-electrophoresis (Figure 21). Ligand blotting using biotinylated IGF II revealed the presence of eight defined mIGFBP-6 spots in the apical (Figure 21 A) and in the basolateral medium (Figure 21 B). The reduced number of IGFBP-6 spots in comparison with the previously shown Figure 16 was due a damage of the basic end of IEF strips, which shortened the pI range from 3-10 to about 3-9.5. The results, however, revealed that spot 7, present in apical medium, was not detected in basolateral medium.

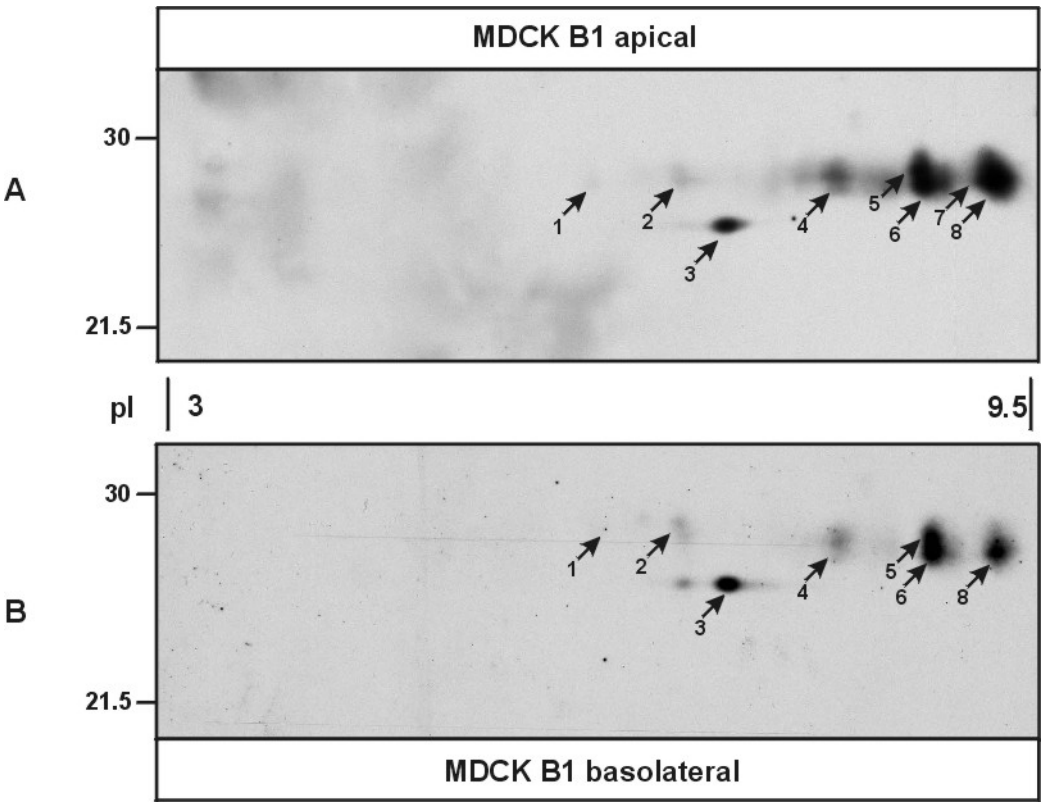

Figure 21: mIGFBP-6 isoforms secreted to the apical or basolateral side of MDCK cells

Conditioned media from MDCK B1 cells grown on polycarbonate filters were collected after 48 h. Proteins in 200 µl apical (A), and 285 µl basolateral medium (B) were precipitated in acetone and subjected to 2D-electrophoresis. Isoforms of mIGFBPs were detected by bIGF II ligand blotting. The detection time of the ECL signal was about 5-times higher in B than in A.

4.3 Characterization of mIGFBP-6 mutants

It has been shown that O-glycosylation delays the proteolysis of IGFBP-6 (Marinaro et al., 2000 b). However, the role of O-glycosylation in other physiological functions or for the transport of IGFBP-6 is unclear. Because it has been suggested that O-glycosylation might be important for the sorting of proteins in polarized cells (Yeaman et al., 1997), potential O-glycosylation sites were changed, followed by stable expression of mIGFBP-6 mutants and analysis of their distribution to the apical or basolateral media. One potential O-glycosylation site (residue 143) in mIGFBP-6 has been found to be conserved and O-glycosylated in human IGFBP-6. A second potential O-glycosylation site (S126) was chosen randomly among two serine and two threonine residues in the central region of mIGFBP-6. Site-directed mutagenesis was carried out to substitute residues S126 and S143 with alanine residues (Figure 22). The mutants were stably expressed in MDCK cells and three cell clones (A126, A143, and A126/143, respectively) expressing similar amounts of mutant mIGFBP-6 forms were used in all further studies.

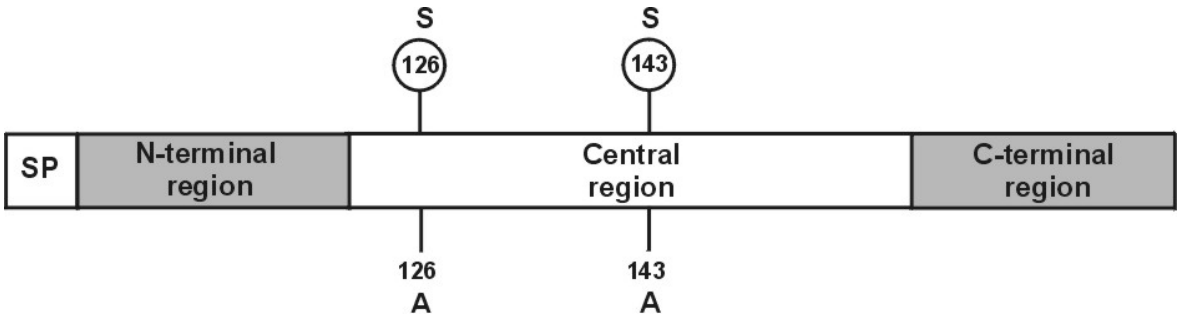

Figure 22: Schematic domain organization and putative O-glycosylation sites in mIGFBP-6

N- and C- terminal regions with amino acid homology among the IGFBPs are indicated as grey boxes. SP represents the signal peptide. The central region is unique to each IGFBP. Serine residues which are potentially O-glycosylated (S126 and S143), were mutated into alanine residues (A126 and A143).

4.3.1 Isoforms of mIGFBP-6 A126 and A143 mutants

Conditioned media from MDCK B1 expressing mIGFBP-6 wild type, A126, and A143 cells grown on plastic dishes were subjected to 2D-electrophoresis with narrow range pI strips (pI 6-11). Ligand blotting using bIGF II revealed that mIGFBP-6 WT is represented by 10 major spots (Figure 23 A). Spots 1 and 2 of mIGFBP-6 WT detected by broad range pI strips (pI 3-7) (Figure 17) were not detectable when narrow range pI strips (pI 6-11) were used. Additionally, two new spots of mIGFBP-6 WT (spot 11 and 12) with apparent molecular masses between 27.5 and 26.5 kDa were detected in the very basic end of the pI

6-11 strip. The 2D-patterns of mIGFBP-6 WT and A126 mutant isoforms were similar, differing mainly in the intensity of spot 12, and in the lack of spot 11 and the appearance of an additional spot with an apparent molecular mass of 26.5 kDa in medium from A126 (marked with an asterisk). These differences, however, have to be proven by additional experiments. The pattern of the mIGFBP-6 A146 isoforms appeared to be different to those of the mIGFBP-6 WT and A126. Thus, Figure 23 C reveals the absence of spots 6, 11, and 12 and the appearance of a new spot with apparent molecular weight of 26.5 kDa (indicated with an asterisk) not present in the mIGFBP-6 WT and A126 mutant. Interestingly, the electrophoretic mobilities of the A143 isoforms were also faster: spots 4, 5, and 7 appeared to have approximate molecular weights of 26.5 kDa, and spots 8, 9, and 10 demonstrated molecular masses of about 26 kDa.

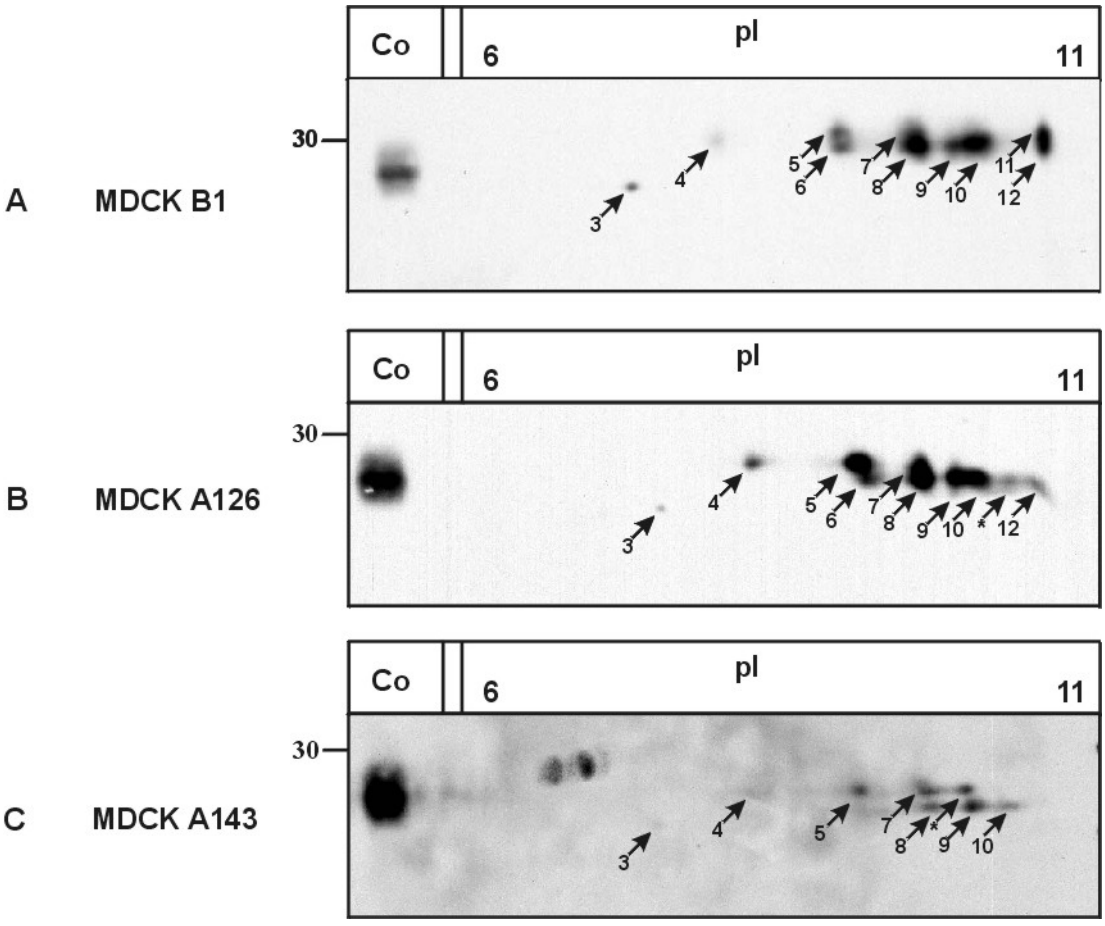

Figure 23: 2D-analysis of mutant IGFBP-6 A126 and A143

Media from MDCK B1 (A), A126 (B), and A146 (C) cells were collected after 48 h of conditioning. Proteins in 300 µl medium were precipitated in acetone and subjected to 2D-electrophoresis with narrow strips range (pI 6-11). mIGFBP-6 spots were detected by bIGF II ligand blotting. New spots appearing in the media from mutant mIGFBP-6 forms are marked with asterisks.

4.3.2 Polarized sorting of mIGFBP-6 mutants in MDCK cells

To examine whether the sorting of A126, A143, and A126/143 mIGFBP-6 mutants differs from the sorting of mIGFBP-6 WT, conditioned media from cells grown on polycarbonate filters were collected after 48 h and subjected to SDS-PAGE. Biotinylated IGF II ligand blotting was used for detection of mIGFBP-6 (Figure 24). The results revealed that the IGFBP-6 mutant MDCK clones showed higher total expression of mIGFBP-6 compared to MDCK B1. The overall mIGFBP-6 apical/basolateral ratio was similar for the wild type and A126 (74% of the total mIGFBP-6 in the apical, 26% in the basolateral) as estimated by densitometry. Interestingly, the percent distribution in MDCK A143 and A126/143 was 65:35% between the apical and basolateral media. Additionally, the electrophoretic mobilities of the A143 and A126/143 mutants appear to be faster than those of the wild type or A126 mutant. Furthermore, in the basolateral medium from MDCK A126 two polypeptides with apparent molecular masses of 27.5 and 26.5 kDa were found, whereas mIGFBP-6 A143 and A126/143 appeared as double band of 26.5-26 kDa. The data suggest that serine 143 is one of the glycosylated site(s) in mIGFBP-6

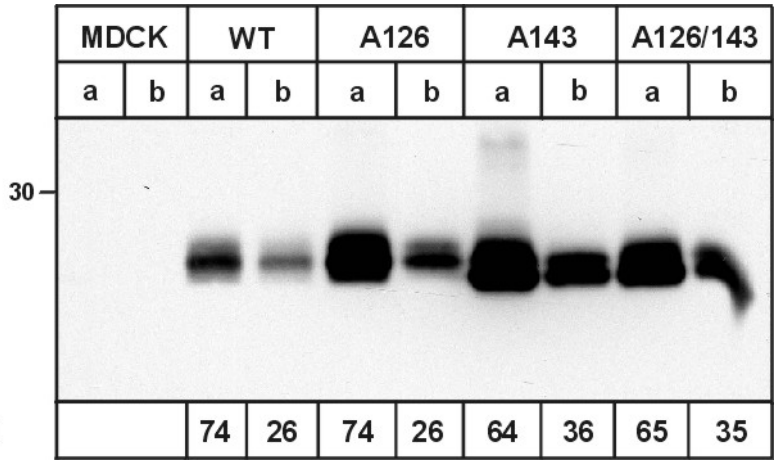

Figure 24: Polarized sorting of mIGFBP-6 mutants in MDCK cells

Apical (a) and basolateral (b) conditioned media from MDCK, MDCK B1, MDCK A126, MDCK A143, and MDCK A126/143 cells were collected after 48 h. Proteins in 200 µl apical or 285 µl basolateral media were precipiated in acetone, and subjected to SDS-PAGE. mIGFBP-6 was detected in bIGF II ligand blotting.

4.4 Effect of mIGFBP-6 on proliferation and migration of MDCK cells

Exogenous IGFBP-6 inhibits the IGF II-stimulated proliferation of different cell lines by forming IGF II/IGFBP-6 complexes preventing the interaction of IGF II with the IGF receptors (Bach et al., 1995; Srinivasan et al., 1996; Putzer et al., 1998). Furthermore, it has been reported that IGF II stimulates the migration and invasiveness of human rhabdosarcoma and of human trophoblast cells (Minniti et al., 1992; McKinnon et al., 2001). To examine autocrine/paracrine effects of IGFBP-6, the proliferation and migration of MDCK, MDCK pGK, and MDCK B1 cells were studied.

4.4.1 Effects of IGF I, IGF II and IGFBP-6 on proliferation of MDCK pGK and MDCK B1 cells

The basal proliferation rates of MDCK, MDCK pGK, and MDCK B1 cells were estimated by 5-bromo-2´-deoxy-uridine (BrdU) incorporation (2.2.4). The results revealed that the proliferation rates of MDCK pGK and MDCK B1 cells were reduced by 25% and 50%, respectively, in comparison with MDCK cells (Figure 25). Because the lower proliferation rates of MDCK pGK and MDCK B1 cells were presumably due to the transfection/selection procedure, in all further studies, MDCK pGK cells were used as a control instead of MDCK cells.

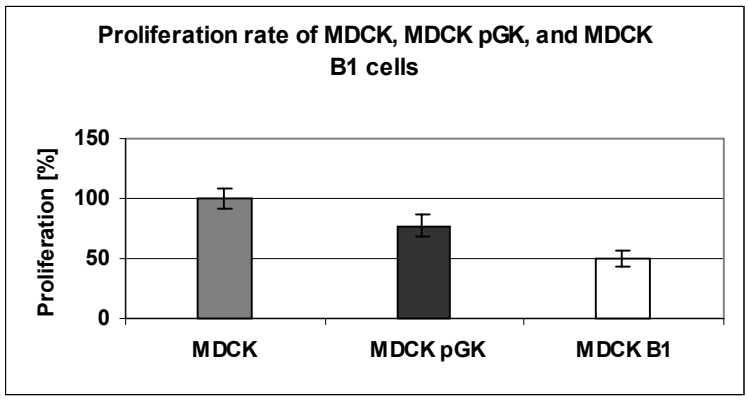

Figure 25: Proliferation rates of MDCK, MDCK pGK, and MDCK B1 cells

Cells (5,000 cells/well) were allowed to attach and grow for 16 h. BrdU was added, and further incubation was carried out for 7.5 h. The proliferation rate is expressed as percentage of the proliferation rate of MDCK cells and represents results from two independent experiments with n=6.

MDCK pGK and MDCK B1 cells were incubated for 14 h in the presence or absence of IGF II (10 nM or 50 nM), IGF I (10 nM), or mIGFBP-6 (0.9 µg/ml) and subsequently labeled with BrdU. The proliferation rates of MDCK pGK and MDCK B1 cells in the presence or absence of factors are presented in Figure 26 as a percentage of the proliferation rate of MDCK pGK control cells. Although MDCK B1 cells demonstrate a lower basal proliferation rate in comparison with the control MDCK pGK, the proliferation response of MDCK B1 cells to all concentrations of IGF II, related to their basal proliferation level, appeared to be higher then of MDCK pGK. Purified mIGFBP-6 in concentration of 0.9 µg/ml increased the proliferation of MDCK pGK by 17%, whereas in MDCK B1 cells it had a marginal effect.

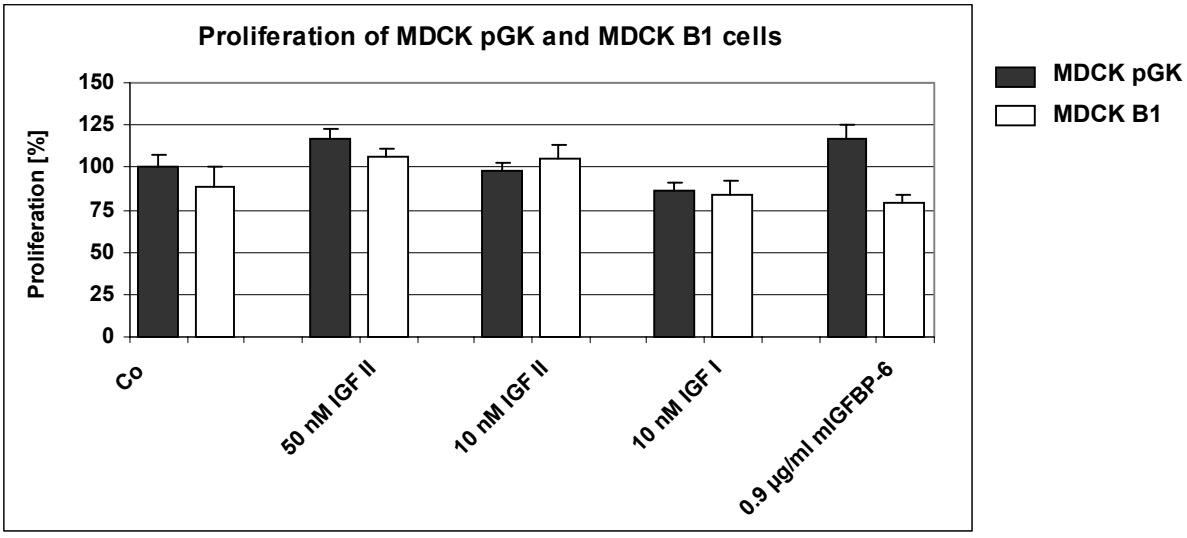

Figure 26: Effects of IGF II (50 nM or 10 nM), IGF I (10 nM), or mIGFBP-6 (0.9 µg/ml) on the proliferation of MDCK pGK and MDCK B1 cells

Cells (5000 cells/well) were allowed to attach and grow for 16 h. They were incubated in presence or absence of IGF II (50 nM or 10 nM), IGF I (10 nM), or mIGFBP-6 (0.9 µg/ml) for 14 h, followed by addition and incubation with BrdU for 7.5 h. The proliferation rate is expressed as percentage of the proliferation rate of MDCK pGK control cells. This represents the results of two independent experiments with n=6 for each condition.

4.4.2 Migration of MDCK pGK and MDCK B1 cells

Boyden chambers were used to examine the effects of the following factors on the migration of MDCK pGK and MDCK B1: VEGF (50 ng/ml), IGF II (50 nM , 10 nM, or 1 nM), IGF I (10 nM), mIGFBP-6 (0.9 µg/ml), 48 h conditioned medium (CM) from MDCK B1 cells, estimated to contain 0.9 µg/ml mIGFBP-6, or MDCK B1 conditioned medium supplemented with 10 nM IGF II. Figure 27 shows the effect of the factors on the migration of MDCK pGK cells. VEGF, a strong migration stimulus for endothelial cells, showing no effect on the migration of MDCK pGK, was used as a negative control. IGF II stimulated the migration of MDCK pGK cells in a dose dependent manner between 43 and 67%, whereas IGF I showed almost no effect on the migration. The addition of mIGFBP-6 inhibited the basal migration rate by 38%. Similarly, conditioned medium from MDCK B1 cells inhibited the migration of MDCK pGK cell by 36%. When the conditioned medium was supplemented with 10 nM IGF II, this inhibitory effect was reduced by 16%.

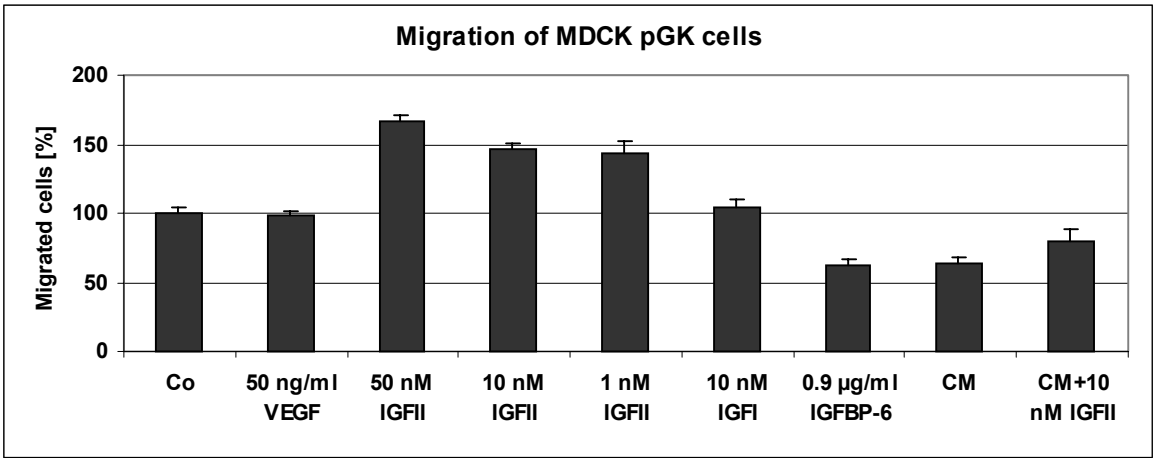

Figure 27: Effects of different factors on the migration of MDCK pGK cells

Modified 96-well Boyden chambers were used to estimate migration. Equal amounts of cells were seeded and incubated in presence or absence of factors in the lower chamber at 37°C for 6 h. Migrated cells were stained and counted under a microscope. The effect of the following factors was estimated: VEGF (50 ng/ml), IGF II (50 nM , 10 nM, or 1 nM), IGF I (10 nM), mIGFBP-6 (0.9 µg/ml), 48 h conditioned medium (CM) from MDCK B1 cells, estimated to contain 0.9 µg/ml mIGFBP-6, or MDCK B1 conditioned medium supplemented with 10 nM IGF II. The results are presented as a percentage of the basal migration rate of control MDCK pGK cells. This represents the results of two independent experiments in triplicate for each condition.

Figure 28 shows the effect of the same factors on the migration of MDCK B1 cells. VEGF increased the basic migration marginally. All tested IGF II concentrations stimulated the migration of MDCK B1 cells between 46 and 123%. IGF I did not affect the cell migration. The addition of recombinant mIGFBP-6 or conditioned medium from MDCK

B1 cells inhibited the migration by 38 and 50%, respectively. The effect of the latter was partially abolished by addition of 10 nM IGF II.

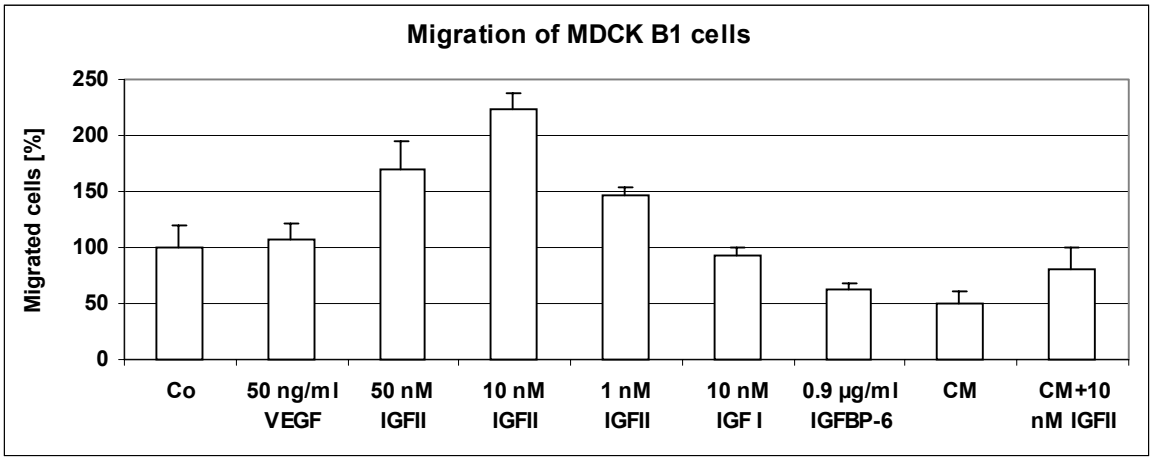

Figure 28: Effect of different factors on the migration of MDCK B1 cells

Boyden chambers were used to estimate migration, as described previously (Figure 27). The effect of the following factors was estimated on the migration of MDCK B1: VEGF (50 ng/ml), IGF II (50 nM , 10 nM, or 1 nM), IGF I (10 nM), mIGFBP-6 (0.9 µg/ml), 48 h conditioned medium (CM) from MDCK B1 cells, estimated to contain 0.9 µg/ml mIGFBP-6, or MDCK B1 conditioned medium supplemented with 10 nM IGF II. The results are presented as a percentage of the basal migration rate of control MDCK B1 cells. The experiment was carried out twice with n=3.

The migration rates of MDCK pGK and MDCK B1 cell in the presence or absence of factors were compared, and expressed as percentage of MDCK pGK cells migrated in absence of factors (Figure 29). The figure demonstrates that the basal and the migration rates in presence of different factors, are generally lower in MDCK B1 cells. These data suggest that the overexpression of mIGFBP-6 inhibits the migration of cells in an autocrine/paracrine manner, which may be abolished by the addition of IGF II.

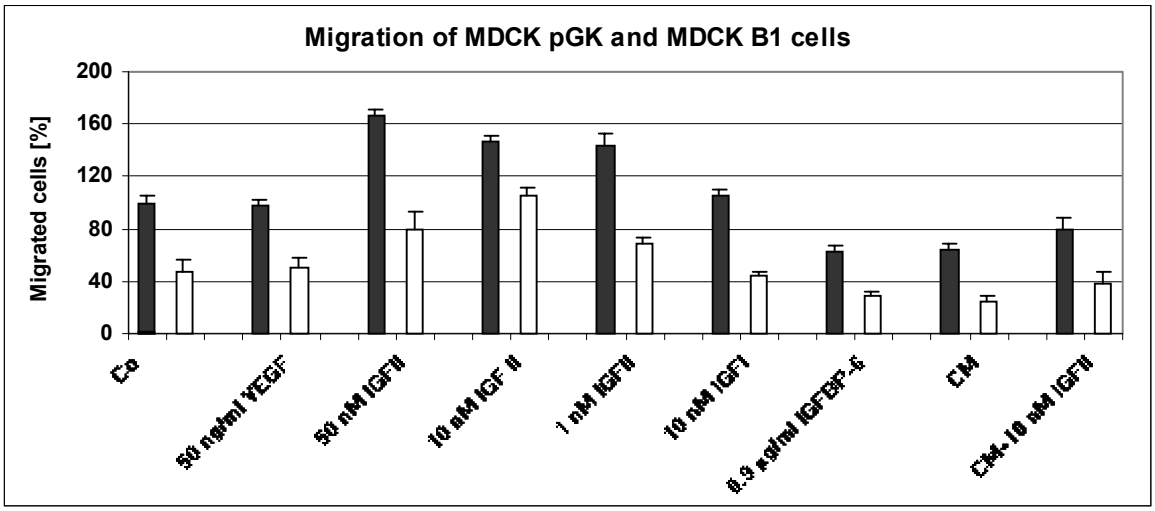

Figure 29: Relative effects of different factors on the migration of MDCK pGK and MDCK B1 cells

5 DISCUSSION

5.1 Secretion of IGFBP proteases from MDCK cells

The normal glomerular capillary wall prevents the ultrafiltration of large amounts of proteins due to its charge and size selectivity. However, small amounts of albumin (68 kDa) and even IgG (158 kDa) are ultrafiltrated physiologically. Urine of normal subjects contains IGFBP-2 and –3 in a reversed ratio compared with serum. (Feld and Hirschberg, 1996). This can be explained: first, that most IGFBP-3 in serum is present in a 150 kDa complex with the acid-labile subunit (ALS) and thereby virtually excluded from glomerular ultrafiltration. Second, some of the urinary IGFBP-3 may result from tubular secretion. Third, the binding or absorption of IGFBPs to the tubule cells during the tubular downstream passage may be different (Feld and Hirschberg, 1996). In the present work, the MDCK cell line was used as a model to examine in more details the components of the IGF system and their regulation in polarized distal/collective tubule kidney cells. It has been described that MDCK cells express IGF 1R and IGF 2R but not the insulin receptor (Magee and Siddle, 1988; Prydz et al., 1990). Additionally, IGF II mRNA but not IGF I mRNA has been detected in MDCK cells (Ernest et al., 1995). However, nothing is known about the other two members of the IGF system, the IGFBPs and the family of IGFBP proteases in MDCK cells. The present study provides evidence that MDCK cells secrete three major IGFBPs and a unique spectrum of neutral IGFBP-2 to -6 proteases.

MDCK cells secrete three IGFBPs with apparent molecular masses of 35, 28 and 25 kDa. The identity of these three IGFBPs remained unknown because none of the tested antibodies directed against human IGFBP-1, -4, and -5, bovine IGFBP-2, mouse or human IGFBP-6 cross-reacted with the canine IGFBPs. According to the molecular masses, these binding proteins may represent IGFBP-2/IGFBP-5, and IGFBP-4 or –6, respectively. Due to the failure of human IGFBP cDNA probes to hybridize with MDCK-derived mRNA in Northern blotting, the identities of the IGFBP species secreted by MDCK cells remains to be determined. Oosterlaken-Dijksterhuis et al. (1999) have identified four canine IGFBPs in conditioned medium from CMT-U335 (canine mammary tumor cell line) using anti-human IGFBP-3, -4, -5, and –6 antibodies, or anti-bovine IGFBP-2 antibody purchased from other companies than those listed in the present study. They have detected IGFBP-2 (35 kDa), IGFBP-4 (24 kDa), a doublet of IGFBP-5 (31/33 kDa), and a doublet of IGFBP-6 (23/25 kDa). Because it has been described that posttranslational modifications

such as glycosylation are altered in tumor cells (Brockhausen, 1999), the data from the canine mammary tumor cell line can not be compared with MDCK cell line.

The proteolysis of IGFBPs plays an important role for the regulation of the extracellular IGFBP-levels and the IGF availability to cell surface receptors, resulting in stimulation of cellular proliferation and differentiation. It has been described that IGFBPs can be degraded in media from cultured cells by acid-activated or neutral proteases that either hydrolyze specifically individual IGFBPs or proteolyse many IGFBPs (Marinaro et al., 1999 a; Gibson and Cohen, 1999). Acid-activated proteolysis of IGFBPs in media from cultured cells is mediated by cathepsin D or cathepsin D-like proteases. Cathepsin D is a lysosomal enzyme which undergoes pH-dependent, intramolecular proteolytic autoactivation. However, 2-20% of the total procathepsin D is secreted into conditioned media by normal cells, whereas cancer cells secrete up to 60% (Marinaro et al., 1999 a). Cathepsin D is able to proteolyse a wide variety of proteins including IGFBP-1 to –5, and IGF II (Claussen et al., 1997). Furthermore, it has been demonstrated that it cleaves IGFBP-3 in acidified media from a variety of normal and transformed human cell lines, and primary rat liver cells (Conover and De Leon, 1994; Scharf et al., 1998 a, b), and IGFBP-4 in acidified media from mouse fibroblasts and isolated rat stellate cells (Braulke et al., 1995; Scharf et al., 1998 a). Recently it has also been shown that IGFBP-6 is degraded in acidified media from HaCaT cells (human keratinocytes) by a cathepsin D-like protease (Marinaro et al., 1999 a). The physiological significance of the acid-activated IGFBP proteolysis remains unclear. Inactive precursor forms of various cathepsins secreted by cultured cells, which undergo autoactivation at low pH (Richo and Conner, 1991), might primarily be responsible for acid-activated IGFBP proteolysis. Therefore, it is rather unlikely, that acid-activated IGFBP proteolysis may contribute to differences in IGFBP abundance observed in conditioned media of MDCK cells. Furthermore, analysis of rat hepatocytes and Kupffer cells in coculture, and of mouse fibroblasts with decreased amounts of lysosomal enzymes, demonstrated delayed intracellular degradation of IGFBP-3, accompanied by an accumulation of IGFBP-3 and its fragments all along the endocytic pathway (Braulke et al., 1999 b; Scharf et al., 2001).

Limited number of studies have described the presence of neutral IGFBP proteolytic activity in media from cultured cells. A neutral disintegrin metalloprotease identical to the pregnancy serum associated IGFBP-3 protease has been reported to degrade IGFBP-3 in media from human placenta trophoblasts (Irwin et al., 2000). IGFBP-4-specific hydrolysis at neutral pH has been detected in media from human ovarian granulosa cells and human

fibroblasts. The IGFBP-4 protease has been identified to be the IGF II-dependent pregnancy-associated plasma protein A (PAPP-A) (Lawrence et al., 1999; Conover et al., 2001). Furthermore, the proteolysis of IGFBP-5 at neutral pH in media from human dermal fibroblasts is cleaved by the serine protease complement component C1s (Busby et al., 2000).

In the present work it is described for the first time that MDCK cells secrete a variety of neutral proteases cleaving recombinant human IGFBPs into fragments of defined sizes (IGFBP-2, -3, -4, and -5), or into small peptides which fail to be detected by SDS-PAGE (IGFBP-6). The number of distinct IGFBP proteases in media of MDCK cells is unknown. Thus, the limited proteolysis of IGFBP-4 revealed the formation of two fragments, suggesting that only one MDCK protease cleaves IGFBP-4. Because the proteolysis of IGFBP-4 is IGF II-independent, it appears that the canine IGFBP-4 protease is different from the IGF II-dependent PAPP-A. In addition, proteolytic pattern and inhibitor profiles demonstrate that different proteases degrade IGFBP-5 in media from human dermal fibroblasts and MDCK cells: the complement component C1s is inhibited by serine protease inhibitors, whereas none of the tested serine protease inhibitors prevented the degradation of the intact IGFBP-5 in media from MDCK. At the concentrations used, TAPI (a specific metalloprotease inhibitor) and aprotinin (serine protease inhibitor) abolished the formation of an 8 kDa IGFBP-5 fragment, resulting in the accumulation of a 16 kDa IGFBP-5 peptide. The data indicate that more than one protease is involved in the degradation of IGFBP-5 in MDCK cells.

Due to its high binding affinity for IGF II (K_D 1~4 x 10^{-11} M; Bach, 1999), IGFBP-6 is an important physiological inhibitor of IGF II actions. Because i) it has been found that MDCK express IGF II but not IGF I (Ernest et al., 1995) and ii) no neutral proteolytic activity against IGFBP-6 in media from cultured cells has been reported so far, the IGFBP-6 protease secreted by MDCK cells was studied in more detail. IGFBP-6 is degraded completely, depending on the incubation time, with the transient formation of fragments as observed for IGFBP-5. However, protease inhibitor profiles reveal that different proteases are involved in the degradation of IGFBP-5 and IGFBP-6 in media from MDCK cells: unlike IGFBP-5, the proteolysis of IGFBP-6 is almost completely abolished by serine and metalloprotease inhibitors. The IGFBP-6 proteases in the conditioned medium separated by ion exchange chromatography into two fractions are inhibited either by serine protease inhibitors or by metalloprotease inhibitors such as 1,10 phenanthroline and the hydroxamic acid-based inhibitor TAPI. The latter has been shown to be a potential inhibitor of tumor

necrosis factor-α converting enzyme (TACE), a member of the disintegrin metalloproteases (Black et al., 1997; Mohler et al., 1994). Several immunoreactive polypeptides including a 44 and a 30 kDa protein band in TAPI-sensitive IGFBP-6 protease fractions were detected with specific antibodies directed against the prodomain, the disintegrin, and the cysteine-rich domain of ADAM 12 S suggesting the involvement of disintegrin metalloproteases in IGFBP-6 proteolysis. ADAM 12 is a member of the fast growing ADAM family (a disintegrin and metalloprotease) comprising almost 30 transmembrane proteins with characteristic conserved domain structure demonstrated in Figure 31. Recently it has been reported that the human ADAM 12, which belongs to the membrane bound disintegrins, undergoes an alterantive splicing resulting in the synthesis of a secreted soluble form named ADAM 12 S (Gilpin et al., 1999). However, it has been demonstrated that purified recombinant human ADAM 12 S degrades IGFBP-3 and IGFBP-5 but not IGFBP-1, -2, -4, and –6 (Loechel et al., 2000). The immunoreactive bands in purified fractions containing IGFBP-6 metalloprotease activity detected by antibodies directed against the highly conserved domains of ADAM 12 S could also be explained by cross-reactivity with an unknown member of the canine ADAM family.

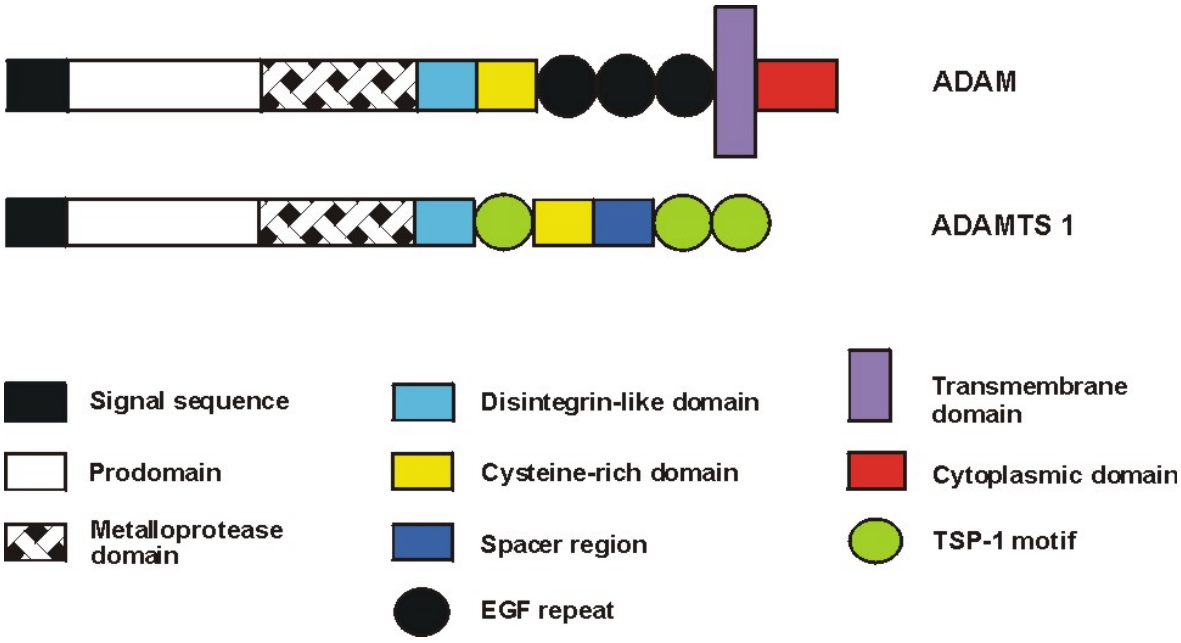

Figure 30: Domain organization of ADAM and ADAMTS metalloproteases

Interestingly, a new family of ADAM-related proteins, known as ADAMTS (ADAM with trombospondin motifs) has been recently identified (Tang, 2001). ADAMTS have the characteristic ADAM-like domains as shown in Figure 31. However they differ from conventional ADAMs by i) a trombospondin type 1 (TSP-1)-repeat found between the disintegrin and the cysteine-rich domain, which may be followed by a varying number of TSP-1-like repeats in the C-terminus, and ii) these proteins lack a transmembrane domain and are, therefore, secreted into the extracellular space. Thus, it can be speculated that ADAMTS-1 might be the IGFBP-6 disintegrin metalloprotease secreted from MDCK cells, because *ADAMTS 1* gene targeted mice exhibit significant growth retardation and changes in the kidney structure (Shindo et al., 2000). The latter is probably due to the high expression of ADAMTS-1 in mouse kidney (Tang, 2001). However, the identity of the IGFBP-6 disintegrin metalloprotease in media from MDCK cells remains to be demonstrated and requires the sequencing/fingerprint mass analysis of the 44 and 30 kDa immunoreactive polypeptides and the analysis of the ADAM/ADAMTS expression pattern in MDCK cells.

Unlike the proteolysis of IGFBP-4 and –5, IGFBP-6 proteolysis was inhibited by IGF II. Claussen et al. (1995) have reported on the inhibition of acid-activated IGFBP-6 proteolysis in conditioned media from NIH-3T3 cells treated with IGF II for 48 h. Furthermore, it has been shown that the direct addition of IGF II to the acidified protease-containing media from NIH-3T3 cells has no effect on the proteolysis of IGFBP-6, suggesting an indirect inhibitory role of IGF II. When MDCK cells were incubated in the presence or absence of IGF II for 24 h, followed by a further incubation with [^{125}I]-IGFBP-6, complete degradation of IGFBP-6 was observed in media from IGF II untreated cells. In contrast, the IGFBP-6 proteolysis was almost completely inhibited in media from IGF II treated cells. Incubation of MDCK cells with [^{125}I]-IGFBP-4 under identical conditions, showed no effect of IGF II on the proteolysis of IGFBP-4, demonstrating that the effect of IGF II is IGFBP/IGFBP-protease-specific. Direct protective effect of IGF II on proteolysis of IGFBP-6, but not of IGFBP-4 and –5, was shown in the cell-free protease assays. The mechanism by which IGF II inhibits the proteolysis of IGFBP-6 appears to depend on the cell line and the proteases investigated. Thus, IGF II inhibits the neutral IGFBP-6 proteolysis in conditioned media from MDCK in a direct manner either by inhibition of the protease(s) or by stabilization and protection of IGFBP-6 due to the formation of IGF II/IGFBP-6 complexes. On the other hand, the acid-activated IGFBP-6 proteolysis in NIH-3T3 cells appears to be inhibited by IGF II indirectly, e.g. by decreasing the amount of

secreted IGFBP-6 proteases or stimulating the secretion of protease inhibitors (Claussen et al., 1995).

There is evidence that both the conserved C- and N-terminal domains of the IGFBPs, responsible for high affinity IGF-binding, are resistant to proteolytic attack. The C- and N-terminal fragments of IGFBP-3 generated by limited proteolysis show an about 100-fold reduced IGF-binding affinity, which is, however, still detectable by ligand blotting (Ho and Baxter, 1997). Proteolysis of glycosylated rhIGFBP-6 in the medium from MDCK cells resulted in a transient formation of immunoreactive fragments of about 28, 24, 22, and 21.5 kDa, which completely lost IGF II-binding properties, as shown by ligand blotting. The inability of the glycosylated IGFBP-6 fragments to bind IGF II indicates the absolute requirement of the full-length IGFBP-6, rather than to sterical hindrance due to glycosylation of IGFBP-6. This is confirmed by studies demonstrating that O-glycosylation does not directly affect high affinity IGF binding of IGFBP-6 (Marinaro et al., 1999 b). Furthermore, it has been demonstrated that proteolysis with chymotrypsin decreases the binding affinity of IGFBP-6 for IGF II, even after a relatively small reduction of the apparent molecular mass (Marinaro et al., 2000 b). Similarly, the truncation of IGFBP-6 in media from MDCK cells by only 1 kDa completely abolished the binding of IGF II. This suggests that the entire IGFBP-6 structure is necessary for binding to IGF II. Therefore, the proteolysis of the IGFBP-6 in media from MDCK cells completely prevents the binding of IGF II to IGFBP-6, which may be an important mechanism to regulate the availability of IGF II.

Neutral IGFBP-6 proteolytic activities were found not only in the media of MDCK cells but also in media from the morphologically and functionally similar bovine kidney distal tubule MDBK cells. The IGFBP-6 fragment pattern and the identical inhibitor profile suggest that similar/identical proteases are involved in the degradation of IGFBP-6 by distal tubule epithelial cells, which might have a physiological relevance for regulation of the IGF system in kidney.

In summary, the present work shows that the MDCK cells originating from distal tubule/collective tubule ducts secrete three major IGFBPs and a variety of proteases degrading specifically IGFBP-2 to –6 at neutral pH. The results demonstrate that IGFBP-4 and IGFBP-5 are hydrolyzed in media from MDCK cells by proteases different to the neutral IGFBP-4 and IGFBP-5 proteases found in media from other cultured cells. Although the identity of the two major IGFBPs secreted by MDCK cells remained unknown, their secretion supports the idea that the IGFBPs found in mammalian urine may

not only originate from the serum, but may be locally produced in different segments of the nephron. Which biochemical processes of distal tubule cells are regulated by the parallel secretion of IGFBPs, IGFBP proteases and IGF II (IGF I has not been detected in MDCK cells; Ernest et al., 1995) remains to be investigated.

5.2 Structural characterization of mouse IGFBP-6 expressed in MDCK cells

In the present work, structural features of mIGFBP-6 stably overexpressed in MDCK (MDCK B1) cells were examined (summarized in Table 5). In conditioned media from MDCK B1 cells mIGFBP-6 appears as a broad band with apparent molecular mass between 27.5 and 26 kDa, as detected by nonreducing SDS-PAGE and subsequent bIGF II ligand blotting or immunoblotting with a specific anti-mouse IGFBP-6 antibody. However, according to the SWISS-PROT database (accsession number P47880), the molecular mass of the unprocessed mIGFBP-6 precursor is 25.4 kDa. Additionally, a high molecular heterogeneity of mIGFBP-6 was demonstrated by nonreducing 2D-electrophoresis. Thus, broad range strips (pI 3-10) revealed 10 major mIGFBP-6 isoforms with apparent molecular masses of 27.5, 26.5, or 26 kDa, and isoelectric points of focusing (pI) as shown in Table 5. When narrow range strips (pI 6-11) were used, two more mIGFBP-6 isoforms were detected (spots 11 and 12) at the very basic end of the strips. The results suggest, that mIGFBP-6 overexpressed in MDCK cells undergoes posttranslational modifications.

mIGFBP-6 spot	1	2	3	4	5	6	7	8	9	10	11	12
Molecular mass (kDa)	27.5	27.5	26	27.5	27.5	26.5	27.5	26.5	26.5	26.5	27.5	26.5
pI	5.5	6.5	7.5	7.7	8	8	9	9	9.6	9.7	10.7	10.7
Phosphate	+	+						+		+		
SO_4					+			+		+		

Table 5: Characteristics of the isoforms of mIGFBP-6 overexpressed in MDCK cells

O-glycosylation is the only known posttranslational modification of IGFBP-6 (Bach, 1999). Although there is one potential N-glycosylation site in the C-terminus of human, but not of mouse IGFBP-6, this site does not appear to be glycosylated (Hwa et al., 1999). Labeling of MDCK B1 cells with [^{3}H]-galactose confirmed the glycosylation of mIGFBP-6. The mobility shift of the [^{35}S]-methionine labeled 27.5 kDa of less than 1 kDa upon O-glycanase treatment indicated that mIGFBP-6 is O-glycosylated to a minimal extent in MDCK cells. Similarly, the endogenous IGFBP-6 secreted by mouse NIH-3T3 cells contains O-linked carbohydrate residues, contributing 1-1.5 kDa to the molecular mass of the protein (Claussen et al., 1995). These findings suggest, that mIGFBP-6 posseses only one or two O-glycosylated sites.

After the enzymatic deglycosylation of mIGFBP-6, however, still two bands were detectable. This may be explained i) by an incomplete enzymatic deglycosylation, or ii) by the presence of other posttranslational modifications. The efficiency of O-glycanase used for enzymatic deglycosylation depends on the presence of sugar residues attached to the O-linked glycan core structure. Residues commonly found attached to the O-linked carbohydrate core include sialic acid, N-acetylglucosamine, and galactose. N-acetylgalactosamine and fucose are presented less frequently (Brockhausen, 1999). In the present study, only pretreatment with neuraminidase was recommended to facilitate O-glycanase-catalized deglycosylation. Because the sugar composition of the five O-linked olygosaccharide chains in hIGFBP-6 overexpressed in CHO cells are different (Neumann et al., 1999), it is still unclear whether the enzymatic deglycosylation of mIGFBP-6 under the conditions used was complete. However, after chemical deglycosylation using TFMS (trifuoromethanesulfonic acid), which removes O-linked glycanes (Naim et al., 1988), two bands of mIGFBP-6 with apparently the same molecular mass as observed after enzymatic deglycosylation, were detected. These results suggest that mIGFBP-6 possesses other posttranslational modifications than O-glycosylation.

Labeling of MDCK B1 cells with [^{33}P]-orthophosphate or [^{35}S]-sulfate, followed by 2D-electrophoresis showed that four isoforms of mIGFBP-6 are phosphorylated (spot 1, 2, 8, and 10) and three are sulfated (spot 5, 8, 10) (Table 5). Another posttranslational modification, which may contribute to the molecular heterogeneity of mIGFBP-6 is a microheterogeneity of the amino acid sequence. It has been demonstrated that 80% of the hIGFBP-6 overexpressed in CHO cells commences at Arg28 and lacks the C-terminal Gly240, and 18% commences at Leu26 (Neumann et al., 1998). Interestingly, the hIGFBP-6 proform, which has been found to represent about 3% of the total amount of protein,

appeared to be nonglycosylated. Together with the O-glycosylation, such posttranslational modification may explain the high molecular heterogeneity of mIGFBP-6 in MDCK cells, but it is rather unlikely that they are the determinants maintaining the unusual basic pI range (between 5.5 and 10.7) of the mIGFBP-6 isoforms. Human IGFBP-6 isolated from serum and cerebrospinal fluid is constituted by five isoforms in the pI range of 4.8-5.8, detected by nonreducing 2D-electrophoresis (Weber et al., 1999). However, the authors have used self-made IPG gels, whereas in the present work only Immobiline DryStrip gels (AmershamPharmaciaBiotech) were used for isoelectrofocusing. Another difference is the origin and preparation of the samples: in the present study, the proteins were extracted from conditioned media by acetone precipitation, whereas Weber and colleagues have immunoprecipitated IGFBP-6 from serum or have directly applied cerebrospinal fluid onto the IPG gels. Attempts, to immunoprecipitate mIGFBP-6 from media of MDCK cells, followed by nonreducing 2D-electrophoresis proved to be unsuccessful. It has to be confirmed whether acetone precipitation affects the pI of isoforms of recombinant IGFBP-6.

Posttranslational modifications are implicated in modulation of the functions and activities of IGFBPs. O-glycosylation has been described to delay the clearance of IGFBP-6 from the circulation by inhibiting binding to specific receptors, such as hepatic asialoglycoprotein receptor (Marinaro et al., 2000 a). Thus, the binding of nonglycosylated recombinant human IGFBP-6 to a range of glycosaminoglycans *in vitro* has been reported to be approximately 3-fold increased, compared with the glycosylated IGFBP-6 (Marinaro et al., 2000 b). Additionally, when bound to glycosaminoglycans, IGFBP-6 has ~10-fold reduced binding affinity for IGF II. These results indicate that O-glycosylation inhibits binding of IGFBP-6 to glycosaminoglycans and cell membranes, thereby increasing the amount of soluble IGFBP-6. Thus, the free IGFBP-6 is able to bind IGF II with high affinity, inhibiting in this manner the action of IGF II. Furthermore, O-glycosylation has been demonstrated to delay the proteolysis of IGFBP-6 (Marinaro et al, 2000 b).

Sulfation of IGFBP-6 has never been described before and its physiological significance and the stochiometry are unknown. Two types of putative sulfation moieties are present in mIGFBP-6: tyrosine residues and O-glycans. O-sulfation of tyrosine residues is a common posttranslational modification of secretory proteins (Kehoe and Bertozzi, 2000). For numerous proteins sulfation appears to be important for biological activity and correct cellular processing (Vishnuvardhan and Beinfeld, 2000). Although it has been demonstrated that elimination of a tyrosine sulfation site by site-directed mutagenesis

results in transport retardation of the *D. melanogaster* yolk protein from TGN to the cell surface (Friederich et al., 1988) the function of sulfated tyrosine residues as sorting signals remains to be elucidated. Sulfation of O-glycans has been shown to play a role in cell adhesion and in regulation of biosynthetic pathways (Tsuboi et al., 1996).

Four mIGFBP-6 isoforms appeared to be phosphorylated by MDCK cells. Interestingly, two of them were sulfated as well. Among the IGFBPs, phosphorylation has been described only for IGFBP-1, -3, and –5 (Hwa et al., 1999). In normal adult human circulation, IGFBP-1 is present as a single highly phosphorylated species, whereas non-phosphorylated variants are markedly increased in fetal serum and during pregnancy (Westwood et al., 1994). Phosphorylation of IGFBP-1 enhances its affinity to IGFs (Westwood et al., 1997) and inhibits the IGF I stimulated amino acid uptake in trophoblast cells (Yu et al., 1998). In contrast, the phosphorylation of IGFBP-3 does not appear to influence its binding to IGFs (Hoeck and Mukku, 1994). To evaluate the role of phosphorylation for IGFBP-6 function, the phosphorylated sites, the phosphorylation stochiometry, the kinases involved and their regulation have to be investigated.

5.3 Polarized secretion of soluble proteins in MDCK cells

In the present work it was shown that three IGFBPs were detected with approximately 4.2-fold higher abundance in the apical than in the basolateral media of polarized MDCK cells. The same media showed higher proteolytic activity against recombinant human IGFBP-4 and IGFBP-6 in the basolateral than in the apical media. The data suggest that IGFBP proteases may degrade IGFBPs secreted to the basolateral media, resulting in an apparent accumulation of IGFBPs in the apical media. In order to establish a model system to investigate the mechanism of polarized distribution of IGFBPs, mouse IGFBP-6 was selected to be expressed in MDCK cells for the following reasons: i) the easy detection and differentiation of mouse IGFBP-6 in the background of MDCK cells due to the inability of canine IGFBPs to bind biotinylated IGF II (Shalamanova et al., 2000); ii) the exclusive secretion of the O-glycosylated IGFBP-6 in HT29-D4 human colon cancer cells to the apical side, whereas IGFBP-2 and IGFBP-4 (devoid O-glycans) are preferentially secreted to the basolateral side (Pommier et al., 1995); iii) the lowest degree of O-glycosylation of mIGFBP-6 compared with the human and rat IGFBP-6 (Claussen et al., 1995; Bach, 1999). The expression of mIGFBP-6 in MDCK cells showed a similar polarized distribution as it was observed for endogenous canine IGFBPs, i.e. higher apical, than basolateral abundance. This may be explained by i) higher basolateral IGFBP-6 proteolytic activity, ii) basolateral secretion followed by transcytosis and apical secretion, or iii) polarized secretion from MDCK cells. The lack of proteolytic activity against [^{125}I]-IGFBP-6 in media from transfected MDCK cells demonstrated that the polar distribution of mIGFBP-6 is protease-independent. Therefore, it appears that the transfection or selection procedures may impair by unknown mechanism the expression or activation of IGFBP-6 proteases in MDCK cells. Additionally, the failure to detect [^{125}I]-IGFBP-6 in basolateral or apical media after addition and incubation of [^{125}I]-IGFBP-6 in the apical or basolateral media , respectively, of polarized MDCK cells, excluded that transcytosis of IGFBP-6 might be the underlying mechanism for polarized abundance of mIGFBP-6. Hence, the abundance of mIGFBP-6 in the apical media from polarized MDCK B1 cells appears to be the result of a direct sorting mechanism, recognizing specific structural determinant(s) of the binding protein.

Structural signals responsible for the polarized sorting of proteins have been mainly studied for membrane proteins. All characterized basolateral determinants of membrane proteins constitute short cytoplasmic peptide sequences (Martens et al., 2000; Kroepfl and

Gardinier, 2001). In contrast, multiple types of signals in the extracellular, transmembrane, and cytoplasmic domains, as well as GPI-anchors, have been described to direct the sorting of membrane proteins to the apical surface. Among these signals, both, N- and O-linked oligosaccharide chains, seem to function as apical sorting signals (Mostov et al., 2000). In comparison with the targeting determinants of membrane proteins, the sorting signals for soluble proteins are far less studied. N- or O-linked oligosaccharides are proposed to promote the apical secretion of several proteins. Thus, N-glycans have been shown to be important for the apical targeting of erythropoetin and rat growth hormone in MDCK cells (Kitagawa et al., 1994; Benting et al., 1999). Furthermore, the O-glycosylated IGFBP-6 has been demonstrated to be secreted apically from human intestinal epithelial cells, whereas IGFBP-2 and –4 (devoid O-glycans) were released basolaterally (Pommier et al., 1995; Remacle-Bonnet et al., 1995).

In the present study, it was shown that mIGFBP-6 expressed in MDCK cells is O-glycosylated at only one or two sites. However, the O-glycosylation sites of the mIGFBP-6 are not known yet (Bach, 1999). Five sites of the human IGFBP-6 expressed in CHO cells are O-glycosylated (Neumann et al., 1998), where only one of them (S144) is conserved in mIGFBP-6 (S143) as shown in Figure 31. To study the role of O-glycosylation as a determinant for apical targeting, the putative O-glycosylation site S143 in mIGFBP-6 was substituted with an alanine residue by site-directed mutagenesis. Another putative non-conserved O-glycosylation site in the same region of mIGFBP-6, S126, was selected randomly and exchanged with an alanine residue as well (Figure 31).

```
Human      122   PQAGTARPQDVNRRDQQRNPGTSTTPSQPNSAGVQ   156
Mouse      121   PQGGASRSRDTNHRDRQKNPRTSAAPIRPNP--VQ   153
```

Figure 31: O-glycosylated residues of hIGFBP-6 and putative O-glycosylation sites in mIGFBP-6

O-glycosylated hIGFBP-6 sites and the conserved putative O-glycosylation site (S143) in mIGFBP-6 are shown in bold and underlined. The non-conserved putative O-glycosylation site in mIGFBP-6 (A126) is underlined and italic. Amino acid numbering is based on the IGFBP-6 entries IBP6_HUMAN (accession number P24592) and IBP6_MOUSE (accession number P47880).

Comparison of the mIGFBP-6 WT with A126 mutant isoforms in 2D-electrophoresis revealed no significant difference in their patterns and electrophoretic mobilities. However, the 2D-pattern of A143 revealed the appearance of a new spot, and a shift of the mobility of all major spots to lower molecular mass, which was confirmed in SDS-PAGE.

Additionally, three of the isoforms of mIGFBP-6 WT and A126 were not detected in A143. Comparison of the sorting of mIGFBP-6 WT and mIGFBP-6 A126, A143, and the double mutant A126/143 in SDS-PAGE showed, that the substitution of S143 by an alanine residue, slightly affected (by 10%) the sorting efficiency of mIGFBP-6. All mIGFBP-6 mutant forms were still detected preferentially in the apical media. To verify whether the lower percentage of A143 and A126/143 IGFBP-6 forms in the apical media are due to the loss of O-linked carbohydrates, analysis of more mutant cell clones is required. Although the data indicate that S126 is not an O-glycosylation site, the A126 mutant may be a suitable internal marker demonstrating the effect of the substitution of a non-glycosylated serine residue with alanine on the molecular heterogeneity of mIGFBP-6. The present data on the O-glycosylation of mIGFBP-6 are too preliminary to allow a conclusion on the functional role of O-linked carbohydrates. Thus, further studies on the ligand binding properties of the A143 mutant (analysis of the structural role by BIACore measurments), or on sorting of IGFBP-6 forms with other substitutions of potential glycosylation sites or introduction of new N- or O-glycosylation sites, remain to be done. Two models are proposed for the role of O-glycosylation as an apical targeting signal. One model considers oligosaccharides to play a structural role in the correct folding of the proteins (Rodriguez-Boulan and Gonzalez, 1999). According to the second model (lectin-based model), the oligosaccharides bind to a hypothetical lectin which mediates association with lipid rafts and promotes apical sorting (Fiedler and Simons, 1994). It is likely that an interaction of mIGFBP-6 with a specific protein(s) (lectine or non-lectine) is required for its apical targeting. The saturation of such an interacting protein may explain the basolateral accumulation of the overexpressed mIGFBP-6 in MDCK cells. It has been reported that VEGF(165) and TGF-β1 overexpressed in epithelial cells are secreted from the apical site at low expression levels, and both from the apical and basolateral sites at high expression levels, suggesting the presence of saturable apical sorting proteins (Marmorstein et al., 2000). It might be that the analysis of cell clones expressing lower amounts of mIGFBP-6 would provide a more specific mIGFBP-6 isoform pattern in apical and basolateral media.

5.4 Biological effects of mIGFBP-6

IGF I and II exert long-term effects on cell proliferation, differentiation, migration, and apoptosis in an endocrine and autocrine/paracrine manner. The IGF actions are mediated by IGF receptors, and are modulated by six IGF-binding proteins. IGFs have higher affinity for IGFBPs (K_D ~10^{-10} M) than for IGF receptors (K_D ~10^{-8}-10^{-9} M). Thus, IGFBPs primarily inhibit the action of IGFs by sequestration, preventing their binding to the IGF receptrs. IGFBP-6 appears to be a specific inhibitor of the IGF II actions due to its highest affinity for IGF II (K_D 1 – 4 x 10^{-11} M) in comparison with the other IGFBPs (Bach, 1999). Thus, it is demonstrated that IGFBP-6 inhibits the IGF II induced but not the basal proliferation of LIM 1215 colon cancer cells or human fibroblasts (Leng et al., 2001; Putzer et al., 1998). Data of the present study show that the basal proliferation rate of mIGFBP-6 overexpressing MDCK cells was lower than of MDCK pGK cells, which suggests that the endogenously produced IGF II (Ernest et al., 1995) functioning in an autocrine/paracrine manner, is sequestrated. Of interest, exogenous mIGFBP-6 had a marginal effect on the basal proliferation of MDCK B1 cells, whereas it stimulated the proliferation of MDCK pGK cells. Extended studies are required to determine the stability of this effect and the underlying mechanism of action. Exogenous IGF II stimulated the proliferation both in MDCK pGK and MDCK B1 cells to a similar extent. It is likely, that the concentration of the mIGFBP-6 secreted in the fresh medium was too low to prevent the IGF II-initiated long-term stimulation of proliferation. Therefore, the proliferation rate should be determined again by addition of IGF II to cell media, which were already conditioned for 24-48 h. In a second biological approach, the migration of MDCK pGK and MDCK B1 cells was tested in dependence of IGF II and IGFBP-6. The basal migration rate of MDCK pGK cells was significantly higher than the migration rate of MDCK B1 cells. These data suggest, that the overexpressed IGFBP-6 either sequestrates the endogenous IGF II required for cell migration, or inhibits directly the cell migration. Both, exogenous mIGFBP-6 (0.9 µg/ml) and conditioned medium from MDCK B1 estimated to contain 0.9 µg/ml mIGFBP-6, inhibited the basal migration of MDCK pGK and MDCK B1 with more than 35%. The results provide evidence, that mIGFBP-6 may be a strong endogenous as well as exogenous anti-migration factor. The concept of an indirect effect of IGFBP-6 on migration by sequestration of IGF II is supported by the fact that IGF II partially reverses the inhibitory effect of conditioned media from MDCK B1 cells on the migration of MDCK pGK and MDCK B1 cells. On another hand, the stimulation of

migration of MDCK pGK and even to a higher extent of MDCK B1 cells by IGF II, does not agree with the sequestration concept. Alternatively, IGFBP-6 may inhibit the migration of MDCK cells in an IGF-independent manner. It has been reported that expression of IGFBP-6 in human neuroblastoma cells coincides with the inability of IGFs, des(1-3)IGF I (which does not bind to IGFBP-6), or insulin to stimulate their proliferation (Babajko et al., 1997). Recent studies have demonstrated that IGFBP-6 activates the apoptosis in non-small cell lung cancer cells (Sueoka et al., 2000). Extended studies on cell migration are required to verify the IGF-dependent or -independent function of IGFBP-6, e.g. by heterologous expression of IGFBP-6 in IGF II-deficient cells or by antisense-mediated suppression of IGF II in MDCK B1 cells.

6 REFERENCES

Alevizopoulos A., Mermod N., (1997): Transforming growth factor-beta: the breaking open of a black box. *Bioessays* 19: 581-91

Alfalah M., Jacob R., Preuss U., Zimmer K. P., Naim H., Naim H. Y., (1999): O-linked glycans mediate apical sorting of human intestinal sucrase-isomaltase through association with lipid rafts. *Curr Biol* 9: 593-6

Artelt P., Morelle C., Ausmeier M., Fitzek M., Hauser H., (1981): Vectors for efficient expression in mammalian fibroblastoid, myeloid and lymphoid cells via transfection or infection. *Gene* 68: 213-9

Babajko S., Leneuve P., Loret C., Binoux M., (1997): IGF-binding protein-6 is involved in growth inhibition in SH-SY5Y human neuroblastoma cells: its production is both IGF- and cell density-dependent. *J Endocrinol* 152: 221-7

Bach L. A., Thotakura N. R., Rechler M. M., (1992): Human insulin-like growth factor binding protein-6 is O-glycosylated. *Biochem Biophys Res Commun* 186: 301-7

Bach L. A., Salemi R., Leeding K. S., (1995): Roles of insulin-like growth factor (IGF) receptors and IGF-binding proteins in IGF-II-induced proliferation and differentiation of L6A1 rat myoblasts. *Endocrinology* 136: 5061-9

Bach L. A., (1999): Insulin-like growth factor binding protein-6: the "forgotten" binding protein? *Horm Metab Res* 31: 226-34

Benting J. H., Rietveld A. G., Simons K., (1999): N-Glycans mediate the apical sorting of a GPI-anchored, raft-associated protein in Madin-Darby canine kidney cells. *J Cell Biol* 146: 313-20

Besnard V., Corroyer S., Trugnan G., Chadelat K., Nabeyrat E., Cazals V., Clement A., (2001): Distinct patterns of insulin-like growth factor binding protein (IGFBP)-2 and IGFBP-3 expression in oxidant exposed lung epithelial cells. *Biochim Biophys Acta* 1538: 47-58

Black R. A., Rauch C. T., Kozlosky C. J., Peschon J. J., Slack J. L., Wolfson M. F., Castner B. J., Stocking K. L., Reddy P., Srinivasan S., Nelson N., Boiani N., Schooley

K.A., Gerhart M., Davis R., Fitzner J. N., Johnson R. S., Paxton R. J., March C. J., Cerretti D. P., (1995): A metalloproteinase disintegrin that releases tumour-necrosis factor-alpha from cells. *Nature* 385: 729-33

Blum H., Hildburg B., Gross H., (1987): Improved silver staining of plant proteins, RNA and DNA in polyacrylamide gels. *Electrophoresis* 8: 93-99

Booth B. A., Boes M., Dake B. L., Linhardt R. J., Caldwell E. E., Weiler J. M., Bar R. S., (1996): Structure-function relationships in the heparin-binding C-terminal region of insulin-like growth factor binding protein-3. *Growth Regul* 6: 206-13

Braulke T., (1999 a): Type-2 IGF receptor: a multi-ligand binding protein. *Horm Metab Res* 31: 242-6

Braulke T., Dittmer F., Gotz W., von Figura K., (1999 b): Alteration in pancreatic immunoreactivity of insulin-like growth factor (IGF)-binding protein (IGFBP)-6 and in intracellular degradation of IGFBP-3 in fibroblasts of IGF-II receptor/IGF-II-deficient mice. *Horm Metab Res* 31: 235-41

Braulke T., Claussen M., Saftig P., Wendland M., Neifer K., Schmidt B., Zapf J., von Figura K., Peters C., (1995): Proteolysis of IGFBPs by cathepsin D in vitro and in cathepsin D-deficient mice. *Prog Growth Factor Res* 6: 265-71

Brewer C. B., Roth M. G., (1995): Polarized exocytosis in MDCK cells is regulated by phosphorylation. *J Cell Sci* 108:789-96

Brockhausen I., (1999): Pathways of O-glycan biosynthesis in cancer cells. *Biochim Biophys Acta* 1473: 67-95

Brodt P., Samani A., Navab R., (2000): Inhibition of the type I insulin-like growth factor receptor expression and signaling: novel strategies for antimetastatic therapy. *Biochem Pharmacol* 60: 1101-7

Busby W. H. Jr., Nam T. J., Moralez A., Smith C., Jennings M., Clemmons D. R., (2000): The complement component C1s is the protease that accounts for cleavage of insulin-like growth factor-binding protein-5 in fibroblast medium. *J Biol Chem* 275: 37638-44

Byun D., Mohan S., Yoo M., Sexton C., Baylink D. J., Qin X., (2001): Pregnancy-associated plasma protein-A accounts for the insulin-like growth factor (IGF)-binding

protein-4 (IGFBP-4) proteolytic activity in human pregnancy serum and enhances the mitogenic activity of IGF by degrading IGFBP-4 in vitro. *J Clin Endocrinol Metab* 86: 847-54

Caplan M. J., (1997): Membrane polarity in epithelial cells: protein sorting and establishment of polarized domains. *Am J Physiol* 272: F425-9

Chen C. and Okayama H., (1987): High-efficiency transformation of mammalian cells by plasmid DNA. *Mol Cell Biol* 7: 2745-2752

Claussen M., Buergisser D., Schuller A.G., Matzner U., Braulke T., (1995): Regulation of insulin-like growth factor (IGF)-binding protein-6 and mannose 6-phosphate/IGF-II receptor expression in IGF-IL-overexpressing NIH 3T3 cells. *Mol Endocrinol* 9: 902-12

Claussen M., Kubler B., Wendland M., Neifer K., Schmidt B., Zapf J., Braulke T. (1997): Proteolysis of insulin-like growth factors (IGF) and IGF binding proteins by cathepsin D. *Endocrinology* 138: 3797-803

Conover C. A., De Leon D. D., (1994): Acid-activated insulin-like growth factor-binding protein-3 proteolysis in normal and transformed cells. Role of cathepsin D. *J Biol Chem* 269: 7076-80

Conover C. A., (2000): In vitro studies of insulin-like growth factor I and bone. *Growth Horm IGF Res* 10 Suppl B: S107-10

Conover C. A., Faessen G. F., Ilg K. E., Chandrasekher Y. A., Christiansen M., Overgaard M. T., Oxvig C., Giudice L. C., (2001): Pregnancy-associated plasma protein-a is the insulin-like growth factor binding protein-4 protease secreted by human ovarian granulosa cells and is a marker of dominant follicle selection and the corpus luteum. *Endocrinology* 142: 2155

Coverley J. A., Baxter R. C., (1997): Phosphorylation of insulin-like growth factor binding proteins. *Mol Cell Endocrinol* 128: 1-5

Creemers E. E., Cleutjens J. P., Smits J. F., Daemen M. J., (2001): Matrix metalloproteinase inhibition after myocardial infarction: a new approach to prevent heart failure? *Circ Res* 89: 201-10

Dennis P. A., Rifkin D. B., (1991): Cellular activation of latent transforming growth factor beta requires binding to the cation-independent mannose 6-phosphate/insulin-like growth factor type II receptor. *Proc Natl Acad Sci U S A* 88 : 580-4

Edge A., Faltynek C., Hof L., Reichert L. Jr., Weber P., (1981): Deglycosylation of glycoproteins by trifluoromethanesulfonic acid. *Anal Biochem* 118: 131-7

Ernest S., Coureau C., Escoubet B., (1995): Deprivation of phosphate increases IGF-II mRNA in MDCK cells but IGFs are not involved in phosphate transport adaptation to phosphate deprivation. *J Endocrinol* 145: 325-31

Fanning A. S., Anderson J. M. (1999): Protein modules as organizers of membrane structure. *Curr Opin Cell Biol* 11: 432-9

Feld S., Hirschberg R., (1996): Growth hormone, the insulin-like growth factor system, and the kidney. *Endocr Rev* 17: 423-80

Fiedler K., Simons K., (1994): A putative novel class of animal lectins in the secretory pathway homologous to leguminous lectins. *Cell* 77: 625-6

Fiedler K., Simons K., (1995): The role of N-glycans in the secretory pathway. *Cell* 81: 309-12

Folsch H., Ohno H., Bonifacino J. S., Mellman I., (1999): A novel clathrin adaptor complex mediates basolateral targeting in polarized epithelial cells. *Cell* 99: 189-98

Forbes B., Ballard F. J., Wallace J. C., (1990): An insulin-like growth factor-binding protein purified from medium conditioned by a human lung fibroblast cell line (He[39]L) has a novel N-terminal sequence. *J Endocrinol* 126: 497-506

Forbes B. E., Turner D., Hodge S. J., McNeil K. A., Forsberg G., Wallace J. C., (1998): Localization of an insulin-like growth factor (IGF) binding site of bovine IGF binding protein-2 using disulfide mapping and deletion mutation analysis of the C-terminal domain. *J Biol Chem* 273: 4647-52

Fowlkes J. L., Thrailkill K. M., George-Nascimento C., Rosenberg C. K., Serra D. M., (1997): Heparin-binding, highly basic regions within the thyroglobulin type-1 repeat of insulin-like growth factor (IGF)-binding proteins (IGFBPs) -3, -5, and -6 inhibit IGFBP-4 degradation. *Endocrinology* 138 (6): 2280-5

Friederich E., Fritz H. J., Huttner W. B., (1988): Inhibition of tyrosine sulfation in the trans-Golgi retards the transport of a constitutively secreted protein to the cell surface. *J Cell Biol* 107: 1655-67

Fullekrug J., Scheiffele P., Simons K., (1999): VIP36 localisation to the early secretory pathway. *J Cell Sci* 112: 2813-21

Gibson T. L., Cohen P., (1999): Inflammation-related neutrophil proteases, cathepsin G and elastase, function as insulin-like growth factor binding protein proteases. *Growth Horm IGF Res* 9: 241-53

Gilpin B. J., Loechel F., Mattei M. G., Engvall E., Albrechtsen R., Wewer U. M., (1999): A novel, secreted form of human ADAM 12 (meltrin alpha) provokes myogenesis in vivo. *J Biol Chem* 273: 157-66

Granerus M., Engstrom W., (2001): Effects of insulin-like growth factor-binding protein 2 and an igf-type i receptor-blocking antibody on apoptosis in human teratocarcinoma cells in vitro. *Cell Biol Int* 25: 825-8

Gut A., Kappeler F., Hyka N., Balda M. S., Hauri H. P., Matter K., (1998): Carbohydrate-mediated Golgi to cell surface transport and apical targeting of membrane proteins. *EMBO J* 17: 1919-29

Hanahan D., (1985): Techniques for transformation of *E. coli*. Glover, D. M., eds., in DNA cloning, IRL press, Oxford.

Hannan L. A., Edidin M., (1996): Traffic, polarity, and detergent solubility of a glycosylphosphatidylinositol-anchored protein after LDL-deprivation of MDCK cells. *J Cell Biol* 133: 1265-76

Ho P. J., Baxter R. C., (1997): Characterization of truncated insulin-like growth factor-binding protein-2 in human milk. *Endocrinology* 138: 3811-8

Hoeck W. G., Mukku V. R., (1994): Identification of the major sites of phosphorylation in IGF binding protein-3. *J Cell Biochem* 56: 262-73

Hwa V., Oh Y., Rosenfeld R. G., (1999): The insulin-like growth factor-binding protein (IGFBP) superfamily. *Endocr Rev* 20: 761-87

Irwin J. C., Suen L. F., Cheng B. H., Martin R., Cannon P., Deal C. L., Giudice L.C., (2000): Human placental trophoblasts secrete a disintegrin metalloproteinase very similar to the insulin-like growth factor binding protein-3 protease in human pregnancy serum. *Endocrinology* 141: 666-74

Jones J. I., Clemmons D. R., (1995): Insulin-like growth factors and their binding proteins: biological actions. *Endocr Rev* 16: 3-34

Kang J. X., Bell J., Beard R. L., Chandraratna R. A., (1999): Mannose 6-phosphate/insulin-like growth factor II receptor mediates the growth-inhibitory effects of retinoids. *Cell Growth Differ* 10: 591-600

Kehoe J. W., Bertozzi C. R., (2000): Tyrosine sulfation: a modulator of extracellular protein-protein interactions. *Chem Biol* 7: R57-61

Kim S. K., (1997): Polarized signaling: basolateral receptor localization in epithelial cells by PDZ-containing proteins. *Curr Opin Cell Biol* 9: 853-9

Kitagawa Y., Sano Y., Ueda M., Higashio K., Narita H., Okano M., Matsumoto S., Sasaki R., (1994): N-glycosylation of erythropoietin is critical for apical secretion by Madin-Darby canine kidney cells. *Exp Cell Res* 213: 449-57

Korner C., Nurnberg B., Uhde M., Braulke T., (1995): Mannose 6-phosphate/insulin-like growth factor II receptor fails to interact with G-proteins. Analysis of mutant cytoplasmic receptor domains. *J Biol Chem* 270: 287-95

Kornfeld S., (1990): Lysosomal enzyme targeting. *Biochem Soc Trans* 18: 367-74

Kroepfl J. F., Gardinier M. V., (2001): Identification of a basolateral membrane targeting signal within the cytoplasmic domain of myelin/oligodendrocyte glycoprotein. *J Neurochem* 77: 1301-9

Kubler B., Cowell S., Zapf J., Braulke T., (1998): Proteolysis of insulin-like growth factor binding proteins by a novel 50-kilodalton metalloproteinase in human pregnancy serum. *Endocrinology* 139: 1556-63

Kurihara S., Hakuno F., Takahashi S., (2000): Insulin-like growth factor-I-dependent signal transduction pathways leading to the induction of cell growth and differentiation of

human neuroblastoma cell line SH-SY5Y: the roles of MAP kinase pathway and PI 3-kinase pathway. *Endocr J* 47: 39-51

Laemmli U., (1970): Cleavage of structural proteins during the assembly of the head of bacteriophage T4. *Nature* 227: 680-685

Larsen J. E., Avvakumov G. V., Hammond G. L., Vogel L. K., (1999): N-glycans are not the signal for apical sorting of corticosteroid binding globulin in MDCK cells. *FEBS Lett* 451: 19-22

Laskey R. A., Mills A. D., (1975): Quantitative film detection of 3H and 14C in polyacrylamide gels by fluorography. *Eur J Biochem* 56: 335-41

Lawrence J. B., Oxvig C., Overgaard M. T., Sottrup-Jensen L., Gleich G. J., Hays L. G., Yates J. R. 3rd, Conover C. A., (1999): The insulin-like growth factor (IGF)-dependent IGF binding protein-4 protease secreted by human fibroblasts is pregnancy-associated plasma protein-A. *Proc Natl Acad Sci USA* 96: 3149-53

Le Maout S., Welling P. A., Brejon M., Olsen O., Merot J., (2001): Basolateral membrane expression of a K+ channel, Kir 2.3, is directed by a cytoplasmic COOH-terminal domain. *Proc Natl Acad Sci USA* 98: 10475-80

Le Roith D., (2000): Regulation of proliferation and apoptosis by the insulin-like growth factor I receptor. *Growth Horm IGF Res* 10 Suppl A: S12-3

Leal S. M., Liu Q., Huang S. S., Huang J. S., (1997): The type V transforming growth factor beta receptor is the putative insulin-like growth factor-binding protein 3 receptor. *J Biol Chem* 272: 20572-6

Leng S. L., Leeding K S., Whitehead R. H., Bach L. A., (2001): Insulin-like growth factor (IGF)-binding protein-6 inhibits IGF-II-induced but not basal proliferation and adhesion of LIM 1215 colon cancer cells. *Mol Cell Endocrinol* 174: 121-7

Lin S., Naim H. Y., Chapin Rodriguez A., Roth M. G., (1998): Mutations in the Middle of the Transmembrane Domain Reverse the Polarity of Transport of the Influenza Virus Hemagglutinin in MDCK Epithelial Cells. *J Cell Biol* 142: 51-57

Lipardi C., Nitsch L., Zurzolo C., (2000): Detergent-insoluble GPI-anchored proteins are apically sorted in fischer rat thyroid cells, but interference with cholesterol or sphingolipids differentially affects detergent insolubility and apical sorting. *Mol Biol Cell* 11: 531-42

Liu B., Lee H. Y., Weinzimer S. A., Powell D. R., Clifford J. L., Kurie J. M., Cohen P., (2000): Direct functional interactions between insulin-like growth factor-binding protein-3 and retinoid X receptor-alpha regulate transcriptional signaling and apoptosis. *J Biol Chem* 275: 33607-13

Liu W., Liu Y., Lowe W. L. Jr., (2001): The role of phosphatidylinositol 3-kinase and the mitogen-activated protein kinases in insulin-like growth factor-I-mediated effects in vascular endothelial cells. *Endocrinology* 142: 1710-9

Loechel F., Fox J. W., Murphy G., Albrechtsen R., Wewer U. M., (2000): ADAM 12-S cleaves IGFBP-3 and IGFBP-5 and is inhibited by TIMP-3. *Biochem Biophys Res Commun* 278: 511-5

Loechel F., Gilpin B. J., Engvall E., Albrechtsen R., Wewer U. M., (1998): Human ADAM 12 (meltrin alpha) is an active metalloprotease. *J Biol Chem* 273: 16993-7

Lowry O., Rosebrough N., Farr A., Randall R., (1951): Protein measurments with the folin phenol reagent. *J Biol Chem* 193: 265-275

Ludwig T., Eggenschwiler J., Fisher P., D'Ercole A. J., Davenport M. L., Efstratiadis A., (1996): Mouse mutants lacking the type 2 IGF receptor (IGF2R) are rescued from perinatal lethality in Igf2 and Igf1r null backgrounds. *Dev Biol* 177: 517-35

Magee A. I., Siddle K., (1988): Insulin and IGF-1 receptors contain covalently bound palmitic acid. *J Cell Biochem* 37: 347-57

Marinaro J. A., Hendrich E. C., Leeding K. S., Bach L.A., (1999 a): HaCaT human keratinocytes express IGF-II, IGFBP-6, and an acid-activated protease with activity against IGFBP-6. *Am J Physiol* 276 (3 Pt 1): E536-42

Marinaro J. A., Jamieson G. P., Hogarth P. M., Bach L. A.., (1999 b): Differential dissociation kinetics explain the binding preference of insulin-like growth factor binding protein-6 for insulin-like growth factor-II over insulin-like growth factor-I. *FEBS Lett* 450: 240-4

Marinaro J. A., Casley D. J., Bach L. A., (2000 a): O-glycosylation delays the clearance of human IGF-binding protein-6 from the circulation. *Eur J Endocrinol* 142: 512-6

Marinaro J. A., Neumann G. M., Russo V. C., Leeding K. S., Bach L. A., (2000 b): O-glycosylation of insulin-like growth factor (IGF) binding protein-6 maintains high IGF-II binding affinity by decreasing binding to glycosaminoglycans and susceptibility to proteolysis. *Eur J Biochem* 267: 5378-86

Marmorstein A. D., Csaky K. G., Baffi J., Lam L., Rahaal F., Rodriguez-Boulan E., (2000): Saturation of, and competition for entry into, the apical secretory pathway. *Proc. Natl Acad Sci USA* 97: 3248-53

Martens A. S., Bode J. G., Heinrich P. C., Graeve L., (2000): The cytoplasmic domain of the interleukin-6 receptor gp80 mediates its basolateral sorting in polarized madin-darby canine kidney cells. *J Cell Sci* 113: 3593-602

McGwire G. B., Becker R. P., Skidgel R. A., (1999): Carboxypeptidase M, a glycosylphosphatidylinositol-anchored protein, is localized on both the apical and basolateral domains of polarized Madin-Darby canine kidney cells. *J Biol Chem* 274: 31632-40

McKinnon T., Chakraborty C., Gleeson L. M., Chidiac P., Lala P. K., (2001): Stimulation of human extravillous trophoblast migration by IGF II is mediated by IGF type 2 receptor involving inhibitory g protein(s) and phosphorylation of MAPK. *J Clin Endocrinol Metab* 86: 3665-74

Minniti C. P., Kohn E. C., Grubb J. H., Sly W. S., Oh Y., Muller H. L., Rosenfeld R. G., Helman L. J., (1992): The insulin-like growth factor II (IGF-II)/mannose 6-phosphate receptor mediates IGF-II-induced motility in human rhabdomyosarcoma cells. *J Biol Chem* 267: 9000-4

Miquelis R., Courageot J., Jacq A., Blanck O., Perrin C., Bastiani P., (1993): Intracellular routing of GLcNAc-bearing molecules in thyrocytes: selective recycling through the Golgi apparatus. *J Cell Biol* 123 (6 Pt 2): 1695-706

Mohler K. M., Sleath P. R., Fitzner J. N., Cerretti D. P., Alderson M., Kerwar S. S., Torrance D. S., Otten-Evans C., Greenstreet T., Weerawarna K., Kronheim S. R., Petersen M., Gerhart M., Kozlosky C. J., March C. J., and Black R. A., (1994): Protection against a

lethal dose of endotoxin by an inhibitor of tumour necrosis factor processing. *Nature* 370: 218-220

Moll M., Klenk H. D., Herrler G., Maisner A., (2001): A single amino acid change in the cytoplasmic domains of measles virus glycoproteins H and F alters targeting, endocytosis, and cell fusion in polarized Madin-Darby canine kidney cells. *J Biol Chem* 276 (21): 7887-94

Monlauzeur L., Breuza L., Le Bivic A., (1998): Putative O-glycosylation sites and a membrane anchor are necessary for apical delivery of the human neurotrophin receptor in Caco-2 cells. *J Biol Chem* 273 (46): 30263-70

Mortensen R., Zubiaur M., Neer E., Seidman J., (1991): Embryonic stem cells lacking a functional inhibitory G-protein subunit (alpha i2) produced by gene targeting of both alleles. *Proc Natl Acad Sci U S A* 88: 7036-40

Mostov K. E., Verges M., Altschuler Y., (2000): Membrane traffic in polarized epithelial cells. *Curr Opin Cell Biol* 12: 483-90

Munger J. S., Harpel J. G., Gleizes P. E., Mazzieri R., Nunes I., Rifkin D. B., (1997): Latent transforming growth factor-beta: structural features and mechanisms of activation. *Kidney Int* 51: 1376-82

Nadler L. S., Kumar G., Nathanson N. M., (2001): Identification of a basolateral sorting signal for the M3 muscarinic acetylcholine receptor in Madin-Darby canine kidney cells. *J Biol Chem* 276: 10539-47

Naim H. Y., Sterchi E. E., Lentze M. J., (1988): Biosynthesis of the human sucrase-isomaltase complex. Differential O-glycosylation of the sucrase subunit correlates with its position within the enzyme complex. *J Biol Chem* 263: 7242-53

Naim H. Y., Joberty G., Alfalah M., Jacob R., (1999): Temporal association of the N- and O-linked glycosylation events and their implication in the polarized sorting of intestinal brush border sucrase-isomaltase, aminopeptidase N, and dipeptidyl peptidase IV. *J Biol Chem* 274: 17961-7

Neumann G. M., Marinaro J. A., Bach L. A., (1998): Identification of O-glycosylation sites and partial characterization of carbohydrate structure and disulfide linkages of human insulin-like growth factor binding protein 6. *Biochemistry* 37: 6572-85

Nishimoto I. (1993): The IGF-II receptor system: a G protein-linked mechanism. *Mol Reprod Dev* 35: 398-406

Nykjaer A., Christensen E. I., Vorum H., Hager H., Petersen C. M., Roigaard H., Min H. Y., (1998): Mannose 6-phosphate/insulin-like growth factor-II receptor targets the urokinase receptor to lysosomes via a novel binding interaction. *J Cell Biol* 141: 815-28

Oh Y., (1998): IGF-independent regulation of breast cancer growth by IGF binding proteins. *Breast Cancer Res Treat* 47:283-93

Oh Y., Muller H. L., Pham H., Rosenfeld R. G., (1993): Demonstration of receptors for insulin-like growth factor binding protein-3 on Hs578T human breast cancer cells. *J Biol Chem* 268: 26045-8

Oka Y., Czech M. P., (1986): The type II insulin-like growth factor receptor is internalized and recycles in the absence of ligand. *J Biol Chem* 261: 9090-3

Oosterlaken-Dijksterhuis M., Kwant M., Slob A., Hellmen E., Mol J., (1999): IGF-I and retinoic acid regulate the distribution pattern of IGFBPs synthesized by the canine mammary tumor cell line CMT-U335. *Breast Cancer Res Treat* 54: 11-23

Parker K., Strominger J., (1983): Localization of the sites of iodination of human β2-microglobulin: Quaternay structure implications for histocompatibility antigens. *Biochemistry* 22: 1145-1153

Peifer M., Tepass U. (2000): Cell biology. Which way is up? *Nature* 403: 611-2

Pommier G. J., Remacle-Bonnet M..M., Tripier S. G., Garrouste F.L., (1995): Differential secretory polarity of IGFBP-6 vs. IGFBP-2 and IGFBP-4 in human intestinal epithelial cells: is it a way of modulating IGF-II bioavailability towards the IGF-responsive basolateral surface? *Prog Growth Factor Res* 6:197-206

Prydz K., Brandli A. W., Bomsel M., Simons K., (1990): Surface distribution of the mannose 6-phosphate receptors in epithelial Madin-Darby canine kidney cells. *J Biol Chem* 265: 12629-35

Putzer P., Breuer P., Gotz W., Gross M., Kubler B., Scharf J. G., Schuller A. G., Hartmann H., Braulke T., (1998): Mouse insulin-like growth factor binding protein-6: expression, purification, characterization and histochemical localization. *Mol Cell Endocrinol* 137: 69-78

Rajah R., Nachajon R. V., Collins M. H., Hakonarson H., Grunstein M. M., Cohen P., (1999): Elevated levels of the IGF-binding protein protease MMP-1 in asthmatic airway smooth muscle. *Am J Respir Cell Mol Biol* 20: 199-208

Rajah R., Bhala A., Nunn S. E., Peehl D. M., Cohen P., (1996): 7S nerve growth factor is an insulin-like growth factor-binding protein protease. *Endocrinology* 137: 2676-82

Rehault S., Monget P., Mazerbourg S., Tremblay R., Gutman N., Gauthier F., Moreau T., (2001): Insulin-like growth factor binding proteins (IGFBPs) as potential physiological substrates for human kallikreins hK2 and hK3. *Eur J Biochem* 268 : 2960-8

Remacle-Bonnet M., Garrouste F., el Atiq F., Marvaldi J., Pommier G., (1995): Cell polarity of the insulin-like growth factor system in human intestinal epithelial cells. Unique apical sorting of insulin-like growth factor binding protein-6 in differentiated human colon cancer cells. *J Clin Invest* 96: 192-200

Richo G., Conner G. E., (1991): Proteolytic activation of human procathepsin D. *Adv Exp Med Biol* 306: 289-96

Rodriguez-Boulan E., Gonzalez A., (1999): Glycans in post-Golgi apical targeting: sorting signals or structural props? *Trends Cell Biol* 9: 291-4

Roghani M., Lassarre C., Zapf J., Povoa G., Binoux M., (1991): Two insulin-like growth factor (IGF)-binding proteins are responsible for the selective affinity for IGF-II of cerebrospinal fluid binding proteins. *J Clin Endocrinol Metab* 73: 658-66

Scharf J. G., Knittel T., Dombrowski F., Muller L., Saile B., Braulke T., Hartmann H., Ramadori G., (1998 a): Characterization of the IGF axis components in isolated rat hepatic stellate cells. *Hepatology* 27: 1275-84

Scharf J. G., Schmidt-Sandte W., Pahernik S. A., Ramadori G., Braulke T., Hartmann H., (1998 b): Characterization of the insulin-like growth factor axis in a human hepatoma cell line (PLC). *Carcinogenesis* 19: 2121-8

Scharf J. G., Braulke T., Hartmann H., Ramadori G., (2001): Regulation of the components of the 150 kDa IGF binding protein complex in cocultures of rat hepatocytes and Kupffer cells by 3',5'-cyclic adenosine monophosphate. *J Cell Physiol* 186: 425-36

Scheiffele P., Peranen J., Simons K., (1995): N-glycans as apical sorting signals in epithelial cells. *Nature* 378: 96-8

Schuller A., Groffen C., van Neck J., Zwarthoff E., Drop S., (1994): cDNA cloning and mRNA expression of the six mouse insulin-like growth factor binding proteins. *Mol Cell Endocrinol* 104: 57-66

Schmidt N., Westphal M., Hagel C., Ergun S., Stavrou D., Rosen E., Lamszus K., (1999): Levels of vascular endothelial growth factor, hepatocyte growth factor/scatter factor and basic fibroblast growth factor in human gliomas and their relation to angiogenesis. *Int. J. Cancer* 84: 10-8

Schmidt K., Schrader M., Kern H. F., Kleene R., (2001): Regulated apical secretion of zymogens in rat pancreas. Involvement of the glycosylphosphatidylinositol-anchored glycoprotein GP-2, the lectin ZG16p, and cholesterol-glycosphingolipid-enriched microdomains. *J Biol Chem* 276: 14315-23

Shalamanova L., Kubler B., Scharf J. G., Braulke T., 2000: Ligand blotting: iodinated vs biotinylated IGF. *Growth Horm IGF Res*10: 294

Shi Z., Xu W., Loechel F., Wewer U. M., Murphy L. J., (2000): ADAM 12, a disintegrin metalloprotease, interacts with insulin-like growth factor-binding protein-3. *J Biol Chem* 275: 18574-80

Shindo T., Kurihara H., Kuno K., Yokoyama H., Wada T., Kurihara Y., Imai T., Wang Y., Ogata M., Nishimatsu H., Moriyama N., Oh-hashi Y., Morita H., Ishikawa T., Nagai R., Yazaki Y., Matsushima K., (2000): ADAMTS-1: a metalloproteinase-disintegrin essential for normal growth, fertility, and organ morphology and function. *J Clin Invest* 105: 1345-52

Srinivasan N., Edwall D., Linkhart T. A., Baylink D. J., Mohan S., (1996): Insulin-like growth factor-binding protein-6 produced by human PC-3 prostate cancer cells: isolation, characterization and its biological action. *J Endocrinol* 149: 297-303

Standker L., Braulke T., Mark S., Mostafavi H., Meyer M., Honing S., Gimenez-Gallego G., Forssmann W. G., (2000): Partial IGF affinity of circulating N- and C-terminal fragments of human insulin-like growth factor binding protein-4 (IGFBP-4) and the disulfide bonding pattern of the C-terminal IGFBP-4 domain. *Biochemistry* 39: 5082-8

Sueoka N., Lee H. Y., Wiehle S., Cristiano R. J., Fang B., Ji L., Roth J. A., Hong W. K., Cohen P., Kurie J. M., (2000): Insulin-like growth factor binding protein-6 activates programmed cell death in non-small cell lung cancer cells. *Oncogene* 19: 4432-6

Sun A. Q., Ananthanarayanan M., Soroka C. J., Thevananther S., Shneider B. L., Suchy F. J., (1998): Sorting of rat liver and ileal sodium-dependent bile acid transporters in polarized epithelial cells. *Am J Physiol* 275: G1045-55

Tang B. L., (2001): ADAMTS: a novel family of extracellular matrix proteases. *Int. J Biochem Cell Biol* 33: 33-44

Towbin H., Staehelin T., Gordon J., (1979): Electrophoretic transferof proteins from polyacrylamide gels to nitrocellulose sheets: Procedure and some applications. *Proc Natl Acad Sci USA* 76: 4350-4354

Tsuboi S., Isogai Y., Hada N., King J. K., Hindsgaul O., Fukuda M., (1996):6'-Sulfo sialyl Lex but not 6-sulfo sialyl Lex expressed on the cell surface supports L-selectin-mediated adhesion. *J Biol Chem* 271: 27213-6

Ullrich A., Gray A., Tam A. W., Yang-Feng T., Tsubokawa M., Collins C., Henzel W., Le Bon T., Kathuria S., Chen E., et al., (1986): Insulin-like growth factor I receptor primary structure: comparison with insulin receptor suggests structural determinants that define functional specificity. *EMBO J* 5: 2503-12

Weber M. M., Spottl G., Gossl C., Engelhardt D., (1999): Characterization of human insulin-like growth factor-binding proteins by two-dimensional polyacrylamide gel electrophoresis and Western ligand blot analysis. *J Clin Endocrinol Metab* 84: 1679-84

Westwood M., Gibson J. M., Davies A. J., Young R. J., White A., (1994): The phosphorylation pattern of insulin-like growth factor-binding protein-1 in normal plasma is different from that in amniotic fluid and changes during pregnancy. *J Clin Endocrinol Metab* 79: 1735-41

Westwood M., Gibson J. M., White A., (1997): Purification and characterization of the insulin-like growth factor-binding protein-1 phosphoform found in normal plasma. *Endocrinology* 138: 1130-6

Wu H. B., Lee C.Y., Rechler M. M., (1999): Proteolysis of insulin-like growth factor binding protein-3 in serum from pregnant, non-pregnant and fetal rats by matrix metalloproteinases and serine proteases. *Horm Metab Res* 31: 186-91

van Doorn J., Ringeling A. M., Shmueli S. S., Kuijpers M. C., Hokken-Koelega A. C., van Buul-Offers S. C., Jansen M., (1999): Circulating levels of human insulin-like growth factor binding protein-6 (IGFBP-6) in health and disease as determined by radioimmunoassay. *Clin Endocrinol (Oxf)* 50: 601-9

Vishnuvardhan D., Beinfeld M. C., (2000): Role of tyrosine sulfation and serine phosphorylation in the processing of procholecystokinin to amidated cholecystokinin and its secretion in transfected AtT-20 cells. *Biochemistry* 39: 13825-30

Yamanaka Y., Fowlkes J. L., Wilson E M., Rosenfeld R. G., Oh Y., (1999): Characterization of insulin-like growth factor binding protein-3 (IGFBP-3) binding to human breast cancer cells: kinetics of IGFBP-3 binding and identification of receptor binding domain on the IGFBP-3 molecule. *Endocrinology* 140 (3): 1319-28

Yeaman C., Le Gall A. H., Baldwin A. N., Monlauzeur L., Le Bivic A., Rodriguez-Boulan E., (1997): The O-glycosylated stalk domain is required for apical sorting of neurotrophin receptors in polarized MDCK cells. *J Cell Biol* 139: 929-40

Yu J., Iwashita M., Kudo Y., Takeda Y., (1998): Phosphorylated insulin-like growth factor (IGF)-binding protein-1 (IGFBP-1) inhibits while non-phosphorylated IGFBP-1 stimulates IGF-I-induced amino acid uptake by cultured trophoblast cells. *Growth Horm IGF Res* 8: 65-70

Zapf J., Walter M., Froesch E. R., (1981): Radioimmunological determination of insulin-like growth factor I and II in normal subjects and in patients with growth disorders and extrapancreatic tumor glycemia. *J Clin Invest* 68: 1321-1330

Zegers M. M., Hoekstra D., (1998): Mechanisms and functional features of polarized membrane traffic in epithelial and hepatic cells. *Biochem J* 336 (Pt 2): 257-69

Zeslawski W., Beisel H. G., Kamionka M., Kalus W., Engh R. A., Huber R., Lang K., Holak T. A., (2001): The interaction of insulin-like growth factor-I with the N-terminal domain of IGFBP-5. *EMBO J* 20: 3638-44

ACKNOWLEDGEMENTS

I would like to express my thanks to the following people for their support during the course of this study.

To Prof. K. von Figura, for reviewing this thesis and for his critical comments.

To Prof. G. Gottschalk, for acting as reviewer.

To Prof. T. Braulke, for his support, guidance, and **patience** during our common work, for his permanent question 'For what.....?', and for the unforgetable professional and personal lessons. ☺

To my wonderful colleagues, Bernd Kübler, Stephan Storch, Peter Breuer, Jens-Gerd Scharf, Udaya Yerramalla, Milena Koleva, Karin Fritsch, Claudia Heine, Sanna Partanen, Uwe Andag, Susanne Hupe, Stefanie Heidrich, Andrea Zeisser, and all the young medical doctors from Kinderklinik, UKE, Hamburg, for their friendship, help, encouragement, high spirit and .....GOOD MOOD. ☺

To my teachers, to Lama Ole and Hannah Nydahl, to my numerous friends in Bulgaria and Germany, who gave and give me moral support and never let me lose my sense of humor.

And last but not least, to my dear Bulgarian-German family: Мамо, татко и Жоро, това което съм постигнала, го дължа на вас! Herzlichen Dank meinen Schwiegereltern, sowie Dana, Katja, Ina, Martin, Angelika und Uwe. Most of all I would like to thank my husband, Peter Malinowski, for his love and unlimited support (Благодаря ти от сърце, моя любов!).

Thank you!

LEBENSLAUF

Am 20. Februar 1972 wurde ich, Liliana Shalamanova-Malinowski, als erstes Kind von Stefka Shalamanova (geborene Tzvetkova) und Dimitar Shalamanov in Sofia, Bulgarien, geboren.

Von 1979 bis 1986 besuchte ich die „10te Grund- und Realschule Hristo Lambov“, Sofia. 1986 setzte ich meine Schulausbildung an Sofias Hochschule für Mathematik, Informatik und Naturwissenschaften fort, und schloss dort 1990 mit dem Abitur ab.

Im Oktober 1990 wurde ich als Student an der „Sofia Universität St. Kliment Ohridski“, Biologische Fakultät, Fachbereich Biochemie, angenommen. Nach Fertigstellung meiner Diplomarbeit „Kinetik der Proliferation von Brustkrebs-Zellen“ am „Nationalen Onkologischen Institut“ in Sofia, erhielt ich im September 1995 mein Diplom in Biochemie.

In der Zeit von Oktober 1995 bis Juni 1998 war ich als wissenschaftliche Mitarbeiterin im Forschungsprojekt „Structure-activity relationships of drugs overcoming multiple drug resistance in tumors“ am Zentrallabor für Biomedizinisches Engineering, Bulgarische Akademie der Wissenschaften, in Sofia angestellt.

Im Juni 1998 begann ich, an der Georg-August Universität Göttingen, an der vorliegenden Doktorarbeit zu arbeiten.